



**Division of Materials, Mechanics and Structures**

Fatigue Behaviour and Reliability of Extended Hollobolt to Concrete

Filled Hollow section

by

Norashidah Abd Rahman

(B.Eng, M.Eng)

Thesis submitted to the University of Nottingham for the degree of

Doctor of Philosophy

October 2012

---

# Abstract

The need to provide mechanical connection from one side for the Hollow section connection has arisen in a number of fields and has resulted in the development of several types of so-called blind fasteners. An experimental blind bolt called the Extended Hollobolt is giving a good behaviour performance in terms of stiffness, strength and ductility. The strength performance of this system has been investigated under both monotonic and cyclic loading. However, the performance of such connections under fatigue loading is still unknown.

The aim of this study was to investigate the behaviour of blind bolt connection to concrete filled hollow section under repeated load. Further aim was to determine the reliability of the Extended Hollobolt to concrete filled hollow section.

The study involved conducting an experimental programme and carrying out fatigue life and reliability analysis. The experiment programme tested 52 specimens of bolts connected to concrete filled hollow sections where 36 tests involved Extended Hollobolt, 10 standard Hollobolt and 6 standard bolts (M16). The test specimens were subjected to tensile fatigue load characteristics with varying stress ranges.

Mathematical methods are used to analyse the fatigue test data using the normal, lognormal and Weibull distributions. Normal and lognormal distributions are more suitable. Therefore, statistical analysis procedure proposed by Eurocode for the statistical analysis is valid for fatigue test data. Statistical analysis was conducted to establish S-N curves and to predict the fatigue life of the proposed blind bolt. This was then compared to the normative regulation in Eurocode 3.

---

The failure mode of the Extended Hollobolt under repeated loading was found to be similar with standard bolt, which is a very positive outcome. Statistical analysis of fatigue test data showed that the fatigue life of Extended Hollobolt is higher than the theoretical design S-N curve which is recommended by Eurocode 3 part 1-9 for the standard bolt. However, the actual fatigue life for the standard bolt appears to be higher than the proposed blind bolt. A design model for predicting the fatigue life using S-N curve for the Extended Hollobolt is proposed. A reliability analysis using FORM (First Order Reliability Method) analysis shows that Extended Hollobolt is reliable in connections to concrete filled hollow sections where the safety index is 4.2.

---

# Table of Contents

Abstract .....	i
Table of Contents .....	iii
List of Tables.....	viii
List of Figures .....	x
Abbreviations .....	xv
Notation.....	xvi
Acknowledgment .....	xvii
Declaration .....	xviii
Chapter 1 : Introduction .....	1
1.1. Bolted connection .....	1
1.2. Fatigue background .....	5
1.3. Research question.....	6
1.4. Research justification .....	7
1.5. Aims and objectives of the research .....	8
1.6. Research methodology .....	9
1.6.1. Literature review .....	9
1.6.2. Experimental work .....	9
1.6.3. Mathematical method.....	10
1.7. Overview of the thesis .....	11

---

Chapter 2 : Literature Review and Related Background .....	12
2.1    Introduction .....	12
2.2    Review of research on blind bolts .....	12
2.2.1    Blind bolt connection .....	13
2.2.2    Extended blind bolt .....	22
2.2.3    Blind bolt connection under cyclic load .....	24
2.3    Review of research in fatigue .....	27
2.3.1    Fatigue load.....	30
2.3.2    Effect of mean stress or stress range .....	34
2.3.3    Effect of frequency.....	35
2.4    Review of research on the fatigue behaviour of bolted connections.....	37
2.4.1    Fatigue failure of bolts .....	38
2.4.2    Fatigue life of the bolt .....	42
2.4.3    S-N Model.....	45
2.5    Concluding remarks .....	47
2.6    Future research directions .....	49
Chapter 3 : Experimental Work .....	50
3.1    Introduction .....	50
3.2    Overview of Fatigue Testing.....	50
3.2.1    Hollow section material .....	51
3.2.2    Bolts .....	53
3.2.3    Concrete material .....	56
3.3    Material geometries .....	56
3.3.1    Hollow section .....	57

---

---

3.3.2	Bolts .....	57
3.3.3	Properties of concrete.....	60
3.4	Test setup and loading procedure .....	63
3.4.1	Fatigue test loading method .....	66
3.4.2	Number of specimens.....	67
3.4.3	Stress range .....	69
3.5	Concluding remark .....	73
Chapter 4 : Experimental Results, Discussions, and Observations.....		74
4.1	Introduction .....	74
4.2	Effect of frequency and stress range determination .....	74
4.2.1	Effect of frequency.....	75
4.2.2	Effect of stress range.....	79
4.2.3	Effect of frequency on the failure mode .....	79
4.3	General observations on Extended Hollobolt under fatigue load.....	80
4.3.1	Fatigue behaviour of the Extended Hollobolt .....	81
4.3.2	Fracture failure of the Extended Hollobolt .....	89
4.4	Comparison among tested bolt types.....	91
4.4.1	Fatigue life of bolt.....	91
4.4.2	Fatigue behaviour of bolts.....	93
4.4.3	Fracture failure of bolt .....	96
4.4.4	EC3 S–N curve classification.....	98
4.5	Effect of concrete strength.....	101
4.6	Chapter summary .....	104

---

Chapter 5 : Statistical and Reliability Analysis.....	105
5.1    Introduction .....	105
5.2    Probability Distribution Function.....	106
5.2.1    Lognormal distribution .....	109
5.2.2    Weibull distribution .....	112
5.2.3    Normal distribution .....	114
5.2.4    Distribution Discussion.....	115
5.3    Extended Hollobolt S-N curve characteristic .....	116
5.3.1    Tolerance Limits .....	119
5.3.2    Confidence limit/level.....	120
5.3.3    Standard deviation.....	123
5.4    Introduction to fatigue reliability .....	124
5.5    Fatigue reliability analysis.....	125
5.5.1    Safety index and probability of EHB .....	127
5.5.2    Discussion on the reliability of the Extended Hollobolt .....	128
5.6    Chapter summary .....	129
Chapter 6 : Conclusions and Recommendations for Future Work .....	130
6.1    Introduction .....	130
6.2    Conclusion.....	131
6.3    Recommendations for further study .....	132
References.....	134
Appendix A.....	142
Appendix B .....	143
Appendix C .....	150

---

---

Appendix D .....	152
Appendix E .....	155

---

# List of Tables

Table 2.1 : Formulation of fatigue rules (Ioannis Vayas et al., 2003) .....	32
Table 2.2 : Comparison table for high cycle and low cycle.....	32
Table 2.3 : Bend fatigue data for four test loading frequencies (R-Fujczak, 1994)...	36
Table 2.4 : Details of the connections tested by Birkemoe (1971) .....	46
Table 3.1 : Sample experimental work specimen details.....	56
Table 3.2 : Material properties of the hollow section .....	57
Table 3.3 : Mechanical properties of the bolts (machined).....	59
Table 3.4 : Mechanical properties of the bolts (full size) .....	59
Table 3.5 : Concrete Mix .....	60
Table 3.6 : Concrete strength of the Extended Hollobolt (EHB C40) .....	60
Table 3.7 : Concrete strength of the standard M16 bolt.....	62
Table 3.8 : Concrete strength of the standard HB .....	62
Table 3.9 : Concrete strength of the Extended Hollobolt (EHB C60) .....	63
Table 3.10 : Number of specimens required, British Standard (BS ISO 12107, 2003). .....	67
Table 3.11 : ASTM Standard Practice recommended sample size (ASTM, 1991). ..	68
Table 3.12 : ASTM Standard Practice replication percentage (ASTM, 1991). .....	68

---

Table 3.13 : Average tensile bolt area.....	70
Table 3.14 : Number of tests per stress range .....	72
Table 4.1: Effect of frequency experimental results .....	76
Table 4.2 : Experimental results of EHB Grade 8.8 C40.....	82
Table 4.3 : Experimental results of standard HB Grade 8.8 C40.....	85
Table 4.4 : Experimental results of standard bolt M16 Grade 8.8 C40 .....	86
Table 4.5 : Experimental results of EHB Grade 8.8 C60.....	87
Table 4.6 : Fatigue life of EHB Grades 8.8 and 10.9.....	89
Table 4.7 : Fatigue life of EHB using C40 and C60 .....	103
Table 5.1: Properties of the normal, lognormal, and Weibull distributions (Walpole et al., 1998).....	108
Table 5.2 : Comparison of the three distributions.....	116
Table 5.3 : S-N Curve result of the EHB .....	123
Table 5.4 : Standard deviation of various types of detail category .....	124
Table 5.5 : Target reliability index $\beta_o$ for class RC2 structural members <sup>1</sup> (BS EN1990, 2002) .....	128

---

# List of Figures

Figure 1.1: Typical extended endplate connection to a tube.....	2
Figure 1.2 : Commercial blind fasteners .....	3
Figure 2.1 : Moment rotation of connection (SCI, 1997) .....	13
Figure 2.2 : Moment rotational diagram (Trahair et al., 2008).....	14
Figure 2.3 : Column flange or bending and bolt strength (SCI, 1997) .....	15
Figure 2.4 : Moment rotation relationship for specimens S1, S2, and S3 (Korol et al., 1993).....	16
Figure 2.5 : T-stub test arrangement with RMH (Barnett et al., 2000).....	17
Figure 2.6 : Load Vs plate separation for the RMH t-stub test (Barnett et al., 2000)	18
Figure 2.7 : Load displacement relationships (Sean Ellison, 2004).....	19
Figure 2.8 : Wall deformation effect of unfilled SHS (Tizani and Ridley-Ellis, 2003); blind bolt to concrete filled tube connection.....	20
Figure 2.9 : Comparison deformation for column face at the bottom flange of beam (mm) (France et al., 1999).....	22
Figure 2.10 : Experimental set up and detail (Yao et al., 2008) .....	23
Figure 2.11: Extended Hollobolt.....	23
Figure 2.12 : Load slip of pullout test under cyclic loading (Yao et al., 2008) .....	25
Figure 2.13 : Details of the connection configuration (Elghazouli et al., 2009).....	26

---

Figure 2.14: Loading protocol (ECCS, 1986).....	26
Figure 2.15 : Top view of the fracture due to low cycle fatigue (Elghazouli et al., 2009).....	27
Figure 2.16 : S-N curves (BS EN1993, 2006) .....	29
Figure 2.17 : Type of applied load (Gurney, 1979) .....	31
Figure 2.18 : Magnitude and stress ratio (Trahair et al., 2008).....	35
Figure 2.19 : Effect of frequency on the fatigue life of Polymer matrix composites (IM7/PET1) (Counts and Johnson, 2002) .....	37
Figure 2.20 : Bolt fatigue failure (ESDEP, 2011).....	38
Figure 2.21 : Fatigue fracture (marinediesels.co.uk) .....	40
Figure 2.22 : Magnification of fatigue failure showing striations (marinediesels.co.uk) .....	40
Figure 2.23 : Fracture failure for bolts loaded axially with a mean stress of 584 MPa (a) and 250 MPa (b) (Hobbs et al., 2000) .....	41
Figure 2.24 : Crack shapes of eccentric loadings (Hobbs et al., 2000).....	42
Figure 2.25 : Comparison between the S-N and Fracture Mechanics models.....	43
Figure 2.26 : Predicted S-N curve using a modified Fracture Mechanics model .....	44
Figure 2.27 : Bolted S-N curve .....	45
Figure 2.28 : Comparison between scatter band of test and normative S-N curve (Schaumann and Marten, 2009) .....	47
Figure 3.1 : Illustration of EHB fatigue test.....	51

---

---

Figure 3.2 : Test arrangement .....	52
Figure 3.3 : Test arrangement using Rig assembly .....	52
Figure 3.4 : Types of bolts for the fatigue test .....	53
Figure 3.5: Actual dimensions of the EHB (all measurements in mm) .....	54
Figure 3.6 : Actual dimensions of the HB (all measurements in mm).....	55
Figure 3.7 : Actual dimensions of the standard M16 bolt (all dimensions in mm)....	55
Figure 3.8 : Coupon piece dimensions .....	57
Figure 3.9 : Bolt tensile test specimens.....	58
Figure 3.10 : Bolt Stress – Strain curve (Machined).....	58
Figure 3.11 : Leveling work.....	64
Figure 3.12 : Bolt connection to the load cell .....	64
Figure 3.13 : Experimental setup .....	65
Figure 3.14 : Loading hysteresis .....	71
Figure 3.15 : Load path .....	71
Figure 4.1 : Cyclic histories at stress $\Delta\sigma_n$ 455 N/mm <sup>2</sup> .....	77
Figure 4.2 : Normalization graph of frequency.....	78
Figure 4.3 : Effect of stress range graph .....	79
Figure 4.4 : Failure mode of Extended Hollobolt .....	80
Figure 4.5 : Normalization graph stress of fatigue life of EHB.....	81

---

Figure 4.6 : Fatigue life displacement graph.....	88
Figure 4.7 : Fracture failure location.....	90
Figure 4.8 : Fracture failure of EHB: a) $\Delta\sigma = 584 \text{ N/mm}^2$ ; b) $\Delta\sigma = 454 \text{ N/mm}^2$ ; c) $\Delta\sigma = 389 \text{ N/mm}^2$ ; d) $\Delta\sigma = 325 \text{ N/mm}^2$ ; e) $\Delta\sigma = 292 \text{ N/mm}^2$ .....	90
Figure 4.9 : S–N curve of bolt comparison .....	92
Figure 4.10 : Comparison fatigue life of bolt at stress range $584 \text{ N/mm}^2$ .....	94
Figure 4.11 : Concrete surface of the standard HB and EHB test specimens .....	95
Figure 4.12 : Static test results of Extended Hollobolt and standard bolt concrete-filled hollow sections .....	95
Figure 4.13 : Fracture failure of bolts: a) $584 \text{ N/mm}^2$ ; b) $519 \text{ N/mm}^2$ ; c) $454 \text{ N/mm}^2$ ; d) $389 \text{ N/mm}^2$ ; e) $325 \text{ N/mm}^2$ .....	97
Figure 4.14 : Micrographic of fracture failure at $\Delta\sigma=454 \text{ N/mm}^2$ .....	98
Figure 4.15 : Sleeve observation after test .....	98
Figure 4.16 : S–N curve according to EC3 characteristics (BS EN1993, 2006) .....	100
Figure 4.17 : Crack propagation on the concrete at stress ranges $584, 455, \text{ and } 325 \text{ N/mm}^2$ .....	101
Figure 4.18 : Fatigue life-displacement graph at $584 \text{ N/mm}^2$ stress range for C40 and C60 .....	102
Figure 4.19 : Fatigue life displacement at $454 \text{ N/mm}^2$ stress range for C40 and C60 .....	103
Figure 5.1 : Probability plot using lognormal distribution.....	110
Figure 5.2 : Lognormal PDF .....	110

---

Figure 5.3 : Lognormal survival graph .....	111
Figure 5.4 : Probability plot using Weibull distribution .....	112
Figure 5.5 : Weibull PDF (Survival graph).....	113
Figure 5.6 : Survival graph using the Weibull distribution of EHB C40 test data ..	114
Figure 5.7 : Probability plot using Normal distribution.....	115
Figure 5.8 : Curve-fitting graph .....	118
Figure 5.9 : Tolerance limit for fatigue test data.....	119
Figure 5.10 : Definition of characteristic resistance .....	122
Figure 5.11 : S-N curve characteristic design .....	123
Figure 5.12 : Geometric representation of the safety index $\beta$ based on the Hesofer–Lind approach.....	127

---

# Abbreviations

EC	=	Eurocode
EC3	=	Eurocode 3
ECCS	=	European Convention for Structural Steelwork
EHB	=	Extended Hollobolt
HB	=	Hollobolt
RMH	=	Reverse Mechanism Hollobolt
FORM	=	First Order Reliability Method
SORM	=	second Order Reliability Method

---

# Notation

$f_{ck,cube(40)}$	=	Concrete strength of cube (C40)
$f_{ck,cube(e)}$	=	Concrete strength of cube (Concrete at test day)
$\Delta\sigma_e$	=	Experimental stress range
$\Delta\sigma_n$	=	Nominal stress range
$P_a$	=	Actual load (experiment)
$S_x$	=	Standard deviation of $x$
$\overline{\log\Delta\sigma}$	=	Mean of stress range
$m$	=	slope
$N_f$	=	Cycles to failure
$P$	=	Probability
$n$	=	number of specimen
$i$	=	specimen at $i=1,2,3\dots n$

---

# Acknowledgment

I would like to take this opportunity to thank the following people who have provided help, guidance and support in completing this work.

Firstly, my greatest appreciation and gratefulness to my supervisor, Dr. Walid Tizani for his valuable guidance, advice, support and supervision. With his effort and advice, I am able to complete this work.

I wish to thank you all the staff in Civil Engineering Laboratory: Mr. Bal Loyla, Mr. Nigel Rook, Mr. Gordan Hardy, Mr. Mike Jones, Mr. Gary Davies, Mr. Jim Bellis and Mr. Jim Meakin for providing assistance during the laboratory testing.

I would like to thank Ministry of Higher Education (MOHE), Malaysia and Universiti Tun Hussein Onn Malaysia for the financial support.

I also would like to express gratitude to Mr. Neil Gill from Lindapter International and Tata Steel Europe (formerly Corus Tubes) for providing technical support and materials for testing.

Most importantly, I wish to thank to all my family members especially to my parents Abd Rahman Tahir and Munah Mohamad for their encouragement and moral support. Finally to all my friends who provided support me throughout the project.

---

# Declaration

I declare that, except where cited in the text, all work contained within this thesis is my own original work, under the direction of my supervisor. The work presented herein was performed at The University of Nottingham between January 2008 and October 2012. This thesis has not been submitted to any institution other than The University of Nottingham for the degree of Doctor of Philosophy.

Norashidah Abd Rahman

---

# Chapter 1 : Introduction

---

## 1.1. Bolted connection

The majority of buildings that incorporate steelwork frames into their structure are usually made up of open-section profile beams and column members. The popularity of steel-framed buildings may be partly attributed to the easy prefabrication and erection of steel members. Structural hollow sections (SHS) are commonly used for columns in multi-storey construction because of their good aesthetic value and high strength-to-weight ratio. However, the close-shaped geometry of hollow sections makes the nut component difficult to manipulate directly to the face of the column. Early solutions for the connection problem include the use of fully welded connections, which is not an attractive option in some countries. The use of standard bolts, which is the main alternative in welding open sections, is impossible in SHS as it requires access to the interior of the tube to facilitate tightening (Barnett et al., 2000). The use of additional components, such as gusset plates and brackets, addresses this problem. However, this use of additional components is not generally considered an acceptable solution for aesthetic reasons.

Hollow section components can also be connected through site welding. Welded connections do not require holes to be drilled into the member, whereas welded joints are more rigid than bolted joints. However, field welding may remain difficult, costly, and time consuming. Welded connections are also susceptible to failure because of cracks caused by fatigue under repeated cycles. Fatigue may result from working loads, such as trains passing over a bridge (high-cycle fatigue) or earthquakes (low-cycle fatigue).

---

The need to provide mechanical connections from one side only started in a number of engineering fields. Blind fastener or blind bolt is a one of the fastening system and the system is applied for installations wherein only one side of the connection can be accessed. For example, blind fasteners can be used to connect the end-plate of a beam to a hollow section, as shown in Figure 1.1.



Figure 1.1: Typical endplate connection to a tube (Lindapter, 2012)

Blind fasteners offer many advantages, including i) high tensile and shear strength, ii) potential use in tension applications and in moment resisting connection, iii) uniform high clamping force, and iv) vibration resistance (Tabsh et al., 1997). Furthermore, blind bolts can easily be installed by unskilled technicians using portable equipment. Many types of blind fasteners are available commercially, including the Flowdrill (Flowdrill B.V Holland), the Huck high strength blind bolt (HSBB), Huck blind oversized mechanically locked bolt (BOM), Ultra Twist (Huck International, USA), and Lindapter Hollobolt (Lindapter International, UK) (Figure 1.2). Each type of fastener differs in terms of the number and design of bolt components, resistance mechanisms, and methods of installation.

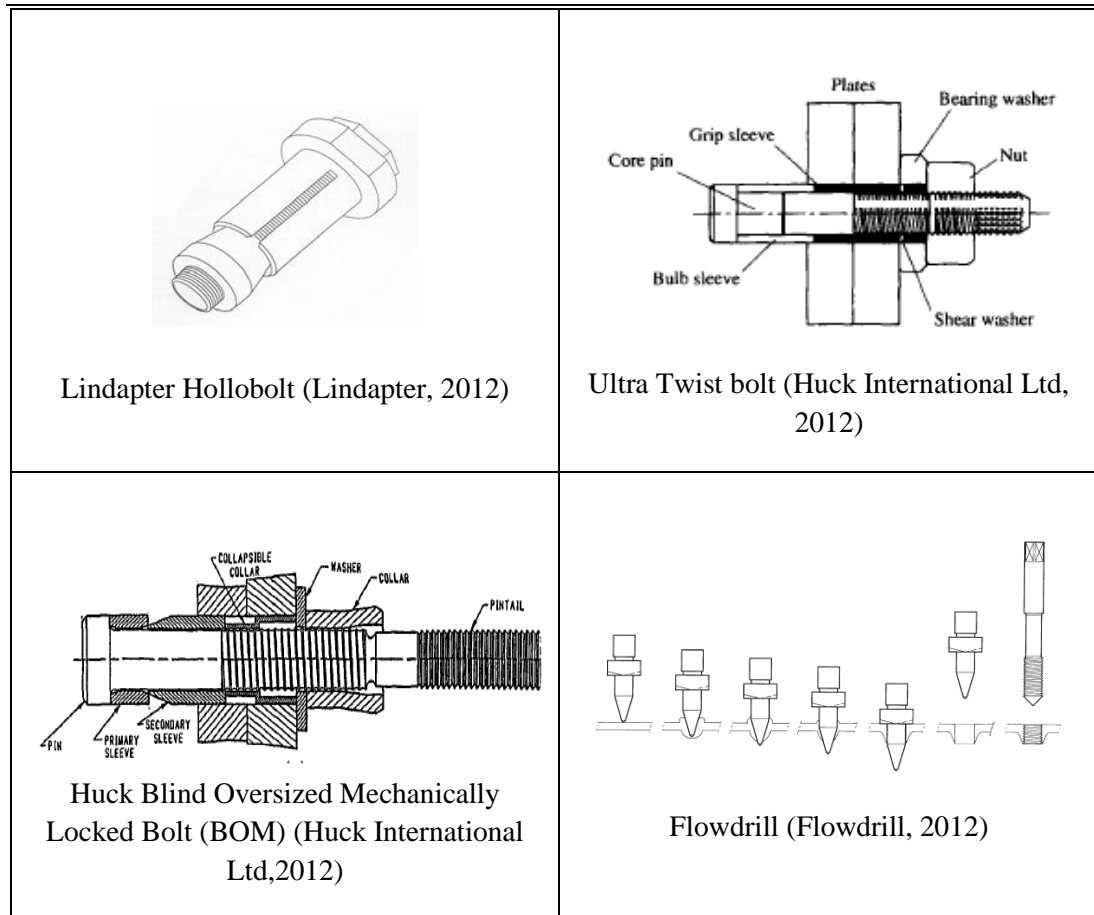


Figure 1.2 : Commercial blind fasteners

The use of blind bolt connections has several advantages, so researchers have investigated the performance of these connections. An experimental test was conducted either under monotonic or cyclic load to investigate the behaviour of blind bolt connection. Barnett (2001) examined the behaviour of the Hollobolt when connected to a hollow section under monotonic load, and the results were compared with the performance of the standard bolt. The findings showed that the behaviour of the Hollobolt is unsatisfactory in terms of stiffness and strength compared with that of the standard bolt. The experiment revealed that the bending of the hollow section dominated the behaviour. Thus, experimental modification was conducted to increase the stiffness and the strength of the Hollobolt. A blind bolt called the Extended Hollobolt was proposed at the University of Nottingham by Tizani and Ridley (2003). This fastener is used in concrete-filled hollow sections, where the concrete is

---

used to prevent the bending of the tube face in order to increase the stiffness and the strength of the connection. The Extended Hollobolt was investigated in pure tension with the use of a T-stub connected to a concrete-filled tube. The results were comparable to conventional connections in terms of stiffness and strength.

Cyclic load testing was conducted in previous research to explore the reliability of the standard Hollobolt for gravity and lateral loads from wind or earthquakes in regions of low to moderate seismicity. Wang (2008) and Elghazouli (2009) investigated the behaviour of the standard Hollobolt when connected to concrete-filled tubes under cyclic loading. Cyclic load testing showed the standard Hollobolt's reasonable energy capability and rotation capacity. The failure mode under cyclic load was similar to that under monotonic test. Elghazouli (2009) provided evidence of fracture caused by low-cycle fatigue, but no further investigation was performed.

As discussed above, recent studies describe the behaviour of the blind bolt when subjected to increasing monotonic load or cyclic loading. Engineers who specify fasteners often base their requirements on strength (tensile strength, yield strength, proof strength, or threaded stripping strength), without taking fatigue and stress concentration into account (O'Brien and Metcalfe, 2009). According to Barsom (1999), most structural components are subjected to repeated fluctuating loads with a below-fracture load magnitude under monotonic loading. Ignoring this issue may result in unfortunate events, as these types of connection are used with a service loading that varies with time.

---

## 1.2. Fatigue background

Events such as the 1994 Northridge earthquake and the I-35 bridge collapse in Minnesota serve as reminders of the importance of fatigue and fracture (Benjamin V. Fell and Kanvinde, 2009). Fluctuating loads must be considered in the design of structural and machine components that are subjected to repeated fatigue (Ayyub et al., 2002). The expected number of loading cycles can vary tremendously during the life of a structure. For example, a beam that supports a crane may be loaded 2,000,000 times in 25 years before it fails to function, whereas an automobile crankshaft might have to be loaded 5,000,000 times before rupture occurs (Beer and E.R.Johnston, 1981).

Investigations on bolted connections under fatigue are not as popular as those on welded connections because welded connections are critical. However, bolted connections under fatigue also require examination to prevent fatigue damage. Although bolted connections are mostly discussed in the field of aeronautics, research related to the behaviour of bolts has also become the subject of discussion within the field of steel structures. Design codes such as EC3 and ECCS provide design procedures for normal bolts under fatigue. These procedures are currently used for fatigue assessment. Studies that aim to predict the fatigue life and the behaviour of bolts have been conducted by researchers such as Birkemoe (1971), Ghazali (2004), and Schaumann (2009). They investigated the behaviour of various types of bolts, such as high-strength bolts. Results in terms of fatigue life and fracture failure showed that the behaviour is compromised compared with that of existing standard bolt design. A fatigue design assessment for the Hollobolt blind bolt has not yet been established, and the same is the case for the Extended

---

Hollobolt. Although the behaviour of the Extended Hollobolt is satisfactory under monotonic or cyclic load, its response under fatigue also requires study. This examination will compare the behaviour and the fatigue life of the Extended Hollobolt under fatigue with the standard bolt with the use of existing design guidance such as Eurocode 3.

### **1.3. Research question**

A study on behaviour of blind bolts, specifically the Extended Hollobolt, was conducted at the University of Nottingham to explore the behaviour of the Extended Hollobolt connection under monotonic load. The Extended Hollobolt was selected because it is easy to handle and install. In terms of stiffness, strength, and failure mechanism, it is also quite comparable to the standard bolt. The experiment clearly demonstrated that this type of connection is reliable as an alternative to welded connections for connecting steel beams to concrete-filled square hollow sections (Barnett et al., 2001). However, this type of bolt has not been examined well under fatigue load. Blind bolt behaviour should be studied further, as low-cycle fatigue was found when the behaviour of blind bolt connections was tested in the cyclic test of Elghazouli (2009).

The research questions are outlined as follows:

- i. What is the behaviour of the Extended Hollobolt under fatigue or repeated load?
- ii. What is the fatigue life of the Extended Hollobolt?
- iii. How can the fatigue life of the Extended Hollobolt be predicted?

- 
- iv. How comparable is the behaviour of the Extended Hollobolt with other types of bolts?
  - v. How reliable is the Extended Hollobolt with respect to fatigue assessment?

#### **1.4. Research justification**

This section explains the need for the present study and provides an overview of the selected parameters.

This work focuses on the investigation of the fatigue life and the reliability of the Extended Hollobolt under tensile fatigue load through experimental work and validation of the test data with the use of statistical analysis. It contributes to existing knowledge by providing information on the behaviour, fatigue assessment, fatigue life prediction, and reliability of the Extended Hollobolt. It also provides guidance for further investigation and design.

The materials and parameters involved in this study were selected from previous studies.

The Extended Hollobolt is comparable to the standard bolt. It has only been studied under monotonic load. Before the present study was conducted, limited information on fatigue load was available. In addition to the Extended Hollobolt, two other types of bolts were investigated, the standard Hollobolt and the standard bolt, which were selected to compare their fatigue behaviour with that of the Extended Hollobolt.

Statistical analysis is the most suitable method to validate and define the reliability of the experimental results. Probability distributions based on previous research

---

findings were selected. These probability distributions were used to define the reliability of the bolt during time service and to predict the fatigue life of the bolt. The reliability function and the prediction equation can serve as foundations and sources of information in assessing the fatigue behaviour of Extended Hollobolts.

### **1.5. Aims and objectives of the research**

This study aims to examine the behaviour of the blind bolt connection of concrete-filled hollow sections using Extended Hollobolts under repeated loading. A further aim is to determine the reliability of Extended Hollobolts for concrete-filled tubes. This research is an extension of an earlier work done at the University of Nottingham. The objectives of the study are as follows:

- i. To conduct experimental tests to investigate the behaviour of Extended Hollobolts under repeated load
- ii. To investigate the effect of the frequency and the stress range of Extended Hollobolts
- iii. To determine the fatigue life and the failure mechanism of the Extended Hollobolt connection in concrete-filled tubes
- iv. To evaluate the performance of the Extended Hollobolt connection and compare it with other types of bolts
- v. To validate the experimental results with a statistical method
- vi. To analyze the reliability of the Extended Hollobolt

---

## **1.6. Research methodology**

This section introduces the methodology used to achieve the aims and objectives of this study. The research objectives outlined in Section 1.5 were accomplished with a combination of experimental work and mathematical method.

### **1.6.1. Literature review**

This stage is important to collate previous research findings and to obtain insights from relevant work. In this section, the researcher proposed relevant areas that should be covered in the study. Previous research on blind bolt connection to hollow section is examined. Blind bolt connection behaviour under monotonic and cyclic tests is discussed. Bolt connection behaviour under fatigue test is also reviewed. Statistical analysis is used to validate fatigue test data.

### **1.6.2. Experimental work**

Necessary tests were performed to determine the behaviour of the Extended Hollobolt on concrete hollow section, as well as the behaviour of other types of bolts compared with the Extended Hollobolt. This study also observed the bolt failure mechanism after failure occurred. The experimental work aims to define the fatigue life and the reliability of the Extended Hollobolt.

A pull out test of a single Extended Hollobolt connected to a concrete-filled hollow section was conducted to achieve the objective of the experimental work. Preparation was undertaken in designing the frame for fatigue testing to ensure that the frame could handle fatigue load. Material properties were determined by coupon and bolt tensile tests. The bolts were tightened to the hollow sections with the use of a

---

conventional torque wrench. Tightening torque was applied according to the suggestions of the supplier. Concrete was then poured into the hollow section. After the concrete was cured properly, the specimen was fixed into the rig frame. Specimen level was checked to ensure it is leveled before the start of the test. All required data such as frequency, amplitude, and mean load were created in the system connected to the load cell. The test commenced when the entire procedure was completed. All readings were logged into the Servocon system connected to the load cell. This load cell was directly connected to the specimen. All the data and the fatigue life of the specimen were recorded.

### **1.6.3. Mathematical method**

Mathematical method was used to validate the experimental data. The reliability of the Extended Hollobolt was also examined to establish the design proposal for the fatigue life of the bolt. At this stage, only Extended Hollobolt connections with concrete strengths of  $40 \text{ N/mm}^2$  were discussed. Other types of bolt were not discussed at this stage.

Statistical analysis was used to validate the experimental data. Data from the experimental work were validated by probability distribution. Three types of distribution, namely, normal, lognormal, and Weibull distribution, were discussed to find a suitable distribution. The reliability of the Extended Hollobolt was then examined. A suitable distribution was subsequently used to predict the fatigue life of the Extended Hollobolt connected to a concrete hollow section. Finally, the predicted fatigue life and the safety index of the Extended Hollobolt were proposed.

---

## 1.7. Overview of the thesis

This thesis comprises six chapters, including the above introduction. An overview of each chapter is provided below.

**Chapter 2** discusses previous findings on blind bolt connection and provides reviews of fatigue and the statistical methods used in analysing fatigue data. This chapter concludes by identifying existing knowledge gaps in this area.

**Chapter 3** presents the experimental work. The design experiment, experimental set-up, and material properties are shown. Fatigue test procedures and instruments are also presented.

**Chapter 4** discusses the results and analysis of the fatigue test data, as well as the comparison of the performances of the proposed blind bolt with the standard Hollobolt and the standard bolt.

**Chapter 5** presents the statistical analysis of the fatigue tests, which define the mean value and the fatigue of the Extended Hollobolt categories. The results are compared with those of the S-N curve provided by Eurocode 3. The reliability of the Extended Hollobolt is also discussed in this chapter.

**Chapter 6** concludes the thesis and makes recommendations for future work.

---

# Chapter 2 : Literature Review and Related Background

---

## 2.1 Introduction

This chapter discusses the past and current research concerning the blind bolt and fatigue behaviour. It also includes background research work in assessing the reliability of the fatigue testing data.

## 2.2 Review of research on blind bolts

Although welding is the most suitable method for connecting structural hollow steel sections, the high cost and labour-intensive procedures have restricted the use of this type of connection. Welding is difficult to inspect, needs high quality control, and must be performed in suitable weather conditions. Site welding is also costlier than site bolting. In contrast, bolted connections are detachable, and are typically selected for onsite assembly in order to avoid site welding, which may result in welding errors during installation, and environmental difficulties. Several types of bolts may be used in structural joints, including ordinary structural and high strength bolts.

The use of bolts often facilitates the assembly of a structure and only requires very simple tools. Unless the joint is located close to the open end of a hollow section member, it is generally difficult to connect two hollow section members or a hollow section with an open profile or a plate directly to each other by bolting. Otherwise, it is necessary to employ measures, such as cutting a hand access hole in the structural hollow section member to enable the bolt to be tightened from the inside or by using “through” or “blind” bolts. Using components such as gusset plates and brackets can

help overcome this problem, but they are not generally considered aesthetically pleasing (Barnett et al., 2000). In recent years, new fastening systems have been developed, resulting in more convenient and efficient connections called blind bolt.

### 2.2.1 Blind bolt connection

The current general practice in analysing a steel structure is to assume that the connections behave either as perfectly pinned or completely fixed elements, as reported by Tanaka (2003) and Azizinamini (2004) and among others.

The properties of beam-column connection behaviour can be obtained from its moment rotational relationship ( $M-\theta$  curve), and is affected by a large number of geometric variables and material properties. The beam-column connection behaviour relates the moment transmitted ( $M$ ) to the relative rotation between the beam end of the adjacent column ( $\theta$ ) (Figure 2.1).

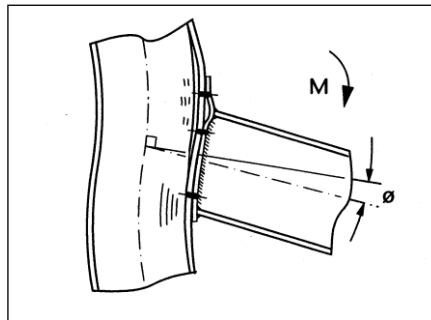


Figure 2.1 : Moment rotation of connection (SCI, 1997)

This connection can be classified in three ways, namely, by strength (i.e., full strength, partial strength, or nominally pinned), by stiffness (i.e., rigid, semi-rigid, or nominally pinned), and by ductility.  $M-\theta$  curves are used to determine the strength, stiffness, and rotational capacity of the connection. Figure 2.2 gives an example of a beam-column connection and its moment rotational diagram. This relationship is

essentially nonlinear, that is, when the rotation is increased, the stiffness is decreased until the moment resistance is reached, which corresponds to the slope of the curve. The moment resistance of the connection is indicated by the peak on the  $M-\phi$  curve, and is considered the most important property of the connection. Ideally rigid, semi-rigid and pinned connections correspond to the vertical and horizontal axes, respectively.

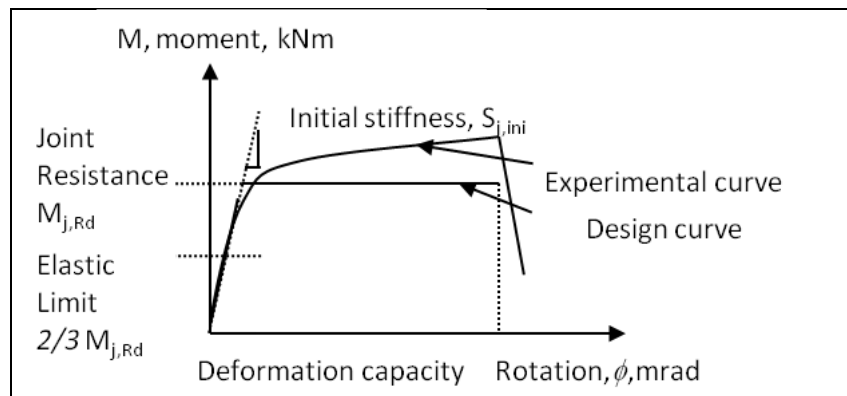


Figure 2.2 : Moment rotational diagram (Trahair et al., 2008)

Of the three characteristics of connection behaviour, the most important is sufficient stiffness, which is required to provide the restraint and transfer the moment, especially in semi-rigid to rigid joint action. The key aspect is the amount of stiffness provided, particularly relative to the stiffness of the connected member. The studies referred to above report that this all depends on the initial joint stiffness ( $S_i$ ) and on the ability of the joints to maintain a sufficiently high stiffness as the maximum load for the structure approaches. Therefore, the  $M-\phi$  curve is important in determining the characteristics of the connection.

Moment connections are widely used in steel structures; they consist of square hollow section (SHS) columns or circular hollow section (CHS) columns, H section beams and plates. Several studies of this type connection have been developed,

whether in design, experimental work, or modelling. For example, Tanaka (2003) proposed a formula for estimating the collapse moment to prevent the local deformation of a hollow section through the application of limit analysis; the author then verified it through comparisons with results from finite element analyses using diagram plates. Studies have also been conducted on the moment connection using blind bolt connection in a hollow section, both with or without concrete infill.

When a plate is used as a connection component, especially in bolted endplate connection, this is referred to as a connection. The T-stub test is a simple test used to understand the behaviour of a connection. Figure 2.3 shows the three possible modes of failures using equivalent t-stub. Tests have also been conducted to determine the failure mode using different plate thickness has been carried out elsewhere (France, 1997, Wang et al., 2009). The thicker plates show higher rigidity compared with thinner plates.

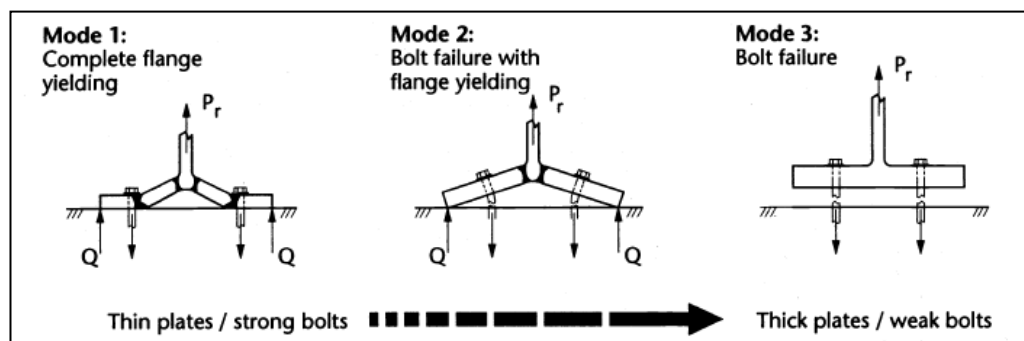


Figure 2.3 : Column flange or bending and bolt strength (SCI, 1997)

To compare the performance of the blind bolt with the standard blind bolt, several types of blind bolts have been tested in previous works. Korol (1993) proposed the bolted moment connection for rectangular hollow steel columns, using high-strength blind bolts to evaluate such a connection in terms of its performance and its failure modes. Five-endplate, bolted beam-column assemblies of various designs were tested

under monotonically increasing load, each having a W-shape beam connected to a square HSS column. While investigating the response of the connection and its elements, the moment rotation relationship of the test connection was also obtained. In evaluating the performance of the connections, a bolted end-plate connection utilizing high-strength blind bolts, as proposed for a W-shape beam and HSS column, appeared very promising as an effective moment connection. Based on the results of Karol (1993), the behaviour of the proposed bolted moment connection involving a W-shape beam and a rectangular hollow section column using high strength blind bolts (HSBB) is judged to be similar to the behaviour of connections using ordinary A325 bolts, in terms of stiffness, moment capacity, and ductility (See Figure 2.4). Thus, HSBB connections have a promising potential in structural connections wherein hollow section columns are employed. A moment connection utilizing blind oversize mechanically locked (BOM) bolts cannot achieve the equivalent strength of A325 bolts. Hence, in applications involving principal shearing action, it may be better to use BOM bolts.

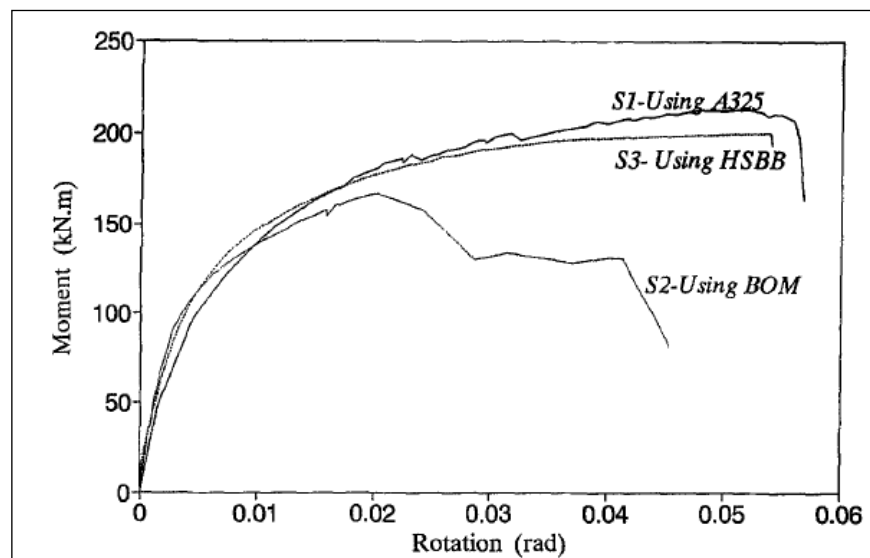


Figure 2.4 : Moment rotation relationship for specimens S1, S2, and S3 (Karol et al., 1993)

Barnett et al. (2000) investigated the performance of blind bolts compared with standard bolts. In their work, they used a new blind bolt with an arrangement designed to represent the tensile region of a moment transmitting endplate connection between a hollow section column and an open section beam. At the early stage of the research project, the original Hollobolt was altered so that the expanding sleeve could be clamped directly to the underside of the joint. Through a series of tests, the arrangement hereafter referred to as the reverse mechanism Hollobolt (RMH), has been shown to significantly improve the clamping force between the connected plies as compared with the original arrangement (Figure 2.5). The design technique considered in this connection is the 'component method'. The connection comprises a series of components, each with a specified design check to be performed. These components, in turn, are based on identification and representation of all possible failure modes and load transfer paths. In the tension region of connection, the bolts and connected plies may be modelled as a pair of equivalent t-stubs representing the flange and web of the column and the web endplate of beam. The standard t-stub tests result indicates that the RMH possesses sufficient strength and stiffness for use in a moment resisting connection (Figure 2.6).

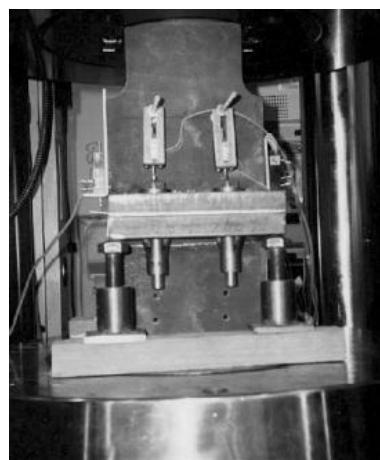


Figure 2.5 : T-stub test arrangement with RMH (Barnett et al., 2000)

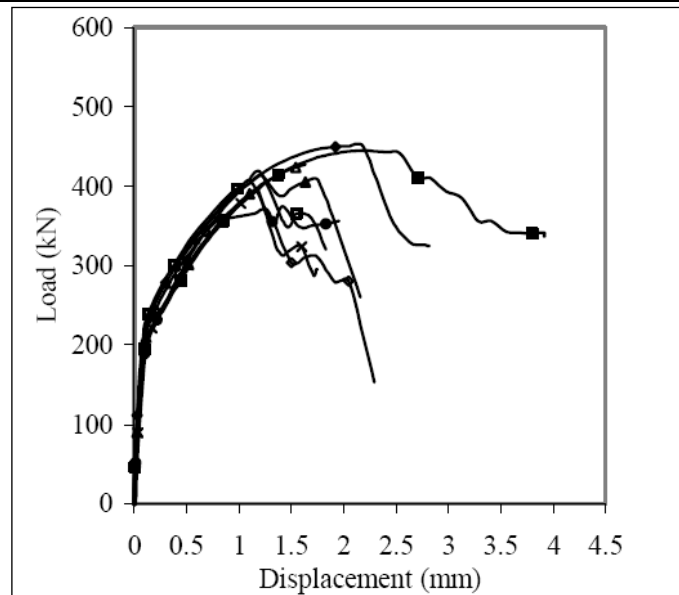


Figure 2.6 : Load Vs plate separation for the RMH t-stub test (Barnett et al., 2000)

It has been demonstrated theoretically that the flexibility of the SHS face may limit the moment capacity of the connection when thin walls and narrow bolt gauges are employed. Thus, Barnett suggested further tests using a modified t-stub arrangement to determine whether or not the full capacity of the RMH may be employed. These tests are anticipated to validate a previously published theoretical model of the tube face failure mechanism. The exploration of newly developed blind bolts continues with the investigation on the performance of new blind bolts for moment resisting connection (Tizani and Ridley-Ellis, 2003). Three main test series of RMH were carried out, namely, t-stub to t-stub, t-stub to SHS, and t-stub to concrete filled SHS. Other types of bolt such as Extended Hollobolt, Hollobolt and standard bolt were also carried out. Throughout the entire test, a relatively rigid t-stub (50 mm thick) was employed to eliminate the influence of endplate bending. The connection behaviour was found to be dependent on the behaviour of the bolts and the interaction between the bolts and the SHS. The tests, which were conducted in displacement control, exerted predominately pure tension forces on the bolts.

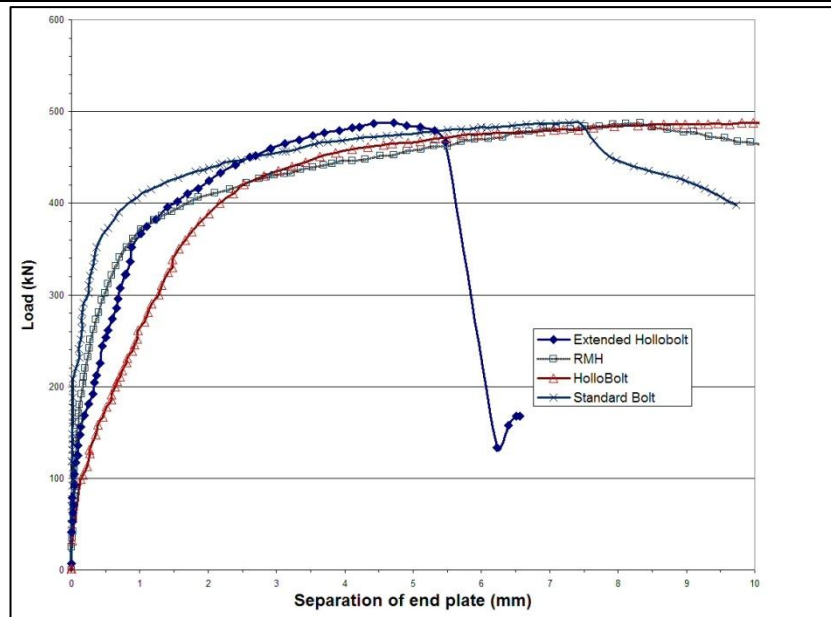


Figure 2.7 : Load displacement relationships (Sean Ellison, 2004)

Indeed, connections made with the RMH were seen to be almost as stiff as those made with standard bolts (Figure 2.7). The behaviour was seen to be comparable at the lower loads and possessed sufficient stiffness to classify the connection as moment-resisting. The results of the initial test showed that the Extended Hollobolt also possessed sufficient stiffness to classify the connection as moment-resisting, but at a lower tensile strength compared with standard bolts. However, a comparison between the hollow section concrete unfilled with concrete infill to the tube shows that the section with concrete fill has an equivalent tensile strength to that of standard bolts; along with the axial stiffness, this indicates a rigid connection classification.

The hollow section concrete unfilled or concrete filled section affects the behaviour of the connection, because the unfilled concrete section apparently deforms the tube and also gives a lower strength to the connection (Figure 2.8). France (1998) studied the effect of tube wall thickness using the flowdrill process. Thicker endplate was also used in the test to eliminate the effect of endplate and study the tube face of columns. Deformation of column faces was observed in every test, and more

deformation was detected in the thinner column face. The behaviour performance of stiffness, strength, and ductility also increased with thicker column face. Aside from increasing the tube face, the other method used to increase the performance of the connection and reduce the deformation of the column face involves adding concrete into the column.

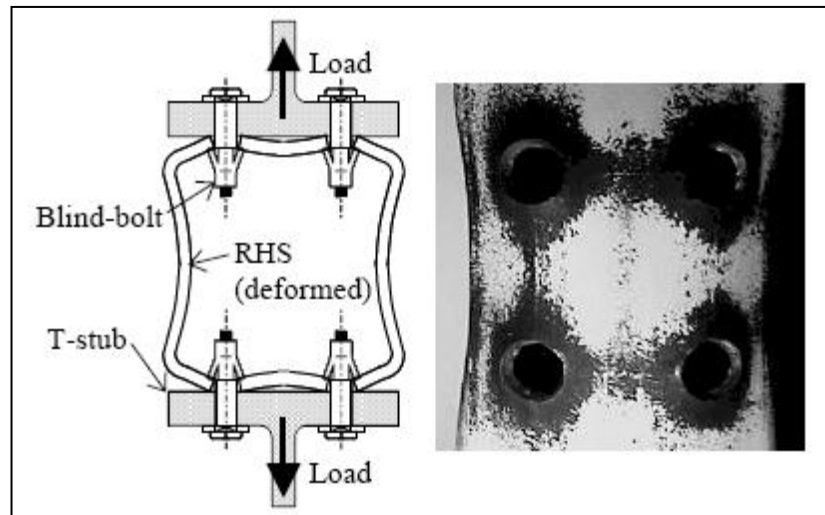


Figure 2.8 : Wall deformation effect of unfilled SHS (Tizani and Ridley-Ellis, 2003); blind bolt to concrete filled tube connection

Connection technology plays an important role in the performance of hollow section structures. A distinction, however, has to be made between CHS and RHS connected members, because the behaviour of joints such as local behaviour of members is different. In particular cases, such as beam-column joints in building frames with concrete filled hollow section (CFHS) columns or concrete filled tube (CFT), both welded and/or bolted connections can be used. Blind bolting technology is also available for beam-column joints on hollow section frames, such as RHS columns and beams or hollow section columns and I or H section beams.

CFHS or CFT provides excellent structural properties, especially for seismic resistance, such as high ductility and large energy absorption capacity. In addition to

---

the enhancement in structural properties, a considerable amount of construction time is reduced because permanent formwork of the concrete is eliminated. Furthermore, the CFT column system has many advantages compared with ordinary steel or the reinforced concrete system (Tan et al., 2003, Hsu and Lin, 2003, Yu et al., 2006, Shosuke Morino and Tsuda, 2002). The main advantages are listed below.

- *Interaction between steel tube and concrete:* local buckling of the steel tube is delayed, and the strength deterioration after the local buckling is moderated due to the restraining effect of the concrete. On the other hand, the strength of the concrete is increased due to the confining effect provided by the steel tube.
- *Cross-sectional properties:* the steel ratio in the CFT cross section is much larger than those in reinforced concrete and concrete-encased steel cross sections
- *Fire resistance:* concrete improves fire resistance, reducing the need for fireproofing.

Therefore, to prevent any inward deformation of blind bolt to hollow section connection, filling the hollow section with concrete is advantageous as it prevents the deformation of tube/column. The comparison between concrete filled and concrete unfilled can be seen in Figure 2.9, which shows that two series of flush endplates for serial beams have been bolted using flowdrill connection to  $200 \times 200 \times 8$  SHS column.

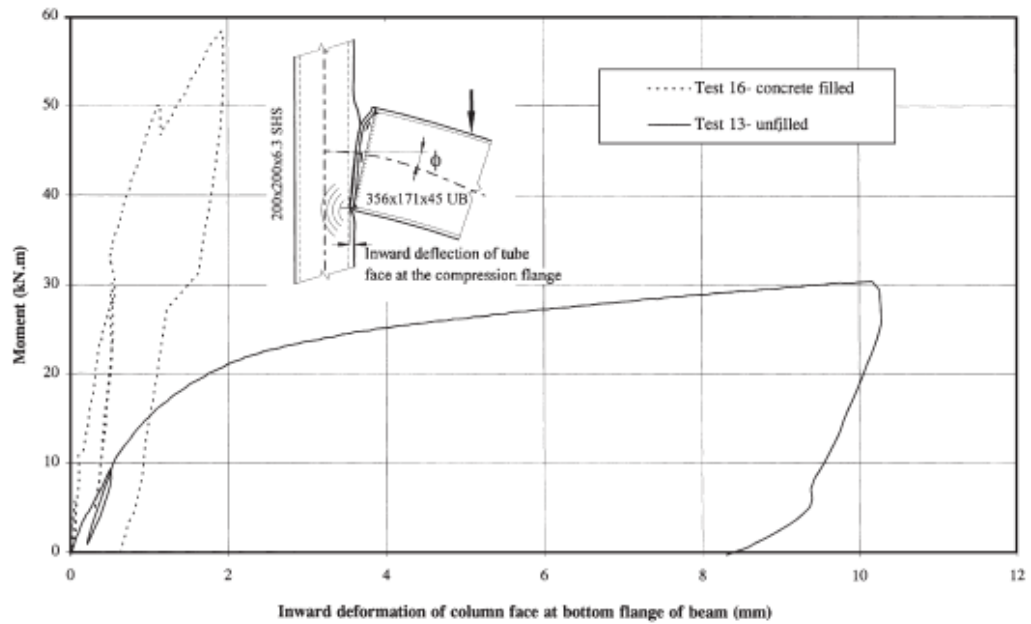


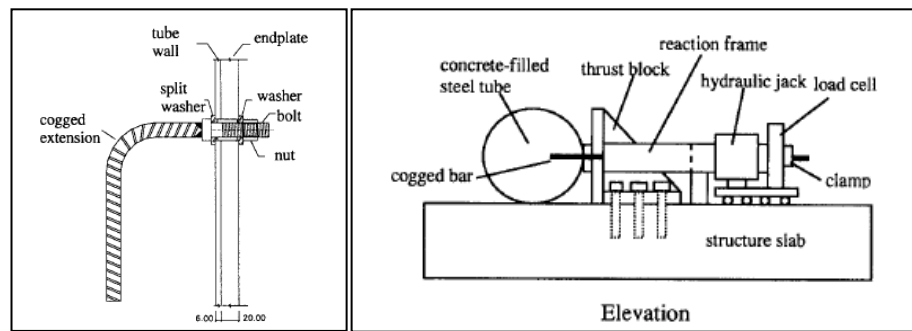
Figure 2.9 : Comparison deformation for column face at the bottom flange of beam (mm) (France et al., 1999)

In a column filled with concrete, the webs of the SHS were restrained from buckling in the region of the compression zone, which shifted the axis of the joint rotation towards the compressive flange of beam. This immediately altered the moment-rotation response by increasing the initial stiffness of the joint. The examination of SHS after each test revealed that the plasticity in the tension zone had been confined to the tube face and did not spread into the adjacent webs. Thus, the additional stiffness from the concrete fill was sufficient to stop any inward deformation of the walls at the location of the top tension bolts.

### 2.2.2 Extended blind bolt

To increase the stiffness of the connection using blind bolts in concrete filled tubes, Yao (2008) introduced the use of an Ajax blind bolt with an extension as shown in Figure 2.10. A series of tests on the blind bolt t-stub connections were conducted to study the behaviour of the connection using a cogged extension. The test results

showed that adding a cogged extension to the blind bolt improved the behaviour of the connection in tension, since the load was shared between the tube wall and cogged anchorage within the concrete. Hence, the cogged extensions prevented the bolts from pulling out of the tube.



a) Blind bolt and cogged extension    b) Pull out test set up

Figure 2.10 : Experimental set up and detail (Yao et al., 2008)

The failure mechanism of the Hollobolt, such as being pulled out from the concrete, is not acceptable in practice. Therefore, further development of this type of bolt is proposed to improve its failure mechanism by increasing the anchorage in concrete. Modification of the original Hollobolt was carried out by extending the shank and adding the nut at the end of the bolt (Barnett et. al, 2000). This new modification is called Extended Hollobolt (EHB) (Figure 2.11). Investigation on the use of this type of Hollobolt was performed through tensile tests in t-stub connection and moment resisting connection. The varied parameters in these tests were tube thickness, bolt gauge, bolt pitch, concrete strength, and bolt grade.



Figure 2.11: Extended Hollobolt

---

The results showed that, compared with the ordinary HB, the EHB showed stiffness improvement and increased tensile capacity (Figure 2.7). The test result shows that the extra anchorage provided by shank length and anchorage nut helped improve the stiffness of the bolt.

### **2.2.3 Blind bolt connection under cyclic load**

One of the most important lessons derived from the Northridge and Hyogo Ken-Nanbu earthquakes is the particular vulnerability of the beam-column connection in steel moment resisting frames and building structures. Starting from this observation, several research programmes have been developed to examine the connection behaviour on connection performance have been underlined, and theoretical models for reliably predicting stiffness, strength, and deformation capacity of the connection.

As bolted and rivet connections performed well in the past earthquake, particularly when encased in concrete (Swanson and Leo, 2000), an innovative beam to concrete filled column connection using blind bolts has been developed for seismic loading condition. At the University of Melbourne, a series of tests on blind bolted t-stub connections were conducted using Ajax blind bolts with or without extension into the concrete of the column (Yao, 2008). By applying a design force of 60 kN (loaded from 0 kN to 60 kN and back to 0 kN), the behaviour of extension was investigated. The performance of the bar was compared with the monotonic curves, as shown in Figure 2.12 (GA: monotonic specimen and GC: cyclic specimens). Based on the superimposed images of the two curves, monotonic curves provided an accurate envelope of cyclic curve, indicating that the extension bar had the same behaviour as the monotonic tests.

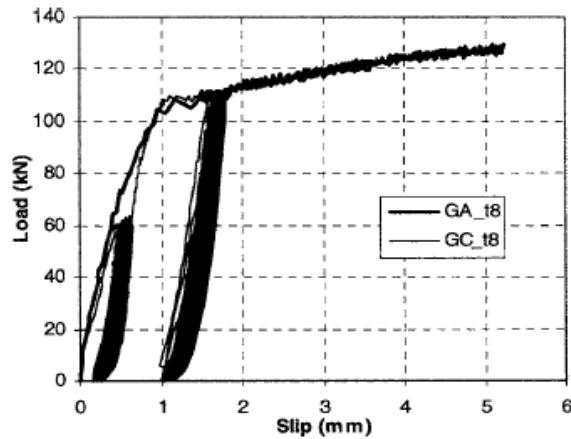


Figure 2.12 : Load slip of pullout test under cyclic loading (Yao et al., 2008)

Wang (2009) and Elghazouli (2009) investigated the complex connections such as the beam-column connection. Wang evaluated the hysteresis performance, failure modes, stiffness degradation, and energy dissipation of four cruciform beams to column connection under cyclic loading in order to investigate the seismic behaviour of blind bolted flush endplate joint. For 28 days, self consolidating concrete (SCC) was used with a compressive cube strength of approximately  $60 \text{ N/mm}^2$ . Under cyclic loading, all specimens displayed large rotation ductile capacities and the majority of failure modes were similar to those under monotonic loading, which were the bolt pullout away from the concrete wall, a longitudinal crack at the corner of the square tube wall, and an endplate inclined and deviated from the column wall (Wang et al., 2009).

Elghazouli (2009) carried out an investigation to find out the behaviour of the blind bolt connection under cyclic load using 17 open beam to tubular column semi-rigid angle connections (Figure 2.13). The cyclic system protocol based on the recommendation provided by ECCS (ECCS, 1986) is shown in Figure 2.14.

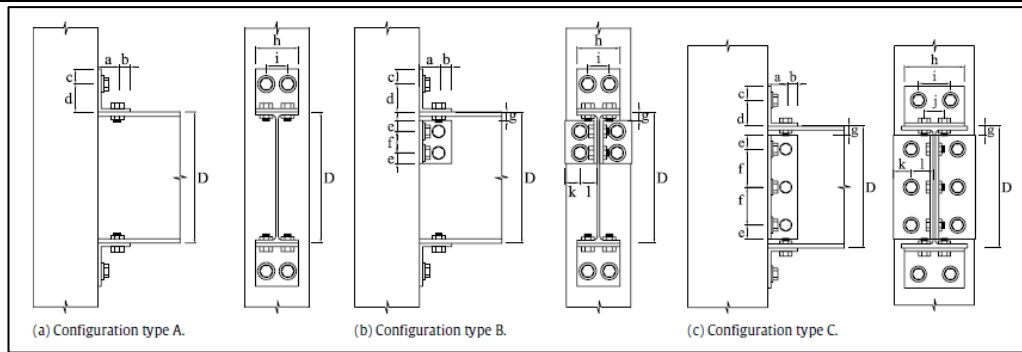


Figure 2.13 : Details of the connection configuration (Elghazouli et al., 2009)

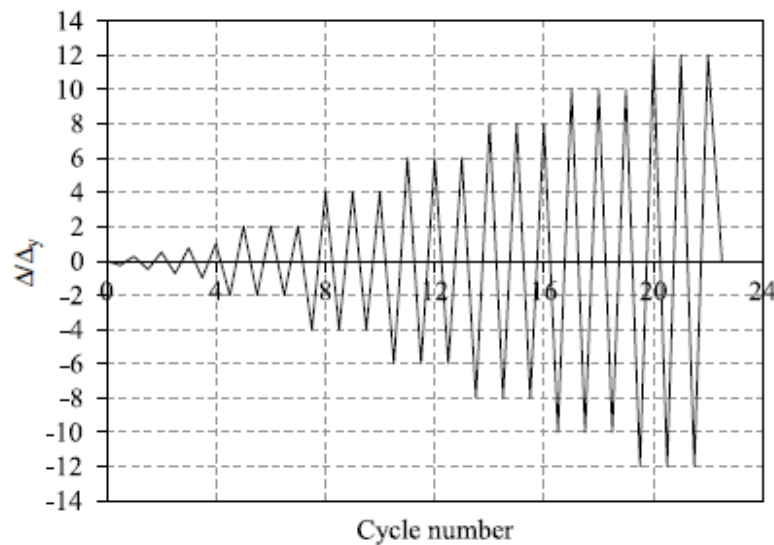


Figure 2.14: Loading protocol (ECCS, 1986)

The test results showed that, with typical design scenarios under cyclic loading, the connection provided a reasonable energy capability and rotational capacity above the required capacity. During the experiment, one of the tests (Figure 2.15) showed that a fracture due to low cycle fatigue occurred during the very last set of cycles at maximum amplitude, in comparison with tests, in which there was no sign of failure when rotation exceeded  $\pm 50$  mrad. However, no further test was conducted, and no further discussion was reported under fatigue load due to the fact that their study's aim was to investigate the behaviour under cyclic test or, specifically, under seismic load test.



Figure 2.15 : Top view of the fracture due to low cycle fatigue  
(Elghazouli et al., 2009)

### 2.3 Review of research in fatigue

Most recent studies describe the behaviour of the blind bolt when subjected to monotonic load or cyclic load. The process of accumulating damage and finally fracture due to cyclic loading is called fatigue. Fatigue load is primarily the type of loading which causes cyclic variations in the applied stress or strain. Fatigue load is categorised as one of the dynamic load groups and dynamic load is related with effectiveness of inertia and damping force. Repeated load or reversed load is the type of cyclic stress applied during the fatigue test. For many years, fatigue has been a significant and difficult problem for engineers, especially for those who design structures such as aircraft, bridges, pressure vessels, cranes, and so on (Sobczyk and Spencer, 1992).

Fatigue is the mechanism whereby cracks grow in a structure. Growth of cracks only occurs under fluctuating stress. Final failure generally occurs in the regions of tensile stress, when the reduced cross-section becomes insufficient to carry the peak load without rupture. While the loading on the structure is stationary, the crack does not grow under normal service temperatures. Many structures, such as building frames,

---

do not experience sufficient fluctuating stress to lead to fatigue problems. Other structures, however, such as bridges, cranes and offshore structures, where the live loading has a higher proportion in the total load experienced fatigue problems.

Since the 19<sup>th</sup> century, when the use of metals in engineering applications increased, it was widely accepted that metal components and structures subjected to repeated load cycles may lead to failure, although the metal components and structures were usually capable of bearing considerably larger loads if the loading were of a static nature. This type of failure, consisting of the formation of cracks under the action of varying loads, is known as fatigue (Ballio and Castiglioni, 1995). According to design standards, such as EC3 (BS EN1993, 2006) and ECCS (1985), fatigue is defined as the damage of a structural part by gradual crack propagation triggered by repeated stress.

The first systematic investigations of fatigue were carried out by Wohler in the 1850s and 60s. Wohler (1871) introduced the concept of fatigue with regards to welded connection, in order to classify material degradation or failure, which was proportional to the number of cycles of applied load. The concept is also known as the Wohler or S-N curve. Wohler or S-N curves (Figure 2.16) are usually applied in design procedures and serve as the design guidelines for welded connections, as stated in Eurocode 3 for fatigue resistance. The design guideline is based on nominal stress ranges and classified construction details. The S-N curve, otherwise known as the stress life method is the basic method for presenting fatigue failure in high cycles ( $N < 10^5$ ). This method implies that the stress level is relatively low and the deformation is in elastic range. These curves relate to the nominal stress range  $\Delta\sigma$ , resisting a certain number of applied loading cycles  $N$ . A log scale is always used for

$N$ . The stress is usually nominal stress and involves no adjustment for stress concentration. They are determined experimentally by means of fatigue tests performed under constant amplitude loading.

The fatigue resistance or fatigue strength of the structure, material, or component can be defined from the curves. The stress produces fatigue failure at a number of stress cycles equal to  $N$ , and the fatigue failure is expressed in terms of a pair of stress components, such as the stress amplitude and the mean stress, or as the maximum and the minimum stress. Further, the curve represents the fatigue life or the fatigue strength of the material, structure or component, where  $m$  is the slope of the curve.

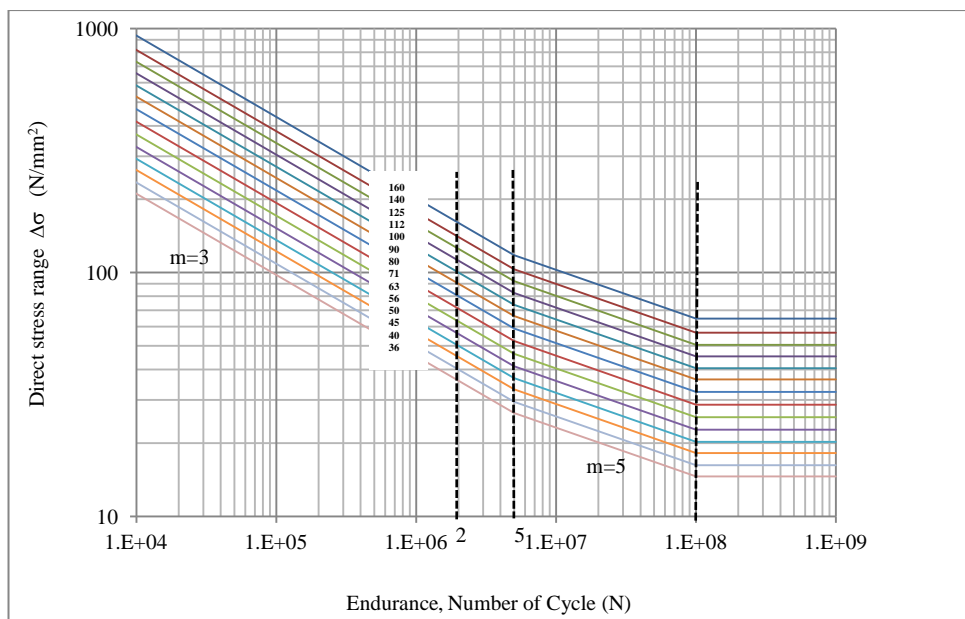


Figure 2.16 : S-N curves (BS EN1993, 2006)

Several factors can influence fatigue life, each resulting in a different S-N curve. The major factors, in order of importance, are as follows:

- 
- type of connection,
  - magnitude of stress executions or variations,
  - mean stress level, and
  - choice of material.

Other conditions, such as corrosive environments and extreme temperatures, also affect fatigue performance.

### 2.3.1 Fatigue load

Through stress analysis, the load spectrum can be defined by the stress range, the mean stress, and the stress sequence to which a detail is subjected. Given that this study considers only fatigue behaviour under constant amplitude stress, the effect of a stress sequence on the fatigue strength of a detail is not discussed. Meanwhile, constant-amplitude cyclic-stress fluctuation is the simplest of cycle histories (Barsom and Rolfe, 1999). This method has been proposed by various researchers in investigating the behaviour of the connection under fatigue load. Fatigue tests are normally carried out using constant stress amplitude for each test sample, because they are easy to do experimentally, and they serve as a straightforward method of presenting data. Constant amplitude can be represented by load (stress) range, mean stress ( $\sigma_m$ ), alternating stress or amplitude ( $\sigma_a$ ), and stress ratio. During a fatigue test, the applied stress conditions can be written as  $\sigma_m \pm \sigma_a$ , where  $\sigma_m$  is the static or mean stress, and  $\sigma_a$  is the alternating stress equal to half the stress range. Figure 2.17 shows the type of fatigue stress in the test. Alternating stress is considered when the applied load is subjected to compression and tension, whereas pulsating tension and fluctuating tension are subjected to tension.

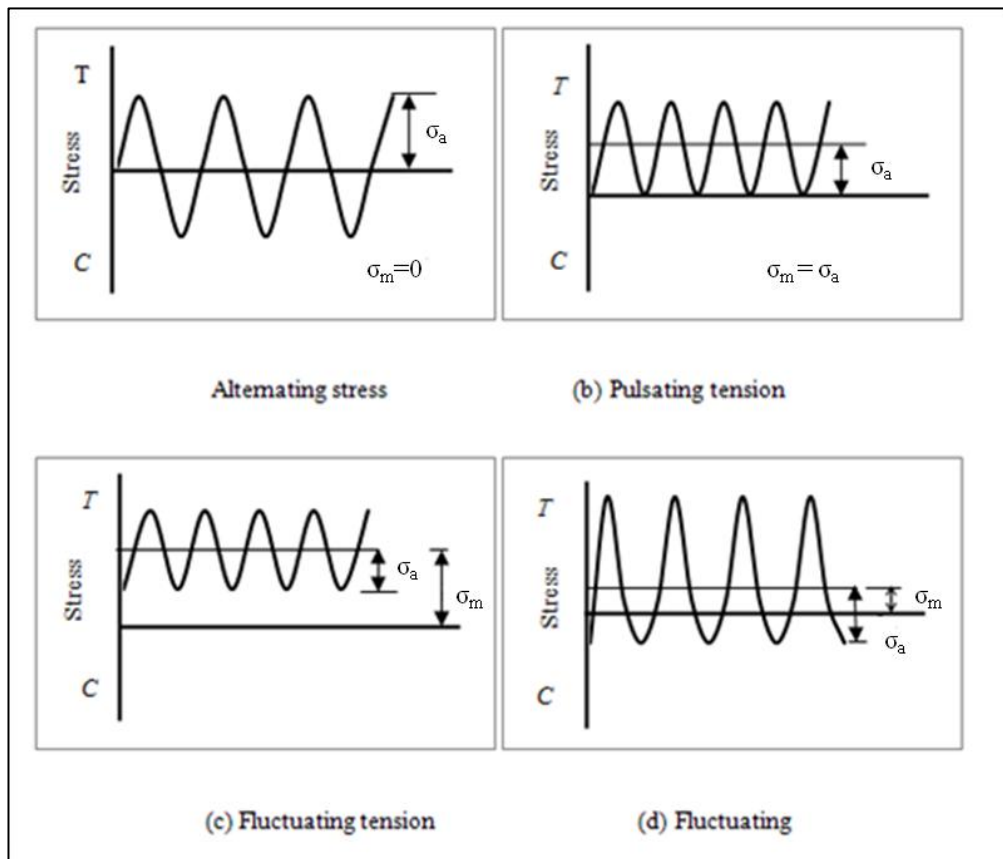


Figure 2.17 : Type of applied load (Gurney, 1979)

Fatigue load can be characterised as either high-cycle or low-cycle fatigue. High-cycle fatigue is generally used in many tests, where stress and strain are largely confined to the elastic region. It has been characterised by a large number of cycles with a nominal stress range in the elastic range  $\Delta\sigma$  or, in other words, low loading amplitude with a long fatigue life. For the high-cycle application, the stress-life (S-N) or total life method is widely used. High-cycle fatigue is associated with life greater than 100,000 cycles.

Typically, low-cycle fatigue tests are used to determine where significant plastic straining occurs. It involves large cycles with significant amounts of plastic deformation and a relatively short life. Low-cycle fatigue is typically associated with

fatigue life between 10 and 100,000 cycles. Table 2.1 provides a summary of the various possible formulations of fatigue analysis. Meanwhile Table 2.2 demonstrates the difference between high-cycle and low-cycle loading applied during the test.

Table 2.1 : Formulation of fatigue rules (Ioannis Vayas et al., 2003)

Structural response	Elastic – Inelastic		
Number of cycles to failure	$\sim 10^4$ to $10^8$	$\sim 10^2$ to $10^4$	$\sim 10^0$ to $10^2$
Fatigue curve for ranges of	Generalised forces	Generalised total deformation	Generalised inelastic deformations
Usual fields of application	Bridges, crane girders, chimneys, masts, and others	Slender plate girders, and others	Buildings under seismic loading

Table 2.2 : Comparison table for high cycle and low cycle

	<b>High-cycle fatigue</b>	<b>Low-cycle fatigue</b>
Amplitude	Stress is low and deformation is primary elastic	Stress is high enough for plastic deformation to occur; stress is less useful and the strain in the material offers a simple description.
Fatigue life	Associated with long life	Associated with short life
Amplitude condition	Should not exceed 1.5 times the yield stress to avoid alternating yielding (Ioannis Vayas et al., 2003)	Stress range concept is not valid and fatigue strength is determined more by strain range

---

Research on the effect and relationship of the fatigue loading type has been carried out (Birkemoe and Srinivasan, 1971, Ballio and Castiglioni, 1995, Plumier et al., 1998, Ghazali and Din, 2004, Birkemoe et al., 1969). The results show that high-cycle fatigue with a small decrease in stress causes a larger number of cycles, whereas a large stress range in low cycle fatigue gives fewer cycles. Thus, the test under low-cycle fatigue can be classified in the same way as the high-cycle fatigue.

Even so, using low-cycle fatigue can save testing time, especially in laboratories, but the existing information more commonly uses high-cycle fatigue. High-cycle fatigue failure initiates local damage due to repeated loads that, in turn, leads to the deformation of a small local crack. The extent of the fatigue crack is gradually increased by the sequence of load repetitions until the effective cross section is finally reduced, leading to catastrophic failure. However, this high-cycle fatigue only becomes a design problem when a large number of loading cycles involving tensile stress are likely to occur during the structure's design life (compressive stress does not cause fatigue). This is often the case for bridges, cranes, and structural support machinery wind and wave loading.

Another kind of fatigue load usually applied during the test is variable amplitude loading. This test is a complex function, in which there is an extremely small probability of the same sequence and the magnitude of stress range recurring at a particular time. Examples of this type of fatigue load histories include wind loading on aircraft, wave loading on ships, and offshore platform and truck loading on bridges.

---

### 2.3.2 Effect of mean stress or stress range

The dependent fatigue life on stress amplitude is represented on the S-N plot. Such data are taken for a constant mean stress,  $\sigma_m$ , often for reversed cycle situation ( $\sigma_m = 0$ ). However, mean stress also affects fatigue life, and its influence may be represented by a series of S-N curves, each measured at different  $\sigma_m$ . Increasing the mean stress level leads to a decrease in fatigue life. A previous study (Bouwman, 1979) investigated the effect of mean stress on the fatigue strength of untightened bolts by applying different minimum values to the system. The experiment results showed that the larger the amplitude, the smaller the number of cycles before fracture occurred. To prove the effect of the stress amplitude, Ballio (1995) and Ghazali (2004) carried out other experiments, in which they applied both low-cycle and high-cycle fatigue. Low-cycle fatigue gives a small number of cycles compared with high-cycle fatigue (Table 2.1), where the number of cycles produced from the testing was less than  $10^3$ .

The effect of the stress magnitude and stress ratio (*R-value*) on fatigue life is demonstrated in Figure 2.18, which shows that maximum tensile stress decreases from its ultimate static value  $f_u$  in an approximately linear fashion as  $N$ , the logarithm of the number of cycles, increases (Trahair et al., 2008).

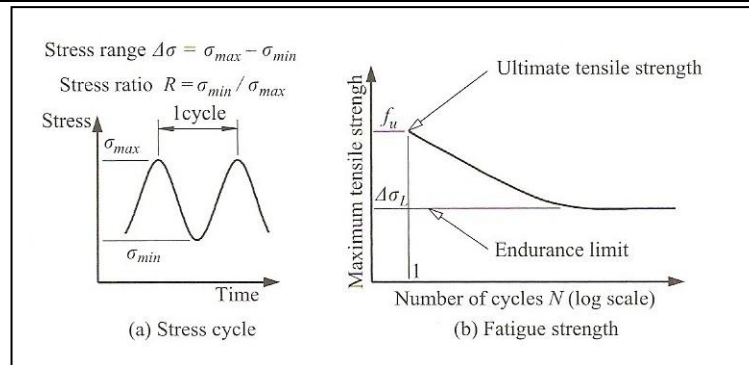


Figure 2.18 : Magnitude and stress ratio (Trahair et al., 2008)

### 2.3.3 Effect of frequency

Fatigue tests carried out in the laboratory are usually conducted at speeds between 3 Hz and 160Hz, depending on the type of specimen and equipment used. In actual structures, however, the frequency of loading may be significantly lower (Gurney, 1979).

There is evidence suggesting that testing at an extremely low frequency, which also implies testing with extremely high stress, tends to result in lower fatigue strength than corresponding tests at higher speeds, even without corrosion. This suggests that structures in service would tend to have lower fatigue strength than those related to similar laboratory-tested specimens.

A difference in frequency during the test may give a different number of cycles to failure, especially at a higher frequency. Furthermore, the difference became more evident when higher frequency was applied on the same stress value, as shown in Table 2.3 (R-Fujczak, 1994, Counts and Johnson, 2002). The bend specimens were tested for failure at different frequencies to examine the effect of fatigue loading frequency on the bending fatigue life of A723 steel. Comparison between 1.5 Hz and 15 Hz indicated slight improvements in fatigue life, but they were small and the

difference within the range was insufficient to be considered significant. However, frequencies from 30 Hz to 75Hz showed slightly larger differences: an average of 50% at 75 Hz compared with 30 Hz.

Table 2.3 : Bend fatigue data for four test loading frequencies (R-Fujczak, 1994)

Load frequency Hz	Stress Ksi (Mpa)	Cycles to failure
1.5	150 (1035)	15,131
	140 (966)	18,908
	100 (690)	112,285
15	150 (1035)	18,500
	140 (966)	25,700
	100 (690)	156,100
30	150 (1035)	58,000
75	140 (966)	210000

According to Counts (2002), frequency under 10 Hz does not greatly affect the fatigue life of Polymer matrix composites material (IM7/PETI-5). This was proven by experimenting with these materials at a temperature of 177 °C and R=0.1, with a difference in frequency at certain stress range (Figure 2.19). Although frequency below 10 Hz does not affect a component's fatigue life, caution is needed when assessing dynamic magnification effects where loading frequencies are close to one of the structure's natural frequencies.

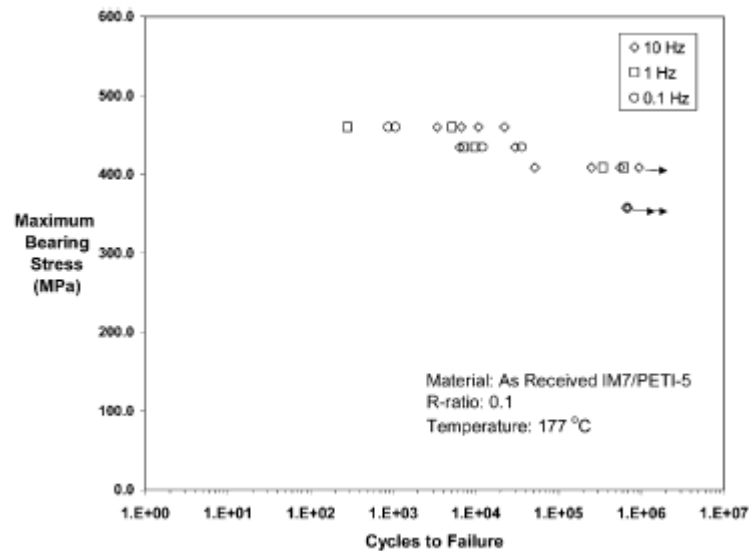


Figure 2.19 : Effect of frequency on the fatigue life of Polymer matrix composites (IM7/PET1) (Counts and Johnson, 2002)

#### 2.4 Review of research on the fatigue behaviour of bolted connections

Engineers specifying fasteners often base their requirements on tensile strength, yield strength, proof strength, or threaded stripping strength without considering fatigue and stress concentration. This lack of concern for fatigue is reflected in the standards for fasteners, which do not recognize the influence of fatigue or explicitly state that fatigue has not been considered (O'Brien and Metcalfe, 2009).

Hence, the type of connection used, together with a service loading that varies with time, is a factor influencing the fatigue life of joints (Ghazali and Din, 2004). The fatigue life of structural components is determined by the sum of the elapsed cycles required to initiate a fatigue crack and propagate the crack from subcritical dimensions to the critical size (Barsom and Rolfe, 1999).

---

### 2.4.1 Fatigue failure of bolts

In the fatigue failure of a threaded bolt, the threads act as a notch, leading to a high stress concentration at the root of the threads. At a location where two threads meet, i.e., at the thread runout, and at the point where the thread and the nut first engage, the stress concentrations can be even higher. The bolt head-shank transition is also a site of stress concentration. For bolted connections, there are basically three locations where a fatigue crack can be initiated in an axially loaded bolt-nut system, as shown in Figure 2.20. These are:

- a) head-shank transition,
- b) thread runout, and
- c) thread at nut.

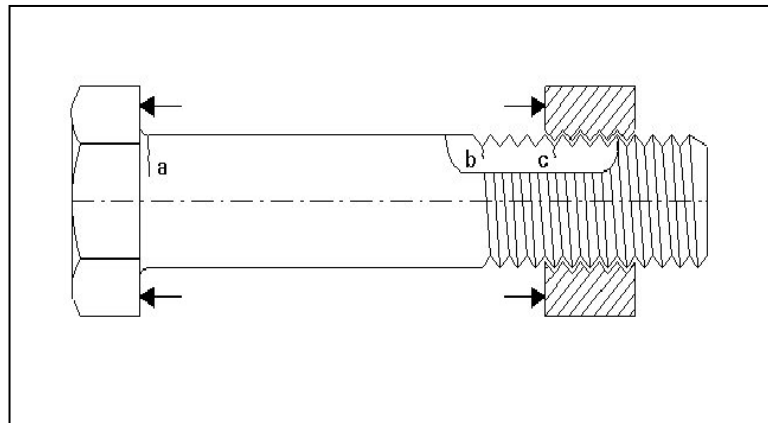


Figure 2.20 : Bolt fatigue failure (ESDEP, 2011)

In standard bolts, the radius at the bolt-head shank transition is usually large enough to prevent fatigue cracks at this point. If fatigue cracks occur, they are located at the first engagement of the threads of the bolt and the nut, as illustrated at point c in Figure 2.20. This is due to the load transfer from nut to bolt. The contacting thread faces of the bolt and the nut result in extra bending stresses in the threads. Furthermore, the load becomes unevenly distributed between the contacting faces of

---

the bolt and the nut, with the stress being higher at the first thread of engagement. Certainly, this depends on the thread form, pitch, and difference in Young's modulus where different materials are used. The load transfer can be more uniform via the plastic deformation of the bolt.

Failure of material due to fatigue can be viewed at a microscopic level, and can be investigated in three steps detailed below.

- **Crack initiation:** The initial crack occurs at this stage due to surface scratches and flaws from the handling or tooling of the material, thread (as in the bolt screw), slip bands, or dislocation intersecting the surface resulting from previous cyclic loading or work hardening.
- **Crack propagation:** The crack continues to grow at this stage due to continuously applied stress.
- **Failure:** This occurs when the material that has not been affected by the crack can no longer withstand the applied stress. This stage occurs quickly.

Fatigue failure can also be identified by examining the fracture. A fatigue fracture has two distinct regions: one is smooth or burnished due to the rubbing of the bottom and the top of the crack as it grows, and the second is granular due to the material's rapid failure (Figure 2.21).

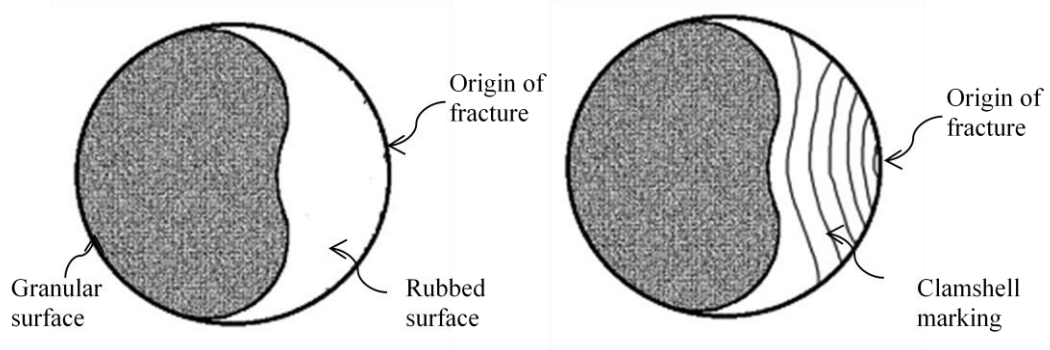


Figure 2.21 : Fatigue fracture (marinediesels.co.uk)

Other characteristics of fatigue fracture are beachmarks and striations. Beachmarks or clamshell marks may be seen in fracture failures of materials that have been used for a certain period, allowed to rest for an equivalent period, and loaded again as in factory usage. Striation, which can be observed through a microscope, is regarded as a step in crack propagation, where the distance depends on the stress range. Beachmarks may contain thousands of striations as shown below.



Figure 2.22 : Magnification of fatigue failure showing striations (marinediesels.co.uk)

The fracture surface of bolts can also be investigated using photography. A previous research (Hobbs et al., 2000) on the effect of eccentric loading on the fatigue performance of high-tensile bolts showed a different result of the load effect. With

---

axial load, it was demonstrated that the crack in the higher mean stress was more akin to a crescent throughout its life (Figure 2.23).

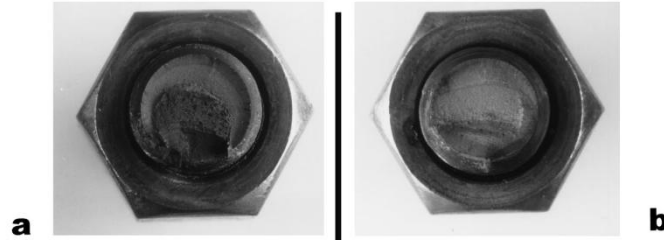


Figure 2.23 : Fracture failure for bolts loaded axially with a mean stress of 584 MPa (a) and 250 MPa (b) (Hobbs et al., 2000)

Figure 2.24 shows the crack shape resulting from the application of eccentric loading, with (c) as the bolt loaded with the eccentricity  $e/D = 0.33$  and (d) as the bolt with the eccentricity of  $e/D = 0.008$ . The global stress amplitude for both bolts loaded with eccentricity decreases from 110 Mpa (top) to 80 MPa (bottom). It can be concluded that the eccentricity level applied on the bolt does not significantly affect the fatigue crack's shape. However, the mean stress level does not have an effect on the shape of fatigue cracks, with the crack front lengthening or broadening around the circumference of the helix as the mean stress increases.

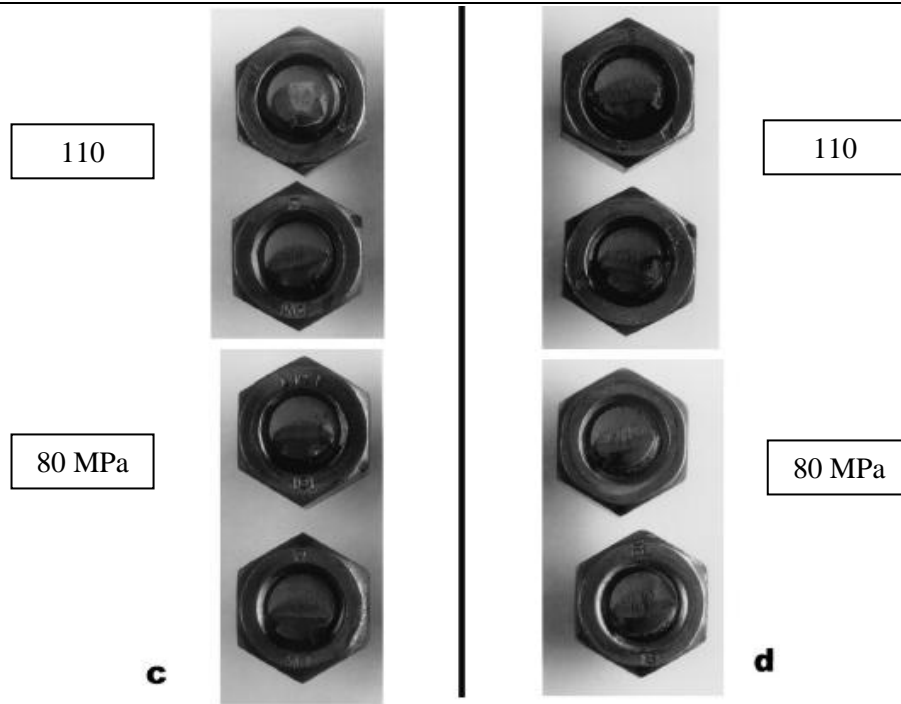


Figure 2.24 : Crack shapes of eccentric loadings (Hobbs et al., 2000)

#### 2.4.2 Fatigue life of the bolt

Fatigue life refers to the number of applications of a given stress, to which a metal sample can be subjected before failing. Fatigue life can be determined through experimental or numerical analysis. The importance of being able to predict the fatigue life of structures was highlighted by the failure of a Norwegian semi-submersible drilling rig, in which a fatigue crack resulted in the death of 123 people in 1980 (Norwegian public commission, 1981).

Several methods have been used in determining the fatigue life of materials and structures. Of these, two models are usually employed to predict fatigue life: the S-N model and the fracture mechanics model.

A conventional model that can predict fatigue life, the S-N model has been widely used by researchers, such as Birkemoe (1971) and Bouwman (1979). The characteristic S-N approach assumes that fatigue damage accumulation is a linear

phenomenon, in accordance with the Miner's rule (Ayyub et al., 2002). This rule states that total fatigue life under various stress ranges refers to the weighted sum of the individual life at a constant stress  $S$ , as given by the S-N curves, each being weighted according to fractional exposure to that level of stress range (Hughes, 1998). Upon crack initiation, cracks propagate based on the fracture mechanics concept (Figure 2.25).

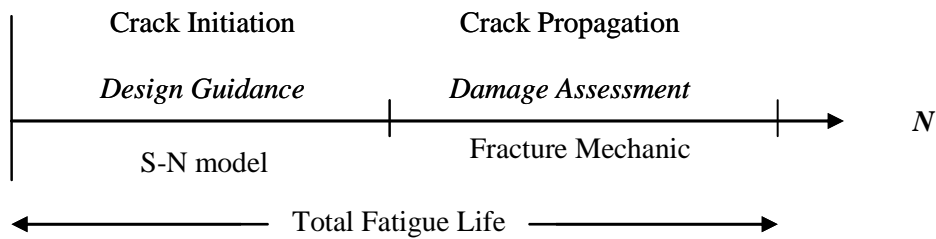


Figure 2.25 : Comparison between the S-N and Fracture Mechanics models

The S-N curves represent the results from the constant cycle fatigue tests conducted to evaluate the fatigue behaviour of different types of structural details. The S-N curve is often presented as a straight line on log-log paper (Figure 2.16). The basic equation to represent the S-N curve is given by:

$$N = \frac{A}{S^m} \quad , \quad \text{Equation 2-1}$$

where  $N$  is the number of cycles to fatigue initiation (failure),  $A$  is the intercept of the S-N curve (with  $S$  being equal to 1),  $S$  is the constant amplitude stress range at  $N$ , and  $m$  is the slope of the S-N curve. Equation 2-1 can also be expressed as:

$$\log N = \log A - m \log S \quad , \quad \text{Equation 2-2}$$

where  $\log$  is to base 10. In general, a least squares analysis of  $\log N$  given  $S$  is used to produce the S-N curve.

Meanwhile, the fracture mechanics model is based on crack growth data. This model was first used by Youngwoo (2007) and Korin (2010) to predict fatigue life of bolts, where variable fatigue load was applied. Estimating fatigue life under variable or random fatigue load usually involved the use of the Fracture Mechanics model (Wirsching, 1998, Tamboli, 1999). This more detailed model examines crack growth and determines the number of load cycles needed for a small initial defect to grow into cracks that are large enough to cause a fracture. In this model, the growth rate is proportional to the stress range, and is expressed in terms of a stress intensity factor  $K$ , which accounts for the magnitude of stress, current crack size, and joint details. The basic equation governing crack growth is given by:

$$\frac{da}{dN} = C\Delta K^m, \quad \text{Equation 2-3}$$

where  $a$  is crack size,  $N$  is the number of fatigue cycle,  $\Delta K$  is the range of stress intensity factor, and  $C$  and  $m$  are the crack propagation parameters derived from fracture mechanics. From the fracture mechanics model, the S-N curve can also be plotted (Figure 2.26).

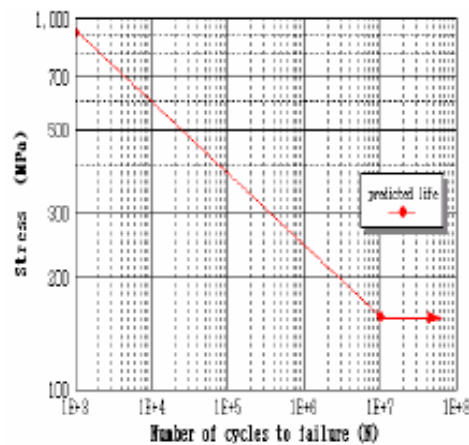


Figure 2.26 : Predicted S-N curve using a modified Fracture Mechanics model  
(Youngwoo Choi et al., 2007)

### 2.4.3 S-N Model

The S-N model is the traditional concept applied in evaluating fatigue life under constant amplitude. In Europe, the fatigue assessment for bolts can be carried out according to EC3. Miscellaneous construction details are dealt with in the Civil Engineering standard EC3, Parts 1 to 9. In EC3, the relevant S-N curve for bolts is classified under category 50. However, test results of some experiments showed that it can be placed at a higher classification. Figure 2.27 from Birkemoe (1971) shows that the connection is stronger or has higher fatigue strength. In the test, two types of loading were applied, namely, tension (T) and compression-tension (C-T). Table 2.4 provides the details of the sample.

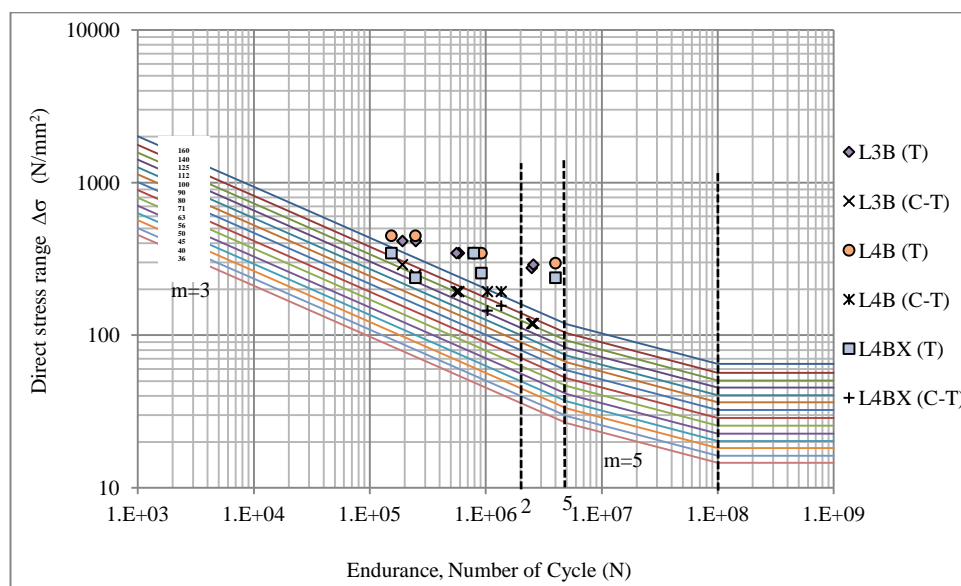


Figure 2.27 : Bolted S-N curve

Table 2.4 : Details of the connections tested by Birkemoe (1971)

Sample	Bolt grade	Steel Grade	Type of load	Other details
L3B	Four bolts of A325	A440	T	-
L3B	Four bolts of A325	A440	C-T	-
L4B	Three bolts of A490	A440	T	-
L4B	Three bolts of A490	A440	C-T	-
L4BX	Three bolts of A490	A440	T	Variation of joint efficiency
L4BX	Three bolts of A490	A440	C-T	

From the figure above, it can be summarized that a bolt under fatigue load can be categorised above class 50, which has greater fatigue resistance. This was also proven by Schaumann (2009) who classified bolts with larger diameters under EC3, indicating that the classification of 50 was for a bolt with a diameter less than 35 mm. Figure 2.28 illustrates that all test results lie above the reduced detail category 50 of EC3. Furthermore, using bolts M48 10.9 HV, with 200 kN applied preload and 60 Hz frequency, a statistical evaluation was calculated, indicating that the survival probability of the stress levels were 97.7%. Based on EC3, this confirmed that the reduced detail category 50 was sufficient for high-strength bolts.

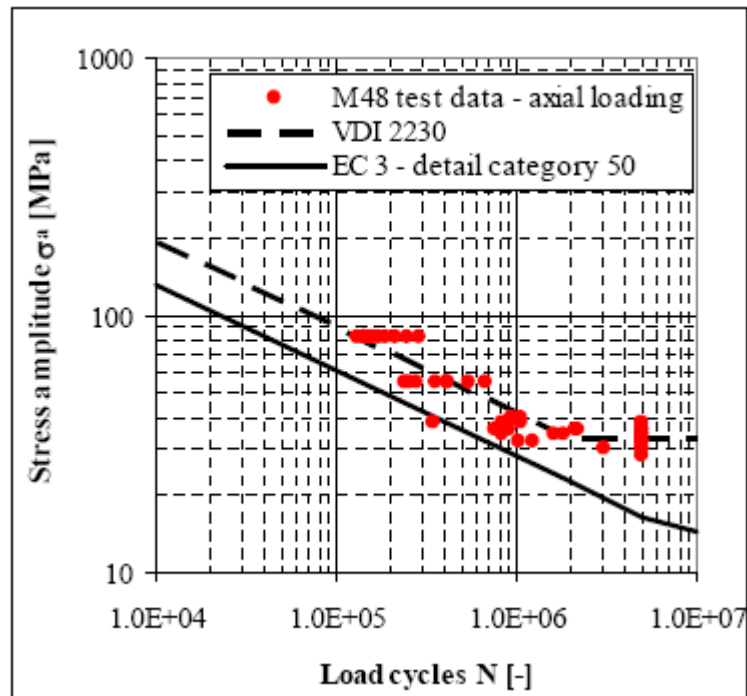


Figure 2.28 : Comparison between scatter band of test and normative S-N curve (Schaumann and Marten, 2009)

It is evident from both experiments that the classification of the EC3 Parts 1-9 (2006) is applicable to the lower fatigue strength classification of the M48 bolt.

## 2.5 Concluding remarks

Based on the discussion of previous and current research on blind bolts and on the fatigue life of bolted connections, the main concluding points are made below.

- The blind bolt is a system that can be used in applications where access installation is done from one side of the connection. The bolt can be installed even by an unskilled technician, implying easy installation.
- The Hollobolt is one of the available blind bolts. Its performance in the hollow section shows less stiffness compared with the standard bolt where deformation of the hollow section occurs. A concrete infill

---

prevents the tube face from bending. Moreover, using a thicker tube wall increases the connection's stiffness.

- A concrete filled tube has excellent structural properties that provide an interaction between the steel tube and the concrete and fire resistance.
- The Extended Hollobolt is a modification of the standard Hollobolt. It is characterised by greater stiffness and strength. Previous studies have shown that by adding anchorage, the blind bolt improves the connection's behaviour because the load can be shared between the tube wall and the anchorage.
- Fatigue is a critical factor, because most structural components are subjected to repeated loads, whose magnitudes are below the fracture load under monotonic loading.
- Based on previous research, load applied at a frequency below 10 Hz does not affect a bolted connection's fatigue life.
- Fatigue life can be predicted using the S-N model and the Fracture Mechanics model. Selecting which model to use depends on the type of fatigue load applied. Specifically, the S-N model can be used for constant loads, whereas the fracture model can be used for variable or random loads.
- Greater focus has been given to the fatigue of welded connections, which has been adopted in many design recommendations, such as EC3, ECC3, and ASTM. In EC3, the fatigue of the bolt has been categorised as class 50 (stress range = 50 N/mm<sup>2</sup>) with a fatigue life of 2 million cycles.

- 
- Extensive design guidance exists for the fatigue life of weld details. However, limited information is available for bolted configurations, because the fatigue of bolts is not considered as critical as the fatigue of welds.

## 2.6 Future research directions

The following are areas that may require further research:

- Cyclic tests of blind bolt connections have been conducted using different types of blind bolts, such as the Hollobolt, the Ajax blind bolt, and the Flowdrill. These tests have demonstrated reliable behaviours of these bolts in concrete filled tubes, but no similar tests have been conducted for fatigue type loading. Furthermore, limited exploratory work with no firm endorsement exists for the low-cycle fatigue of the standard Hollobolt.
- The Extended Hollobolt to concrete filled tube demonstrated more reliable behaviour than the standard Hollobolt. However, there is insufficient knowledge about Extended Hollobolt fatigue that is comparable to the EC3 fatigue assessment. Thus, the Extended Hollobolt's fatigue behaviour must be tested to further investigate its behaviour under repeated loads.

---

## Chapter 3 : Experimental Work

---

### 3.1 Introduction

This research uses experimental work to investigate the behaviour of blind bolt connections. Fatigue testing is conducted to determine fatigue life and failure mode when subjected to a prescribed sequence of stress amplitude (Weibull, 1961). In the course of this research, a series of blind-bolt-to-column-joint tests is conducted to investigate the behaviour of blind bolts when subjected to repeated loads. This chapter describes the details of the experimental program, including materials used, test setup, and test procedure.

### 3.2 Overview of Fatigue Testing

Previous study shows the HB has a higher shear capacity than standard bolts due to its larger shear area, which is a result of the bolt area being expanded to the area of the sleeve of the HB ( Sean Ellison, 2004). Load is applied directly to the shank of the bolt, making the area to which the tension load is applied difficult to predict. Therefore, loading the bolt in tension is the most appropriate method when investigating EHB behaviour in a moment connection. In the current study's tests, the EHB was connected to a concrete-filled hollow section using a thick plate further connected to the load cell. Figure 3.1 illustrates the test arrangement. The following sections describe the materials and the test setup.

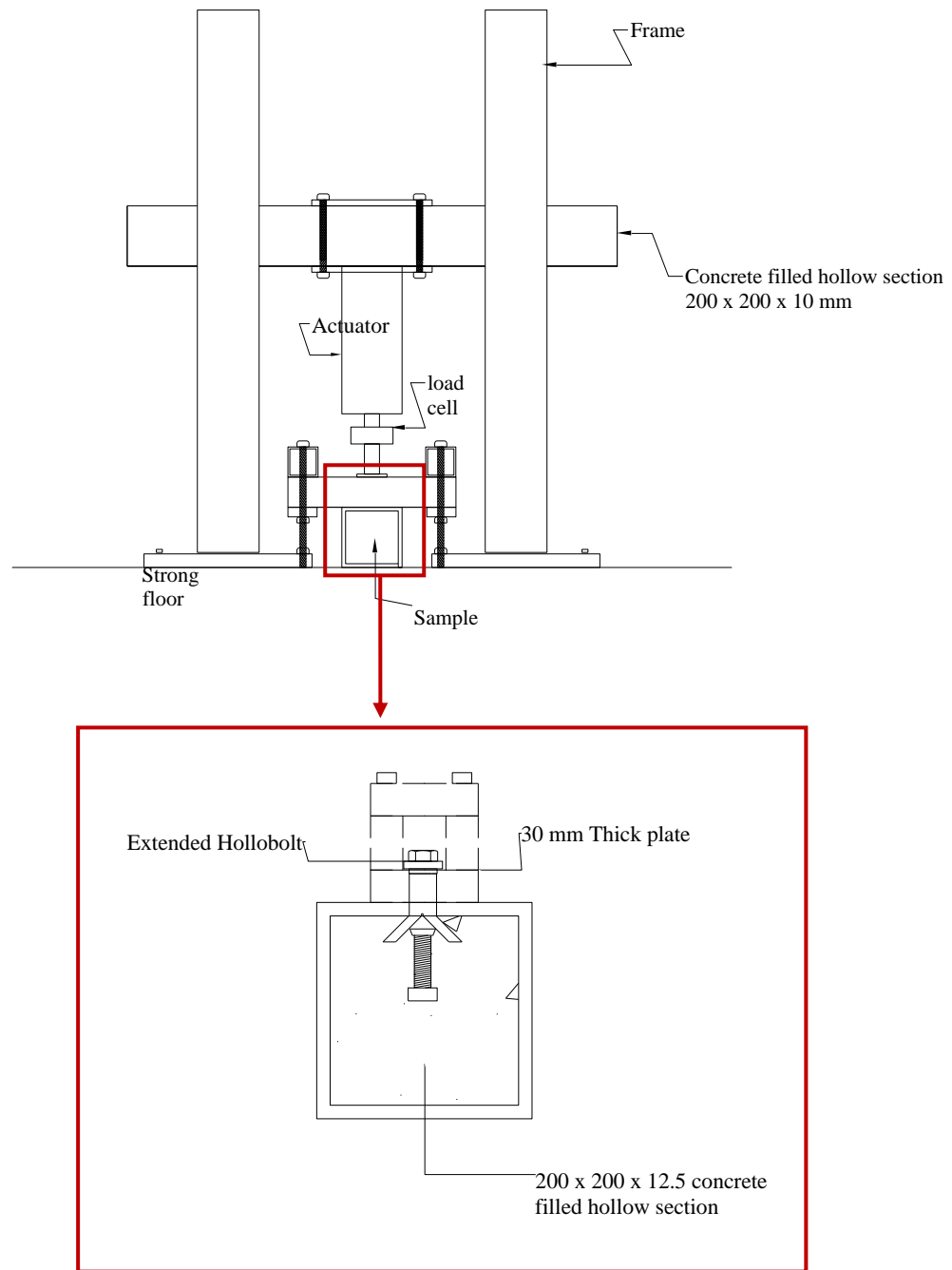


Figure 3.1 : Illustration of EHB fatigue test.

### 3.2.1 Hollow section material

For the purposes of this research, the “thick plate and hollow section” configuration was selected to eliminate the effects of tube face bending and plate bending during the experiment. A Grade S355 concrete-filled tube having dimensions of  $200 \times 200 \times$

12.5 was used in the experiment (Figure 3.2). A 12.5 mm hollow section was used to eliminate the flexibility,  $B/t$  (where  $B$  is width of tube section and  $t$  is thickness of tube wall), in the tube wall and tube face (Al-Mughairi, 2009). The steel tube was connected to the blind bolt using a 30 mm thick plate.

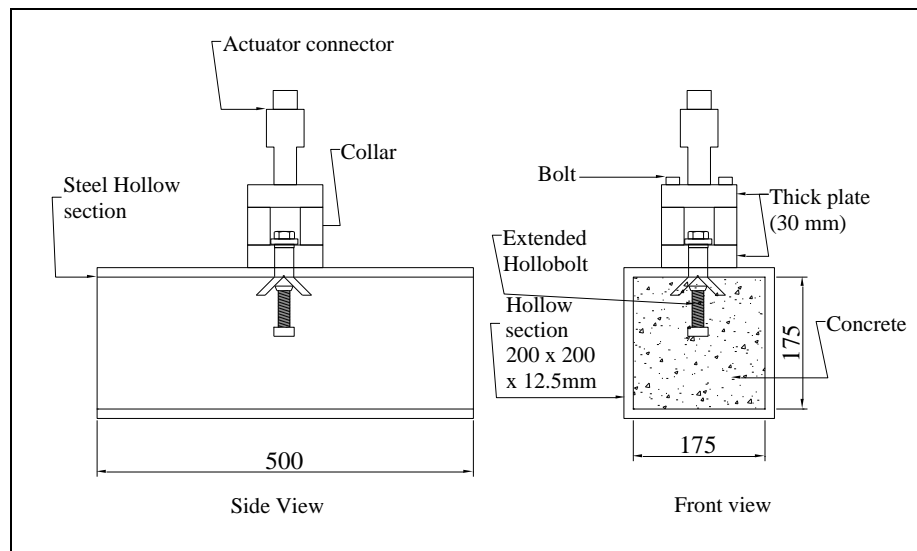


Figure 3.2 : Test arrangement

A hollow section was initially used; however, this was later replaced due to lack of availability. Therefore, a rig was prepared to complete the fatigue test, as shown in Figure 3.3.

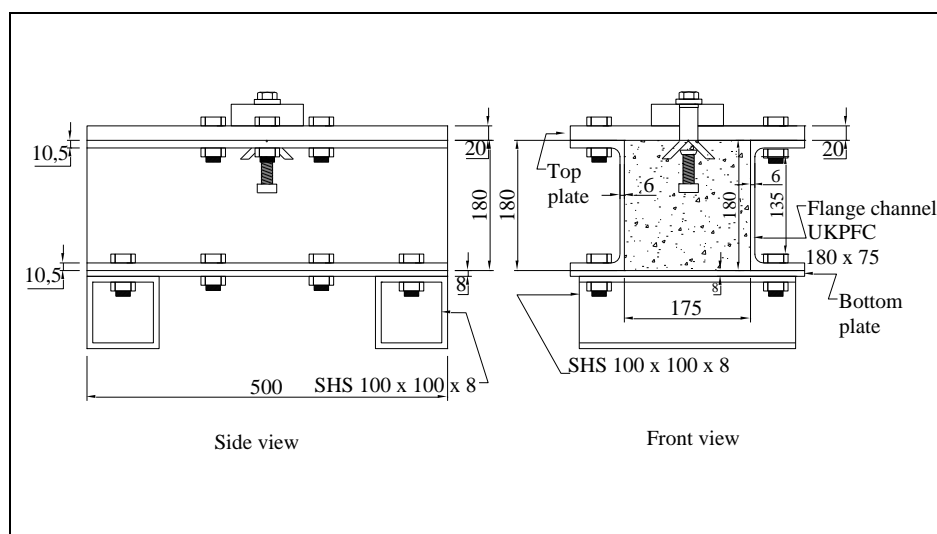


Figure 3.3 : Test arrangement using Rig assembly

---

The steel rig was used repeatedly for the bolt-fatigue testing. Thus, a 20 mm thick top plate was used to avoid deformation. Other component choices, such as plate thickness for the connection between bolt and top plate, were similar to those in the hollow section setup.

### 3.2.2 Bolts

Three types of Grade 8.8 bolts were used: a standard bolt, a standard HB, and an EHB (Figure 3.4). The fatigue lives of the standard M16 bolt and standard HB were determined for comparison with that of the EHB. The standard HB and standard M16 bolts were selected because under static loads, standard HB exhibit less strength and stiffness compared to EHB, whereas standard bolts exhibit more strength and stiffness than EHB under the same conditions.



Figure 3.4 : Types of bolts for the fatigue test

All the bolts were tightened by applying 190 Nm torque, as proposed by Lindapter (2011). The dimensions of the bolts, such as length and shank diameter, were measured, and the measurements were used to calculate the actual dimensions of the material for data analysis.

Figure 3.5 to Figure 3.7 present the actual dimensions of the EHB, the standard HB, and the standard M16 bolt. The dimensions of each bolt, such as outer and inner diameters, were used to determine the actual stress range value. The outer and inner diameters of the bolt shank were measured using shadowgraph and validated using a point micrometer. Shadowgraph is the optical system that enables to measure the part to a higher degree of accuracy.

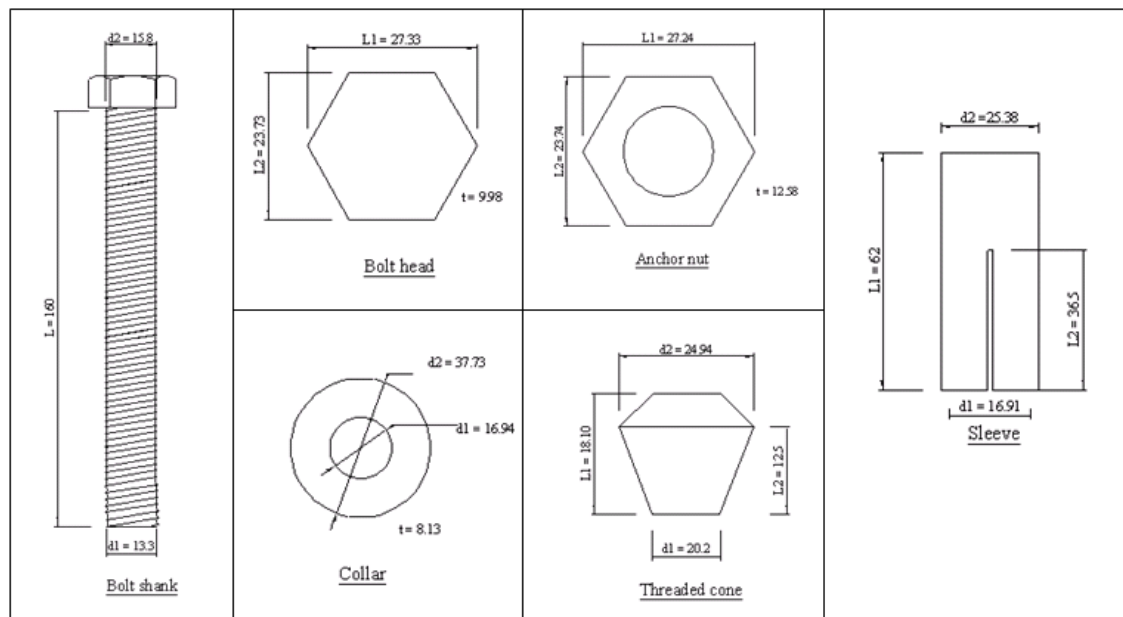


Figure 3.5: Actual dimensions of the EHB (all measurements in mm)

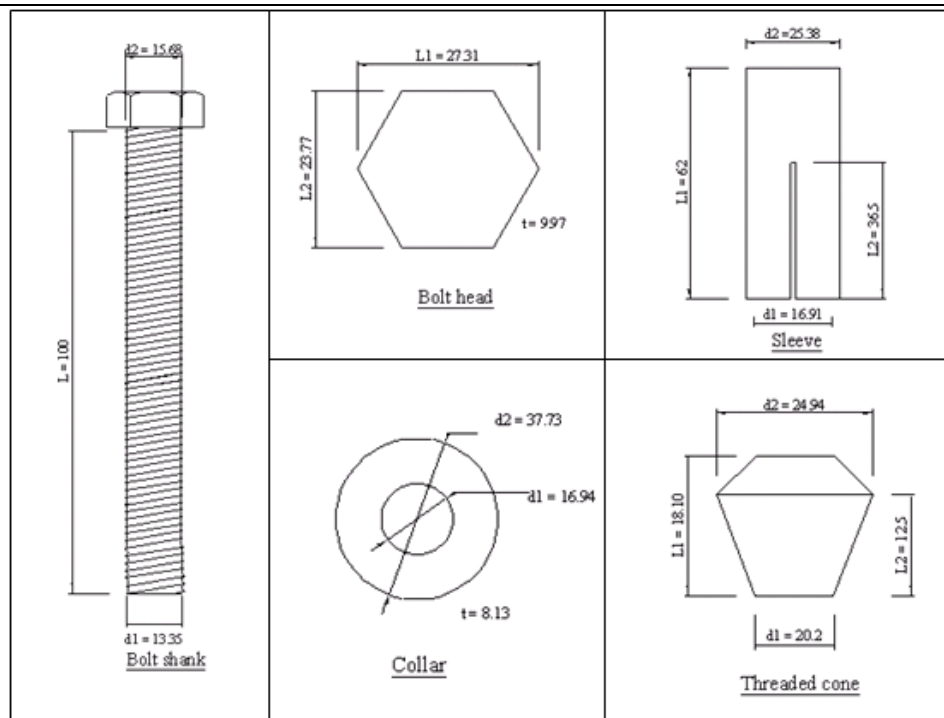


Figure 3.6 : Actual dimensions of the HB (all measurements in mm)

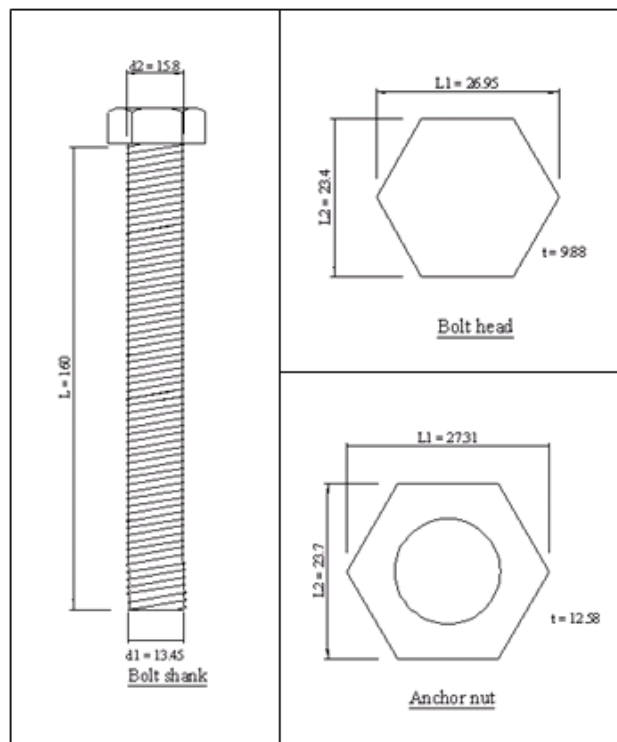


Figure 3.7 : Actual dimensions of the standard M16 bolt (all dimensions in mm)

---

### 3.2.3 Concrete material

Concrete with 40 N/mm<sup>2</sup> strength was used for the fatigue test. The mix was designed for early strength, thereby ensuring reliable results after only seven days of curing. This situation would probably not be the case in real life; however, due to limited time and resources, this approach was deemed the best. Concrete with strength of 60 N/mm<sup>2</sup> was also used to compare the effects of concrete strength on the fatigue life of the EHB.

Table 3.1 : Sample experimental work specimen details

Bolt type	Bolt Grade	Concrete design strength at Day 7 N/mm <sup>2</sup>
Extended Hollobolt	8.8	40
Extended Hollobolt	8.8	60
Standard bolt	8.8	40
Standard Hollobolt	8.8	40

### 3.3 Material geometries

This section discusses the mechanical and material properties of the components used, including stress–strain relationship, yield stress, Young’s modulus, and ultimate strength, as well as the methods used to measure these properties. Cube compressive tests were performed to determine the compressive strength of the concrete.

### 3.3.1 Hollow section

The mechanical properties of the hollow section used in the early stages of the experiment were determined using coupon tensile tests. The geometry of the coupon pieces was specified according to the EN 10002-1:2001 Annex D (BS EN, 2001), as shown in Figure 3.8.

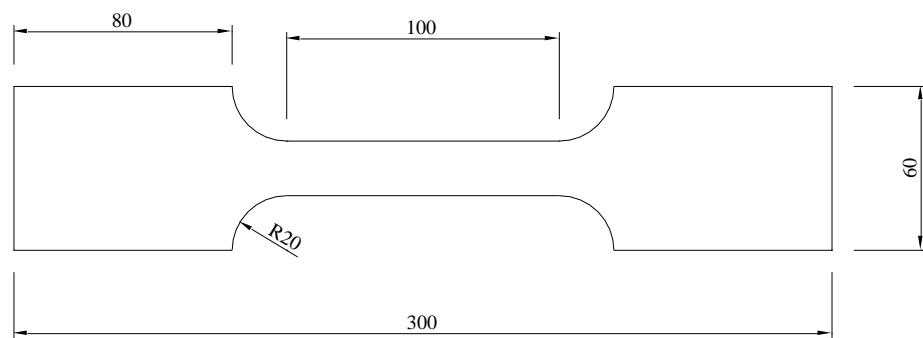


Figure 3.8 : Coupon piece dimensions

The hollow section's yield strength, Young's modulus, and ultimate tensile strength are summarized in Table 3.2.

Table 3.2 : Material properties of the hollow section

Hollow section	Yield strength N/mm <sup>2</sup>	Ultimate Tensile strength N/mm <sup>2</sup>	Young's Modulus kN/mm <sup>2</sup>
200 × 200 × 12.5	393.404	501.076	205.174

### 3.3.2 Bolts

Tensile tests were conducted to determine the mechanical properties of the bolts. According to BS EN ISO 898-1: 2009, two different tests as shown in Figure 3.9

(i.e., full bolt and machining bolt tests) should be run to determine the mechanical properties of a bolt (Table 3.3).

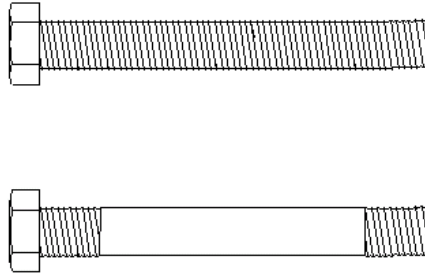


Figure 3.9 : Bolt tensile test specimens

The actual yield strengths and tensile strengths of the bolts were defined using the stress strain graph in Figure 3.10 and summarized in Table 3.3 and Table 3.4.

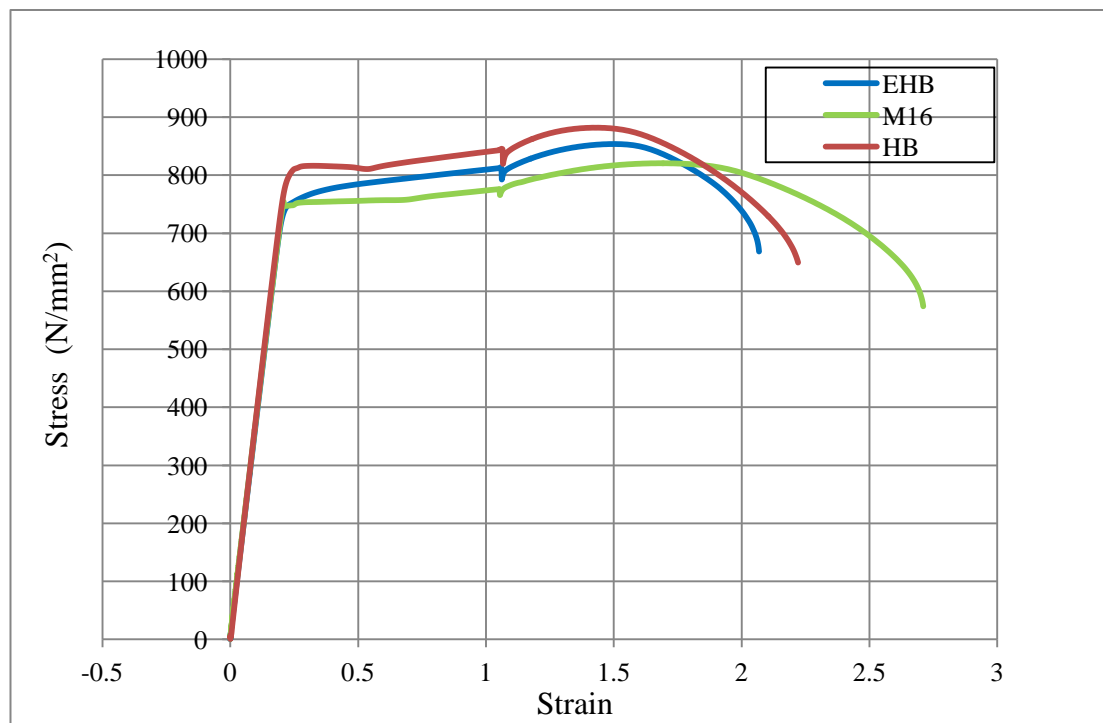


Figure 3.10 : Bolt Stress – Strain curve (Machined)

Table 3.3 : Mechanical properties of the bolts (machined)

	<b>Ultimate load (kN)</b>	<b>Yield stress (N/mm<sup>2</sup>)</b>	<b>Ultimate tensile stress (N/mm<sup>2</sup>)</b>	<b>Young's modulus (N/mm<sup>2</sup>)</b>
Extended Hollobolt (EHB) (Grade 8.8)	131.082	813.197	852.39	204.701
Standard Bolt (M16) (Grade 8.8)	128.461	851.353	925.923	208.115
Hollobolt (HB) (Grade 8.8)	135.894	816.025	967.132	209.444

Table 3.4 : Mechanical properties of the bolts (full size)

	<b>Ultimate load (kN)</b>	<b>Yield stress (N/mm<sup>2</sup>)</b>	<b>Ultimate tensile stress (N/mm<sup>2</sup>)</b>	<b>Young's modulus (N/mm<sup>2</sup>)</b>
Extended Hollobolt (EHB) (Grade 8.8)	146.247	859.288	948.855	204.095
Standard Bolt(M16) (Grade 8.8)	139.551	806.241	891.415	190.461
Hollobolt (HB) (Grade 8.8)	149.064	946.841	967.132	174.644

### 3.3.3 Properties of concrete

Concrete samples with compressive cube strengths of approximately and 60 N/mm<sup>2</sup> were used after seven days of curing. The mixes of concrete were as shown in Table 3.5. Concrete strength was determined using standard cube tests. Cube strength was recorded on Day 7, the day of testing, and Days 14 and 28.

Table 3.5 : Concrete Mix

Concrete strength	Cement kg/m <sup>3</sup>	Coarse aggregate Kg/m <sup>3</sup>	Water Kg/m <sup>3</sup>	Fine aggregate Kg/m <sup>3</sup>
C40	440	1020	210	735
C60	570	826	206	753

Table 3.6 : Concrete strength of the Extended Hollobolt (EHB C40)

Sample No.	Input load range (kN)	Concrete strength (N/mm <sup>2</sup> )			
		Day 7	Test day	Day 14	Day 28
S1	90	35.80	35.80	41.70	46.30
S2	70	38.85	35.85	40.55	47.40
S3	45	40.00	40.00	45.56	50.63
S4	90	39.50	42.50	44.20	50.10
S5	60	40.00	40.00	45.10	49.80
S6	50	39.80	43.55	47.20	51.67
S7	45	39.33	39.33	43.45	48.00
S8	70	38.90	40.96	43.60	48.70
S9	70	38.90	40.96	43.60	48.70
S10	70	38.70	38.70	-	-
S11	70	41.00	41.00	46.90	51.10
S12	70	41.00	41.00	46.80	51.50

Sample No.	Input load range (kN)	Concrete strength (N/mm <sup>2</sup> )			
		Day 7	Test day	Day 14	Day 28
S13	45	38.70	38.70	46.20	49.70
S14	60	37.40	37.40	41.70	47.40
S15	50	37.40	37.40	41.70	47.40
S16	50	40.90	40.90	45.20	51.23
S17	50	40.90	40.90	45.20	51.23
S18	60	41.90	41.90	48.60	52.20
S19	60	41.80	41.80	49.15	51.77
S20	60	41.80	42.50	49.15	51.77
S21	60	40.25	40.25	46.53	51.83
S22	60	40.25	41.15	46.53	51.83
S23	90	40.30	40.30	43.43	50.27
S24	90	40.30	40.30	43.43	50.27
S25	60	38.40	39.25	-	48.20
S27	60	37.60	37.60	43.70	47.67
S28	45	37.60	38.50	43.70	47.67
S29	45	38.10	38.10	43.30	47.23
S33	50	41.22	41.22	45.33	50.55
S34	50	41.22	42.67	45.33	50.55

Table 3.7 : Concrete strength of the standard M16 bolt

Sample No.	Input load range (kN)	Concrete strength (N/mm <sup>2</sup> )			
		Day 7	Test day	Day 14	Day 28
B1	90	36.90	36.90	42.5	46.35
B2	90	36.90	36.90	42.5	46.35
B3	90	39.40	39.40	40.5	46.03
B4	70	36.80	36.80	40.5	46.03
B5	70	36.80	38.17	43.45	47.93
B6	70	39.40	39.40	43.45	47.93
B10	80	39.30	41.87	-	48.34
B11	80	39.30	41.87	-	48.34
B12	80	41.22	41.22	45.33	50.55
B13	80	41.22	41.22	45.33	50.55

Table 3.8 : Concrete strength of the standard HB

Sample No	Input load range (kN)	Concrete strength (N/mm <sup>2</sup> )			
		Day 7	Test day	Day 14	Day 28
C1	90	38.00	38.00	43.30	47.23
C2	90	38.00	38.00	43.30	47.23
C3	70	38.80	38.80	41.05	47.40
C4	70	38.80	38.80	43.10	47.40
C5	60	38.80	38.80	43.10	48.45
C6	60	38.80	38.80	43.10	48.45
C7	50	39.30	39.30	45.10	47.80
C8	50	39.30	39.30	45.00	47.80
C9	50	39.75	39.75	45.00	48.97
C10	50	39.75	39.75	45.00	48.97

Table 3.9 : Concrete strength of the Extended Hollobolt (EHB C60)

Sample No	Input load range (kN)	Concrete strength (N/mm <sup>2</sup> )			
		Day 7	Test day	Day 14	Day 28
D1	90	64.50	64.50	69.50	74.33
D2	90	64.50	64.50	69.50	74.33
D3	70	59.80	59.80	64.50	68.77
D4	70	59.80	59.80	64.50	68.77
D5	90	62.25	62.25	66.37	-
D6	70	62.25	62.25	66.37	-

### 3.4 Test setup and loading procedure

The specimen was positioned within the hydraulic system. Before the load cell and the sample were connected, precaution was taken during tightening to ensure that the load was zero before the test started. Leveling work was done to ensure that the specimen was leveled and placed in the correct position, as shown in Figure 3.11 and Figure 3.12. The three bolts at the top flange were tightened to ensure that the specimen was properly connected to the load cell. Each load increment was monitored during tightening to keep extra load from being applied to the system before the test began.

All of the specimens were tested in a 100-kN capacity Servocon Hydraulic System. Each specimen was fitted with the support at the end of the specimen edge and supported by a frame, as shown in Figure 3.13.



Figure 3.11 : Leveling work

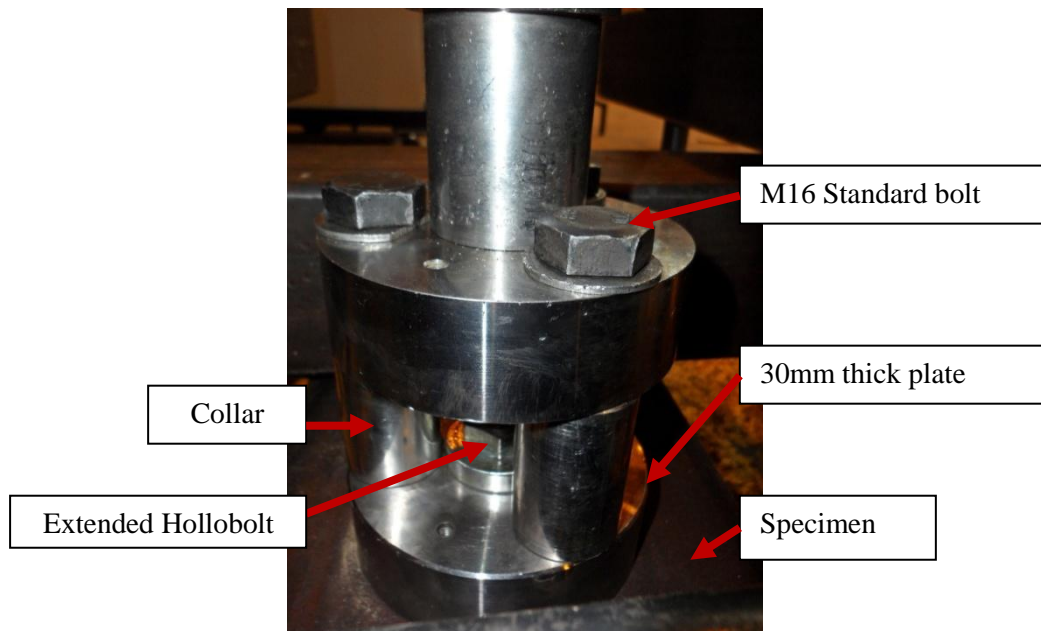


Figure 3.12 : Bolt connection to the load cell

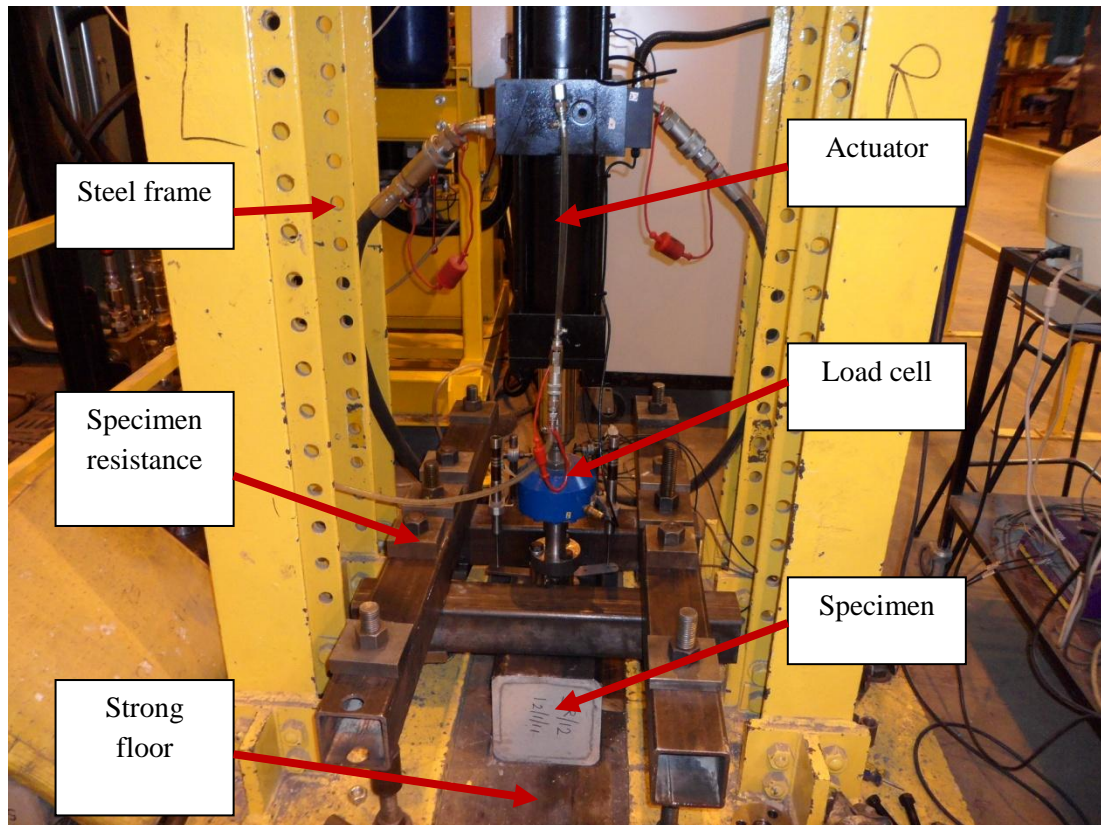


Figure 3.13 : Experimental setup

In the early stage of testing, the frequency was maintained within the range of 0.25 Hz to 5 Hz. Due to time limitations, the effects of frequency on EHB fatigue life were investigated to determine the highest frequency that could be applied to the Servocon system. The frequency was later fixed at 3 Hz for the rest of the test. Further justification for this 3 Hz setting is given in Chapter 4. The test was conducted under load control to maintain a constant load. After the specimen was positioned in the test area, the load was manually increased to the mean load in order to ensure that the correct load/range was applied. Because the experiment was intended to investigate the fatigue behaviour of the blind bolt under a working load, the benchmark or maximum load applied was set at 90 kN. Maximum load relates to

---

bolts' tension resistance, according to EC3 Part 1-8 (Appendix A). The machine was then set for automatic operation to  $N$  number of cycles or until the specimen failed.

### 3.4.1 Fatigue test loading method

Standard tests are generally the most suitable methods for determining the S–N curve. Response tests (constant amplitude) or increasing amplitude tests are most suitable (ASTM, 1963) for determining long-life fatigue strength or fatigue limit. The latter method, which was used in this research, is discussed in detail in this section. Two types of standard test may be carried out using either a single test specimen or groups of specimens at each stress level.

In the standard test, each fatigue specimen is cycled in constant stress or strain amplitude at different stress level until fracture occurs. Stress levels usually range from a high value, at which failure will occur quickly, to a lower value, at which failure only occurs after an extremely large number of cycles. If the primary interest is the long-life end of the S–N curve, often called the fatigue limit, the stress level is usually selected somewhere above this estimated fatigue limit. If the interest depends on the results of the first test, then subsequent specimens are tested at stress levels either above or below first test result until a point is found at which the specimen does not fail, in effect finding the fatigue limit.

A single test specimen at each stress level is generally used when a relatively small number of specimens are being tested, such as when the fatigue specimens are expensive or in short supply, or when machine parts, full size section, or assemblies are being tested.

Because the standard test using only one specimen at each stress level gives very little information concerning the variability of the material or component and the test procedure, it is better to test several specimens, each at various stress levels. In this test, each group should consist of at least four specimens in order to estimate the variability of the data. Ten or more specimens are preferred to gain some indication of the fatigue life values' distribution shapes. Generally, at least four stress levels are used in tests for determining S–N curves.

### 3.4.2 Number of specimens

The reliability of test results is primarily dependent on the number of specimens tested. This reliability increases as more tests are run. Table 3.10 gives the typical quantities of specimens for the reliability test. The numbers in the confidence level column in Table 3.10 corresponding to a confidence level of 95% were used to calculate the reliability for design purposes, those at the 90% confidence level were used for general engineering applications, and those at 50% were used for exploratory tests.

Table 3.10 : Number of specimens required, British Standard (BS ISO 12107, 2003).

Probability of failure P (%)	Confidence level, 1- $\alpha$ (%)		
	50	90	95
	Number of specimen , n <sup>a</sup>		
50	1	3	4
10	7	22	28
5	13	45	58
1	69	229	298

<sup>a</sup>The value of n are rounded to the nearest whole number

The ASTM Standard Practice (ASTM, 1991) offers guidance concerning the minimum number of S–N data points that should be included in the statistical analysis. Their recommendation assumes that the data are based on random samples

of the material and that the test data contains no run-outs (the specimen did not fail) or suspended tests (Herbet J. Sutherland and Veers, 2000, Wirsching, 1983, Beretta et al., 1995). These recommendations are summarized in Table 3.11.

Table 3.11 : ASTM Standard Practice recommended sample size (ASTM, 1991).

<b>Type of test</b>	<b>Minimum number of specimens</b>
Preliminary & Exploratory	6 to 12
Research and Development	6 to 12
Design allowable	12 to 24
Reliability	12 to 24

In addition to the number of specimens, ASTM offers replication guidelines. The percentage of replication  $R$  is defined as

$$R = 100 \left[ 1 - \frac{l}{n} \right] \quad \text{Equation 3-1}$$

where  $n$  is the number of specimens for different stress levels in the test data. The minimum replication is given in Table 3.12. Replications in the table indicate the test repetitions.

Table 3.12 : ASTM Standard Practice replication percentage (ASTM, 1991).

<b>Type of test</b>	<b>Percent replication (minimum)</b>
Preliminary & Exploratory	17 to 33
Research and Development	33 to 50
Design allowable	50 to 75
Reliability	75 to 88

Therefore, considering the suggestions provided by ASTM and British Standard, using five levels of stress and thirty fatigue tests of the EHB of Grade 8.8 with C40, the replication level of the test was 83%, which falls within the reliability guideline. The replication levels for the standard Hollobolt and normal M16 bolt tests were 60% and 70%, respectively. This number of specimens was deemed acceptable for comparison purposes. The 67% replication level of the Grade 8.8 EHB test using C60 also shows an acceptable number of specimens for comparison purposes. Table 3.14 shows the number of samples used in the fatigue testing.

### 3.4.3 Stress range

Tension tests were conducted to determine the fatigue behaviour of the proposed connection. The stress range was calculated using the tensile stress area of the bolts, as in Equation 3-2:

$$\sigma = \frac{P_a}{A_t} \quad \text{Equation 3-2}$$

where

$P_a$  = actual load during test

$A_t$  = tensile area of bolt according to BS EN ISO898:1:2009 (2009)

$$= \pi / 4 \left( \frac{d - \frac{3}{8}H + d_o - \left(\frac{H}{6}\right)}{2} \right)^2 \quad \text{Equation 3-3}$$

---

where	$H$	=	Height of fundamental triangle
		=	$8/5(d-d_o)/2$
	$d$	=	thread outer diameter
	$d_o$	=	thread root diameter

Table 3.13 : Average tensile bolt area

<b>Bolt type</b>	<b>d</b>	<b>d<sub>o</sub></b>	<b>Tensile area (A<sub>t</sub>)</b>
Extended Hollobolt	15.8	13.3	154.13
Standard M16 Bolt	15.8	13.45	156.55
Standard Hollobolt	15.68	13.45	154.13

While under load control, a constant tensile force was applied, as shown in Figure 3.14 and load path of the fatigue test is shown in Figure 3.15. This constant applied load had a simple loading history compared with the variable applied load, which has more complex fluctuating histories. Different load/stress ranges were applied based on the design yield stresses of the bolt, which, according to the Eurocode 3 Part 1-8 (BS EN1993, 2005), is at  $640 \text{ N/mm}^2$  for bolts of Grade 8.8. Five different load ranges were used: 90, 70, 60, 50, and 45 kN, which equate with nominal stress ranges of 584, 455, 390, 325, and  $292 \text{ N/mm}^2$ , respectively (Table 3.14). Unlike the EHB and standard HB, the applied stress ranges for the standard M16 bolt were 90, 80, and 70 kN, equating to stress ranges of 584, 519, and  $390 \text{ N/mm}^2$ , respectively.

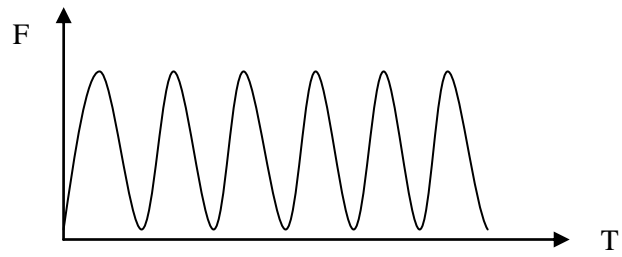


Figure 3.14 : Loading hysteresis

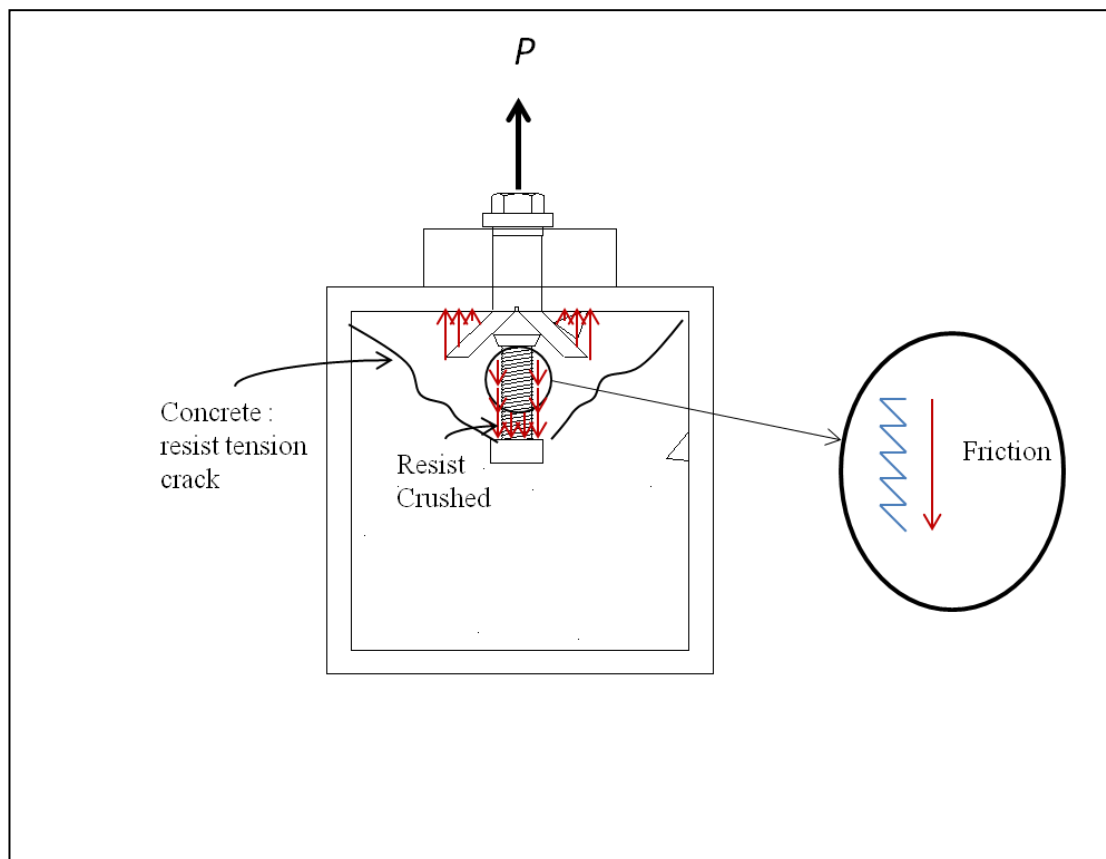


Figure 3.15 : Load path

Table 3.14 : Number of tests per stress range

Nominal Load (kN)	Nominal Stress range (N/mm <sup>2</sup> )	Number of samples tested			
		Concrete grade			
		C40	C40	C40	C60
		Extended Hollobolt	Standard Bolt M16	standard Hollobolt	Extended Hollobolt
90	584	4	3	2	3
80	519	0	4	0	0
70	454	6	3	2	3
60	389	6	0	2	0
50	325	9	0	4	0
45	292	5	0	0	0
Total		30	10	10	6

The tension fatigue test was selected because it is the most appropriate type of bolt fatigue test. The tension–tension cycle fatigue test is also the most uniform and severe form of fatigue loading. The selected loading waveform (sinusoidal) represents the most practical waveform in actual fatigue cases because it does not imply holding periods. In this study, the repeated load (stress) loading condition varied in tensile load range, which in practice is a normal stress condition.

---

### **3.5 Concluding remark**

Fatigue testing was conducted to determine the fatigue life of a Grade 8.8 EHB in comparison with a Grade 8.8 standard bolt M16 and a Grade 8.8 standard HB. 12.5mm thickness of tube wall and 30mm thickness of plate are used to eliminate the effect of tube wall and plate. The bolts were connected to concrete-filled hollow sections, and constant fatigue tensile tests were applied under load control. Frequencies between 0.25 and 5 Hz were used to investigate the effects of frequency on the proposed system's fatigue test. Due to time constraints, a frequency of 3 Hz was later applied to the rest of the fatigue tests and will explain later in Chapter 4.

---

# Chapter 4 : Experimental Results, Discussions, and Observations

---

## 4.1 Introduction

To understand the behaviour of the EHB under fatigue loading, a testing program was undertaken. The EHB was connected to a concrete-filled hollow section, as detailed in Chapter 3.

This chapter presents the results obtained from the experimental tests. Observation, comparison, and discussion of the results are provided to explain the effect of the frequency and failure mode of the EHB under different frequencies and stress ranges. The fatigue life of different types of bolts, specifically that of the EHB, the standard HB, and the standard bolt (M16), is the key characteristic used as the basis for comparison and discussion. The suitable frequency for the fatigue test is discussed, and general observations regarding the specimens after failure are provided.

## 4.2 Effect of frequency and stress range determination

To minimize the experimental variables, the effects of frequency and stress range for the EHB were investigated. The effect of frequency between 0.25 Hz and 5 Hz was investigated to define the highest frequency applied for all the tests in order to save time considering that a longer experimental time may be required for failure mode to be reached. The effect of the stress range was investigated to determine the fatigue life of the bolt when a higher load or a lower load is applied.

---

### 4.2.1 Effect of frequency

In fatigue testing, reaching the number of necessary cycles for specimen failure can take a long time. Therefore, the effect of frequency should be analyzed to define the suitable frequency to shorten the testing time and to confirm that the results are not significantly affected when a different frequency is applied.

To determine the suitable frequency for the proposed test, frequencies between 0.25 Hz and 5.0 Hz were applied. The results in Table 4.1 show the various frequency tests of EHB samples. To investigate its effect, of the frequency stress range ( $\Delta\sigma_n$ ) of 584, 454, 389, and 325 N/mm<sup>2</sup> was employed.

Table 4.1 shows that fatigue life at stress  $\Delta\sigma_n$  584 N/mm<sup>2</sup> increased by approximately 16% for S4 (1.0 Hz) and by 30% for S23 (at 3.0 Hz) from S1 (0.25 Hz). These three samples had a similar average loads during the test, and exhibited slightly different fatigue lives. However, a large difference occurred when a stress range of  $\Delta\sigma_n = 454$  N/mm<sup>2</sup> was applied. The large difference in fatigue life at this stress range was due to the fact that the stress range increased when higher frequency was used. Therefore, in this case, we can conclude that the stress range can be affected by the frequency. We can see that, at a frequency of 5 Hz, the load increased with an average of 6 kN from the applied load and reached at the negative value, as shown in Figure 4.1, which illustrates the effect of frequency on the actual load during the fatigue test with frequencies of 1, 3, and 5 Hz. This is probably due to the acceleration of the system at higher frequency is higher compared to the lower frequency. Therefore, a higher load range at higher frequency is obtained throughout this test. Figure 4.1 shows negatives load at higher frequency, these negative values

are not taken in the data analysis shown in later chapters. Overall, the results showed that 3 Hz is the most reliable frequency to use so that the actual load is close to the applied load during the test.

Table 4.1: Effect of frequency experimental results

No	Actual load range $P_a$ (kN)	Actual stress range $\Delta\sigma_a$ (N/mm <sup>2</sup> )	Number of cycles $N_f$	Frequency (f)	Fracture failure
S1	89.67	581.78	8,025	0.25	Shank
S4	89.93	583.48	9,314	1.0	Shank
S23	89.89	583.24	10,489	3.0	Shank
S24	90.20	585.26	12,063	3.0	Near head
S2	69.90	453.51	20,608	0.25–1.0	Shank
S11	71.91	466.81	28,331	3.0	Shank
S12	73.80	478.82	28,632	3.0	Shank
S9	76.10	493.75	20,649	5.0	Near head
S10	76.44	495.94	21,441	5.0	Head
S5	60.60	393.17	55,822	1.0–2.0	Shank
S25	60.93	395.34	58,142	3.0	Near head
S27	60.86	394.85	63,314	3.0	Shank
S17	49.93	323.95	78,803	2.0	Shank
S15	51.13	331.73	89,300	3.0	Shank
S16	50.88	330.11	91,878	3.0	Near head

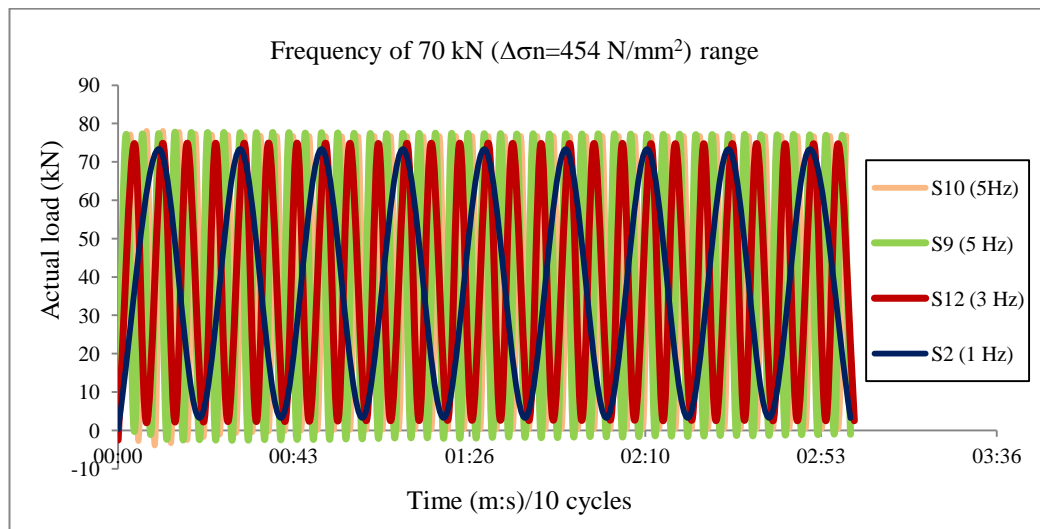


Figure 4.1 : Cyclic histories at stress  $\Delta\sigma_n$  455 N/mm<sup>2</sup>

Figure 4.2 shows the effect of frequency on the fatigue life of the EHB at different stress ranges, where  $\Delta\sigma_n$  is the actual stress range and the  $x$ -axis (fatigue life) is normalized with the concrete strength ( $f_{ck,cube}$ ). Although similar mix proportions were used for the concrete infill, the concrete strengths were different among samples at Day 7 and the test day. The strength varied between 35 N/mm<sup>2</sup> and 43 N/mm<sup>2</sup>.

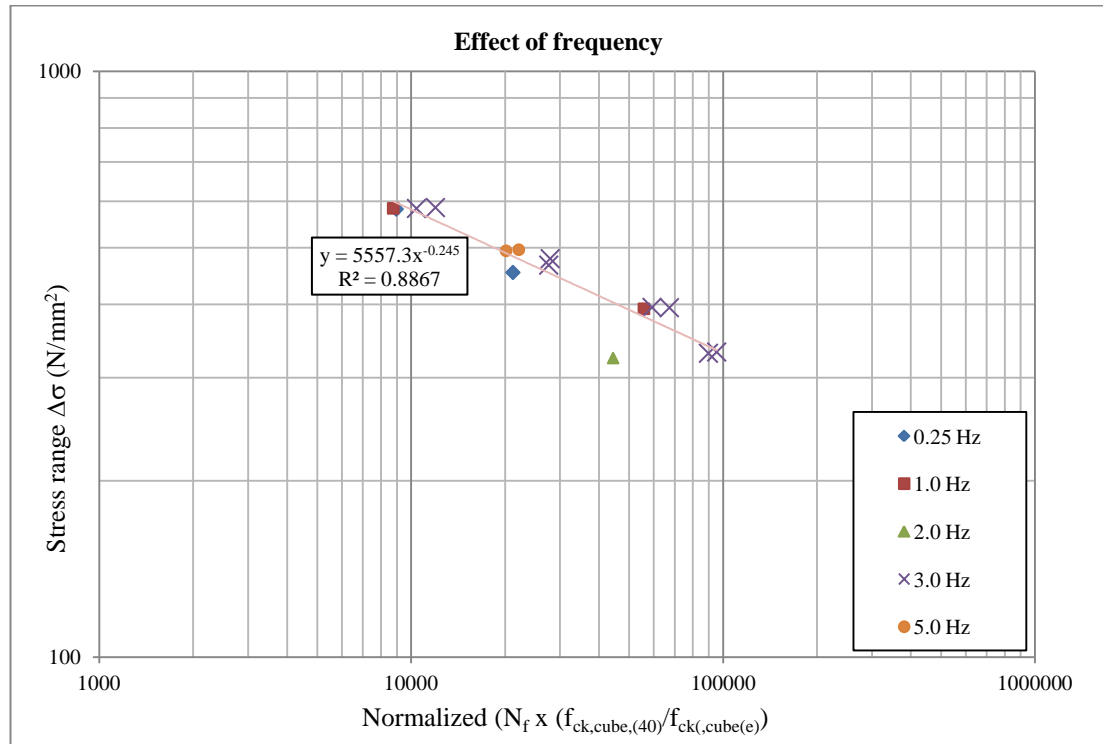


Figure 4.2 : Normalization graph of frequency

Figure 4.2 illustrates that the fatigue life increases according to the frequency of the system. At the stress range of 389 N/mm<sup>2</sup>, the fatigue life did not have a large influence; from 2 Hz to 3 Hz, the difference was merely 4%. With the same frequency, the fatigue life of the EHB increased by 9%.

For greater detail, the least squares method is used explain that the correlation coefficient or R-square for the sets of data is 0.8867. A good logarithmic straight-line fit is demonstrated, showing that fatigue life decreases slightly with the frequency at lower stress.

### 4.2.2 Effect of stress range

The stress range below the yield stress was applied to investigate the behaviour of the EHB under service load. As expected, the number of cycles to failure increased when the stress range was decreased (see Figure 4.3). This result demonstrated that the EHB behaves in a similar manner to the standard bolt, whose fatigue life increases relative to the stress range (Bouwman, 1979).

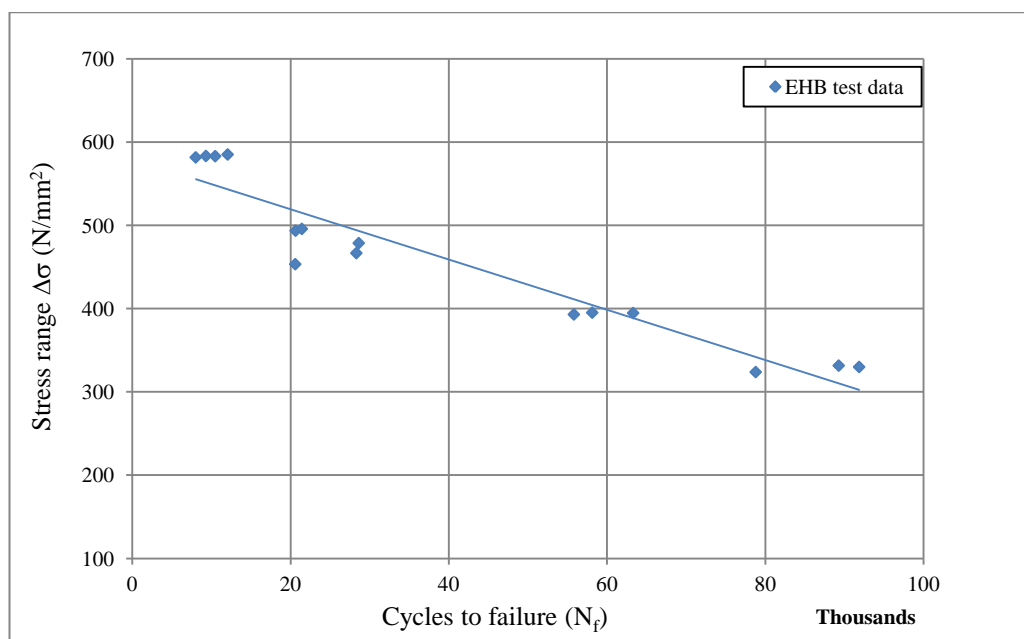


Figure 4.3 : Effect of stress range graph

### 4.2.3 Effect of frequency on the failure mode

The failure mode of the EHB was due to bolt fracture. Figure 4.4 shows the final failure of the bolts. The difference in the location of the fracture between the bolts was due to the position of the bolt during the test, despite the fact that, before the test was started, caution was taken to ensure that the specimen was levelled and that the load was working axially. However, occasionally, in the middle of the test, the actuator did not move axially, causing the bolt to have a different location of failure.

Nevertheless, the fatigue life of the test bolt was not significantly affected by the final fracture position. For example, at  $\Delta\sigma_n = 325 \text{ N/mm}^2$ , the difference between S15 and S16 was only 3%. Overall, the failure mode of the EHB was located in the shank of the bolt. Another factor influencing the final fracture was the uneven joint surface. Such problems are common, and usually originate from a manufacturing problem that results in the joint surface not being square in relation to the bolt hole.



Figure 4.4 : Failure mode of Extended Hollobolt

### 4.3 General observations on Extended Hollobolt under fatigue load

Experimental results were collected from the final failure fatigue test on the EHB. The fatigue life of the bolt can be determined from the bolt failure, which is known as the number of cycles to failure ( $N_f$ ). Meanwhile, the fatigue strength is defined as the stress applied during the fatigue test. Finally, a comparison and discussion of the different types of bolts are presented in Table 4.2 to Table 4.5, which show the

overall test results from the fatigue tests of the EHB, the HB, and the standard bolt, respectively.

### 4.3.1 Fatigue behaviour of the Extended Hollobolt

The 30 fatigue tests conducted on the EHB revealed the fatigue life of the sample to be dependent on the stress range. The fatigue life is presented in the S–N normalized graph in Figure 4.5.

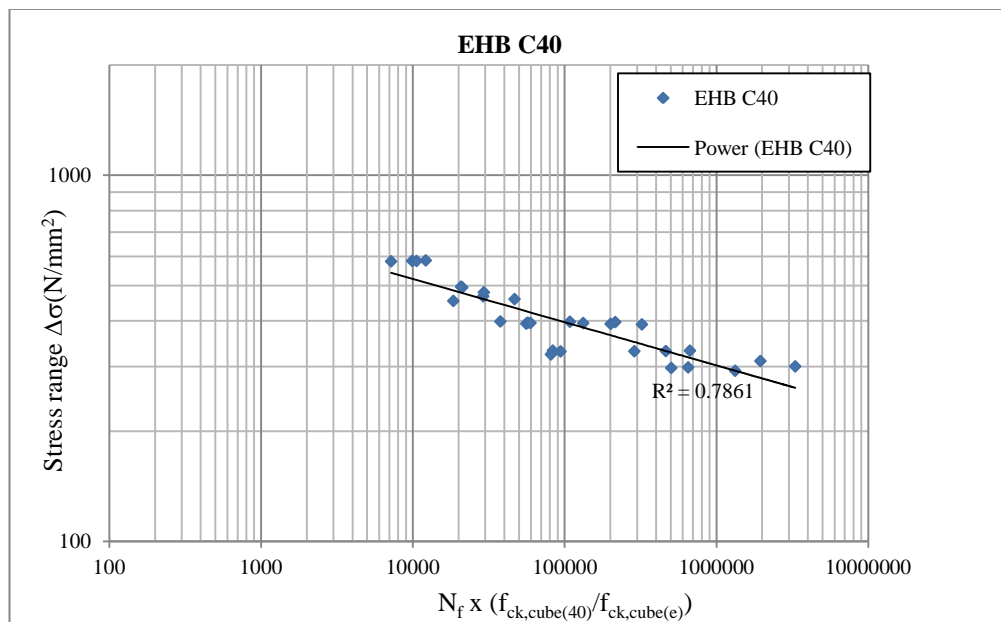


Figure 4.5 : Normalization graph stress of fatigue life of EHB

At the high stress range of 584 N/mm<sup>2</sup>, the EHB demonstrated consistent fatigue life, with a difference of less than 20% among four tests despite the different applied frequencies among the specimens. At the low stress range, the number of cycles to failure varied by more than 50% at the same frequency. Fatigue life began to spread wider when a lower range was used. For example, at stress range 389 N/mm<sup>2</sup>, the value of the fatigue life ranged between 40000 cycles and 300000 cycles. This pattern became more obvious at stress ranges of 325 and 292 N/mm<sup>2</sup>.

Table 4.2 : Experimental results of EHB Grade 8.8 C40

No.	Sample Number	Concrete strength at Day 7 (N/mm <sup>2</sup> )	Concrete strength at test days (N/mm <sup>2</sup> )	$\Delta F$ (kN)	Load Amplitude ( $F_{\max} - F_{\min} / 2$ ) (kN)	Number of cycles (N)	Average actual load range (kN)	Average actual Stress range $\Delta\sigma_a$ (N/mm <sup>2</sup> )	Frequency (Hz)	Fracture failure	Fracture position from bottom of head (mm)
1	S1	35.80	35.80	90	45	8025	89.67	581.77	0.25	Shank	51
2	S4	39.50	42.50	90	45	9314	89.93	583.46	1.0	Shank	52
3	S23	40.30	40.30	90	45	10489	89.90	583.22	3	Shank	49
4	S24	40.30	40.30	90	45	12063	90.21	585.24	3	Near Head	0
5	S2	35.85	35.85	70	35	20608	69.90	453.50	0.25-1.0	shank	50
6	S8	38.90	40.96	70	35	45631	70.70	458.68	3	Near Head	5
7	S9	38.90	40.96	70	35	20649	76.10	493.74	5	Near Head	0
8	S10	38.70	38.70	70	35	21441	76.44	495.93	5	Near Head	0
9	S11	41.00	41.00	70	35	28331	71.95	466.79	3	shank	52
10	S12	41.00	41.00	70	35	28632	73.80	478.80	3	Shank	50

No.	Sample Number	Concrete strength at Day 7 (N/mm <sup>2</sup> )	Concrete strength at test days (N/mm <sup>2</sup> )	$\Delta F$ (kN)	Load Amplitude ( $F_{\max} - F_{\min} / 2$ ) (kN)	Number of cycles (N)	Average actual load range (kN)	Average actual Stress range $\Delta\sigma_a$ (N/mm <sup>2</sup> )	Frequency (Hz)	Fracture failure	Fracture position from bottom of head (mm)
11	S5	40.00	40.00	60	30	55822	60.60	393.16	1.0–2.0	Shank	49
12	S14	37.40	37.40	60	30	40297	61.43	398.57	3	Near Head	0
13	S18	41.90	41.90	60	30	191710	60.50	392.52	3	Near head	4
14	S19	41.80	41.80	60	30	126731	60.81	394.54	3	Shank	50
15	S20	41.80	42.50	60	30	202742	61.20	397.08	3	Near head	4
16	S21	40.25	40.25	60	30	107526	61.33	397.90	3	Shank	51
17	S22	40.25	41.15	60	30	313697	60.31	391.28	3	Near Head	3
18	S25	38.40	39.25	60	30	58142	60.93	395.32	3	Shank	52
19	S27	37.60	37.60	60	30	63314	60.86	394.85	3	Shank	56
20	S6	39.80	43.55	50	25	264135	50.94	330.46	2	Near Head	4
21	S15	37.40	37.40	50	25	89300	51.13	331.72	3	Shank	53
22	S16	40.90	40.90	50	25	91878	50.88	330.10	3	Near Head	4

No.	Sample Number	Concrete strength at Day 7 (N/mm <sup>2</sup> )	Concrete strength at test days (N/mm <sup>2</sup> )	$\Delta F$ (kN)	Load Amplitude ( $F_{\max} - F_{\min} / 2$ ) (kN)	Number of cycles ( $N_f$ )	Average actual load range (kN)	Average actual Stress range $\Delta\sigma_a$ (N/mm <sup>2</sup> )	Frequency (Hz)	Fracture failure	Fracture position from bottom of head (mm)
23	S17	40.90	41.20	50	25	78803	49.93	323.94	2	Shank	53
24	S33	41.23	41.23	50	25	450044	50.99	330.82	3	Shank	49
25	S34	41.23	42.67	50	25	626804	51.12	331.63	3	Shank	48
26	S3	40.00	40.00	45	22.5	1328102	45.05	292.27	1.0 -2	Near head	4
27	S7	39.33	39.33	45	22.5	3358810	46.30	300.41	3	Near head	3
28	S13	38.70	38.70	45	22.5	2012778	47.89	310.72	3	Shank	49
29	S28	37.60	38.50	45	22.5	676386	46.02	298.59	3	Shank	34
30	S29	38.10	38.10	45	22.5	528703	45.86	297.53	3	Shank	56

Table 4.3 : Experimental results of standard HB Grade 8.8 C40

No.	Sample Number	Concrete strength at 7 days (N/mm <sup>2</sup> )	Concrete strength at test days (N/mm <sup>2</sup> )	$\Delta F$ (kN)	Load Amplitude ( $F_{\max}-F_{\min}/2$ ) (kN)	Number of cycles ( $N_f$ )	Average actual load range (kN)	Average actual Stress range $\Delta\sigma_a$ (N/mm <sup>2</sup> )	Frequency (Hz)	Fracture failure	Fracture position from bottom of head (mm)
1	C1	38.00	38.00	90	45	12174	89.20	578.74	3	Near head	4
2	C2	38.00	38.00	90	45	10756	88.98	577.28	3	Near head	2
3	C3	37.57	37.57	70	35	20817	69.14	448.54	3	Near head	1
4	C4	38.80	38.80	70	35	20034	69.42	450.39	3	Near head	3
5	C5	38.80	38.80	60	30	29779	60.10	389.92	3	Near head	4
6	C6	38.80	38.80	60	30	38491	60.24	390.83	3	Near head	3
7	C7	39.30	39.30	50	25	110000	49.80	323.09	3	Near head	2
8	C8	39.30	39.30	50	25	39671	49.54	321.41	3	Near head	3
9	C9	39.75	39.75	50	25	60577	50.45	327.32	3	Near head	3
10	C10	39.75	39.75	50	25	62401	50.32	326.47	3	Near head	3

Table 4.4 : Experimental results of standard bolt M16 Grade 8.8 C40

No	Sample Number	Concrete strength at 7 days (N/mm <sup>2</sup> )	Concrete strength at test days (N/mm <sup>2</sup> )	$\Delta F$ (kN)	Load Amplitude ( $F_{\max}-F_{\min}/2$ ) (kN)	Number of cycles ( $N_f$ )	Average actual load range (kN)	Average actual Stress range $\Delta\sigma_a$ (N/mm <sup>2</sup> )	Frequency (Hz)	Fracture failure	Fracture position from bottom of head (mm)
1	B1	36.90	36.90	90	45	16957	89.17	577.01	3	Shank	43
2	B2	36.90	36.90	90	45	14806	89.33	578.05	3	Shank	42
3	B3	39.40	39.40	90	45	17020	89.24	577.47	3	Shank	43
4	B10	39.30	41.87	80	40	80293	79.69	515.64	3	Near head	2
5	B11	39.30	41.87	80	40	14018	79.94	517.26	3	Shank	44
6	B12	41.22	41.22	80	40	32193	80.53	521.09	3	Shank	44
7	B13	41.22	41.22	80	40	27514	80.51	520.99	3	Shank	44
8	B4	36.80	36.80	70	35	320684	70.11	453.68	3	Shank	42
9	B5	36.80	38.17	70	35	254351	70.25	454.59	3	Shank	44.5
10	B6	39.40	39.40	70	35	300387	70.59	456.79	3	Shank	44

Table 4.5 : Experimental results of EHB Grade 8.8 C60

No	Sample Number	Required Concrete strength at 7 days (N/mm <sup>2</sup> )	Concrete strength at test days (N/mm <sup>2</sup> )	$\Delta F$ (kN)	Load Amplitude ( $F_{\max} - F_{\min} / 2$ ) (kN)	Number of cycles (N)	Average actual load range (kN)	Average actual Stress range $\Delta\sigma_a$ (N/mm <sup>2</sup> )	Frequency (Hz)	Fracture failure	Fracture position from bottom of head (mm)
1	D1	64.50	64.50	90	45	13840	90.86	587.96	3	Near head	4
2	D2	64.50	64.50	90	45	21624	90.32	584.46	3	Near head	1
5	D5	62.25	62.25	90	45	17707	90.01	582.43	3	Shank	42
3	D3	59.80	59.80	70	35	27919	70.88	458.65	3	Shank	48
4	D4	58.90	59.80	70	35	42862	70.22	454.40	3	Shank	49
6	D6	62.25	62.25	70	35	88765	70.68	457.40	3	Near head	9

The large scatter of the data at the low stress range is shown in Figure 4.6. The graph illustrates that the fatigue life of the EHB was related to the concrete-filled hollow section against the actuator movement. The actuator movement is discussed because of the difficulty in measuring the movement of the bolt directly near it. The available data logger also could not manage to capture the peak values during the test.

In terms of stiffness, the bolt behaved similarly at a higher stress range, but behaved differently at a lower stress range. In the bolt test, higher stress showed that the bolt had nearly equal stiffness as when lower stress was applied. This behaviour can be attributed to the increasing plasticity at higher strength and the increasing elasticity at lower strength.

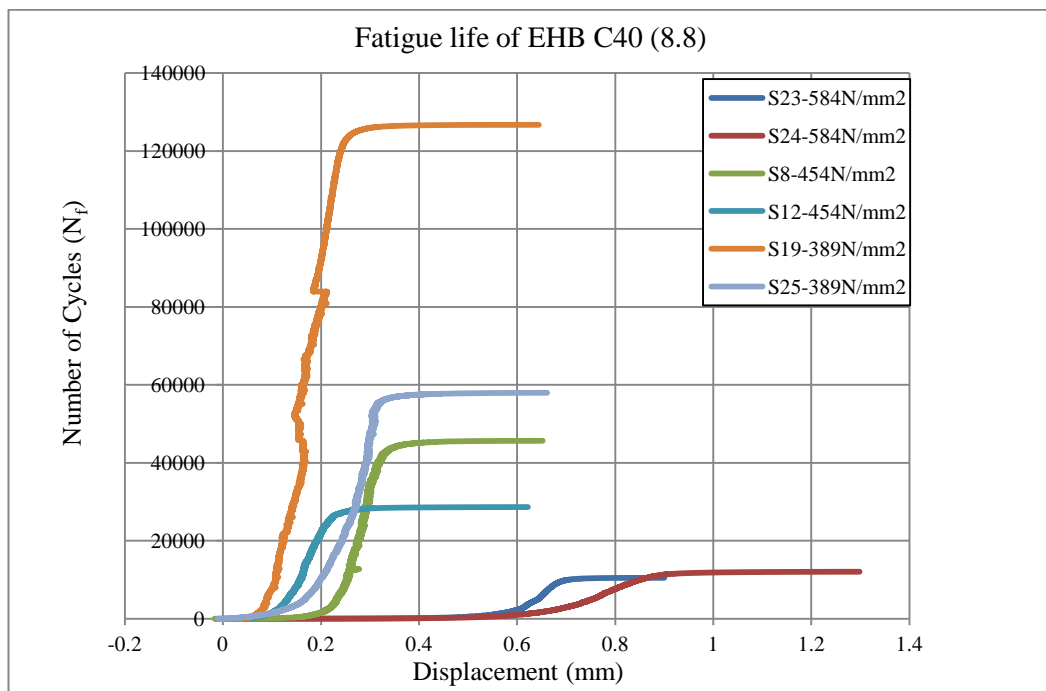


Figure 4.6 : Fatigue life displacement graph

Compared with the Grade 10.9 EHB (Jiani, 2012), the fatigue life of the EHB grade 8.8 is lower at stress range  $584 \text{ N/mm}^2$  (see Table 4.6) because the yield of the former is higher than that of the latter. However, no further conclusion can be made

at a lower range because, in Grade 8.8 EHB, fatigue life is scattered. Therefore, no absolute fatigue life or fatigue strength can be observed between those grades unless the S–N curve is plotted via more tests on Grade 10.9 EHB.

Table 4.6 : Fatigue life of EHB Grades 8.8 and 10.9

Stress range $\Delta\sigma_n$ (N/mm <sup>2</sup> )	Grade 8.8		Grade 10.9	
	Sample No.	Fatigue life (N <sub>f</sub> )	Sample No.	Fatigue life (N <sub>f</sub> )
584	S23	10,489	Test 1	13,281
454	S9	20,649	Test 2	29,854
389	S14	40,297	Test 3	67,257
	S27	63,314		

### 4.3.2 Fracture failure of the Extended Hollobolt

The failure mode of all tests was due to bolt failure known as Failure Mode 3, as described in Chapter 2. This failure caused the bolts to reach their ultimate capacity, thereby minimizing the contribution of the components. This type of failure mode could help explain how the EHB would behave under fatigue load.

To anticipate the failure mode, we have to describe the component used in the test. The selected plate was thick to prevent any significant bending of the loaded face. A thick hollow section was used for the same purpose. The hollow section was filled with concrete to prevent deformation. The fracture failure of the bolt under fatigue tension load was expected to occur at the shank, as discussed in Chapter 2. For this test, the location of the fracture failure is indicated in Figure 4.7.

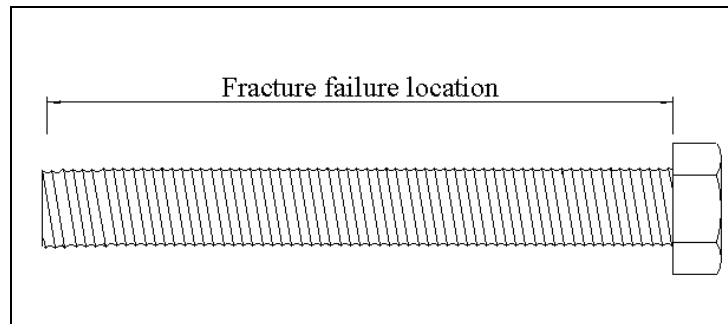


Figure 4.7 : Fracture failure location

According to the experiments, failure occurred near the head and in the middle of the shank, as anticipated. The fracture failure of the bolt can be examined by taking a photograph of the fracture. Images of a typical fracture surface are shown in Figure 4.8.

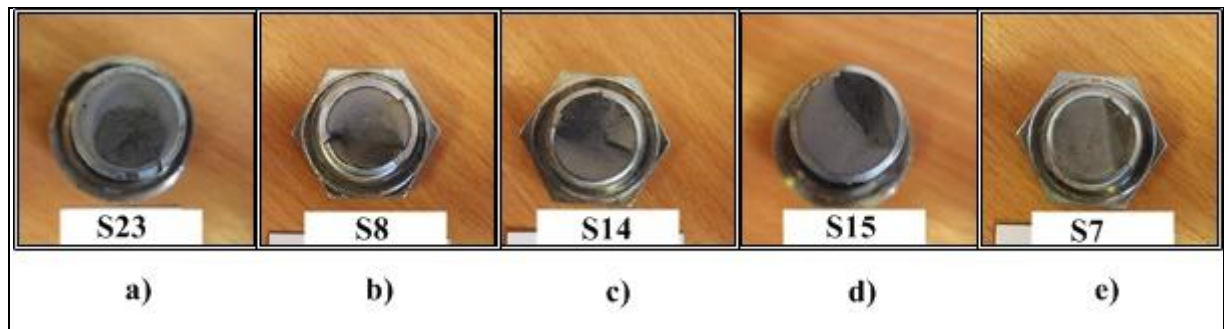


Figure 4.8 : Fracture failure of EHB: a)  $\Delta\sigma = 584 \text{ N/mm}^2$ ; b)  $\Delta\sigma = 454 \text{ N/mm}^2$ ; c)  $\Delta\sigma = 389 \text{ N/mm}^2$ ; d)  $\Delta\sigma = 325 \text{ N/mm}^2$ ; e)  $\Delta\sigma = 292 \text{ N/mm}^2$

Shape trends are clear between S23 (stress range at  $584 \text{ N/mm}^2$ ) and other stress ranges, such as S8 ( $389 \text{ N/mm}^2$ ) and S14 ( $325 \text{ N/mm}^2$ ). This change may be attributed to increased plasticity in the thread root with higher stress range causing load shedding along the helix thread. Such load shedding can result in crack growth around the helix.

---

#### **4.4 Comparison among tested bolt types**

A preliminary series of fatigue tests using different bolt types, the standard HB and the standard bolt M16 was performed. The tests on the standard HB used the rig (an alternative material for the hollow section) with dimensions of 200 mm × 200 mm × 20 mm. The test on the standard bolt M16 was performed by using a 200 mm × 200 mm × 12.5 mm hollow section. Other conditions of the test, such as loading rate, frequency, and experimental setup, were similar to the EHB concrete-filled hollow section test.

##### **4.4.1 Fatigue life of bolt**

Fatigue life describes the failure of the material due to fatigue. In this study, fatigue life occurs when the bolt has failed. The fatigue failure of the bolt is recorded for each stress range. To describe the linear relationship between applied stress and the number of cycles to failure, curve fitting can be applied. The different concrete strength rates of the specimen during the test are presented in the S–N graph plotting, where the ratio of concrete strength during the test is considered in calculating the number of cycles. An assumption of fatigue life increases relatively when concrete strength is used to normalize the number of cycles from the test. This assumption is based on the findings from the previous study (Al-Mughairi, 2009). For the standard HB under fatigue load, a different rig with a 20 mm thick steel plate was used. The fatigue life of the bolt is discussed according to the S–N curve graph in Figure 4.9.

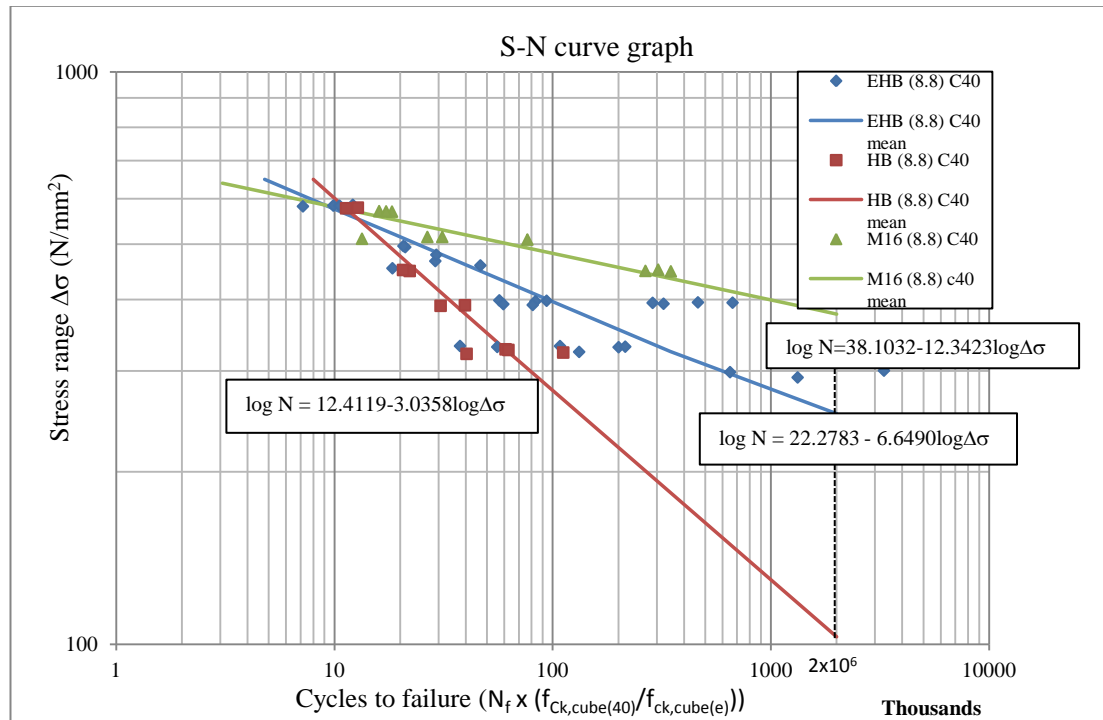


Figure 4.9 : S–N curve of bolt comparison

The figure reveals that EHB have a longer fatigue life than standard HB. It also shows that the EHB has higher fatigue strength compared to a standard HB. However, in terms of fatigue life, a standard HB exhibits a behaviour opposite to that of the EHB. The standard HB has less scatter life throughout the different stress ranges. Furthermore, the longer shank and the nut also provide extra fatigue life to the EHB. The bond between the nut and the shank with concrete prevents the EHB from pulling out, and provides the EHB additional fatigue strength.

The standard bolt M16 exhibited a longer fatigue life when it was connected to the concrete-filled hollow section. The M16 bolt had greater fatigue strength than the EHB. The sleeve of the HB functioning as the nut to the standard bolt did not totally contribute to a longer fatigue life; however, it provided the EHB much better fatigue strength and fatigue life compared with the standard HB. Even though the M16 exhibited a longer fatigue life than the EHB, both intercepted results at a higher

---

stress range ( $\Delta\sigma_n = 584 \text{ N/mm}^2$ ). Thus, the fatigue life of bolts is nearly the same when higher stress is applied. For the standard HB, the fatigue life at a higher stress range might have a higher degree of plasticity. Overall, we can conclude that the mean stress and material properties affect the fatigue life of the EHB.

#### 4.4.2 Fatigue behaviour of bolts

To investigate the stiffness of the EHB during fatigue tests, data from the actuator movement were used due to the difficulties in positioning the other instrumentation. This indicative approach is the most appropriate method to measure the displacement of the bolt during the test, given the difficulty of recording the movement of the bolt and the plate of the specimen under higher frequency. Therefore, determination of the bolt movement during the test was based on the actuator position.

A comparison of the fatigue life among the three investigated types of bolts is presented in Figure 4.10. The three bolts were at the stress range of  $584 \text{ N/mm}^2$ . The graph shows that the EHB is stiffer than the standard HB, and is less stiff compared to the standard M16 bolt.

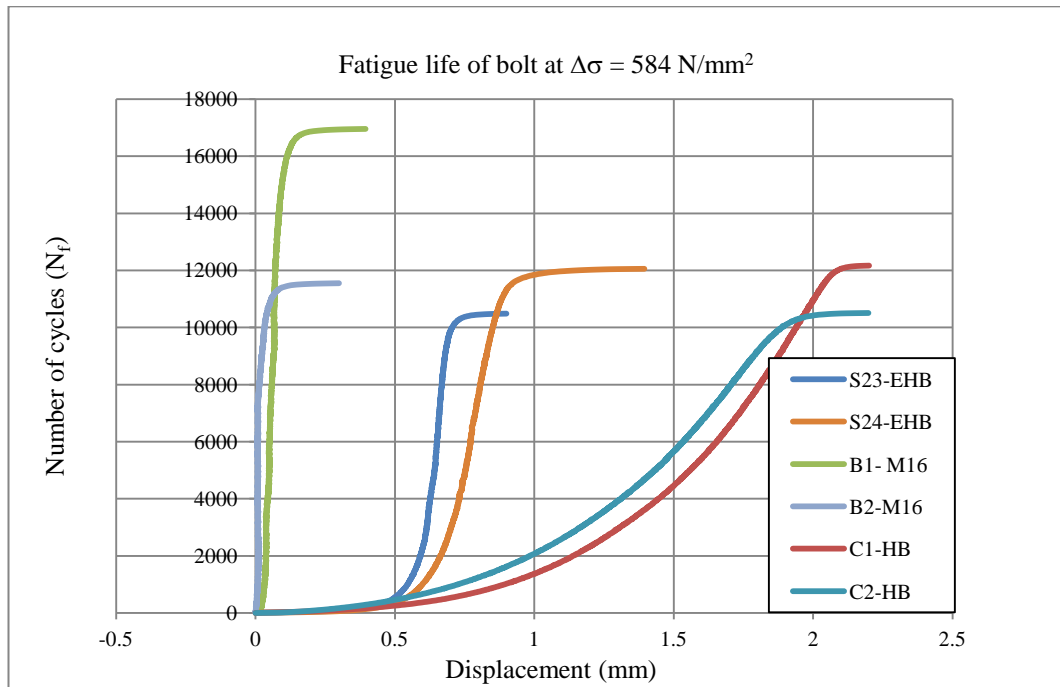


Figure 4.10 : Comparison fatigue life of bolt at stress range  $584 \text{ N/mm}^2$

Our observation showed that, after the rig section was removed, the HB was pulled out of the concrete, which was not the case with the EHB (Figure 4.11). However, the fatigue life of the M16 bolt was longer than that of the EHB when the bolt was connected to the concrete-filled tube. This result was expected considering that, in the static test, the M16 bolt was stiffer than the EHB, as shown in Figure 4.12. The life of the M16 bolt increased when a lower stress range was applied. The same result was also observed in the EHB and the standard HB. For both the M16 bolt and the EHB, the bolt remained inside the concrete when the steel section was cut. The concrete continued to hold the nut placed at the end of the EHB, thereby preventing the bolt from pulling out during the fatigue test. This phenomenon indicates that the EHB has longer fatigue life of the than that of the standard HB.

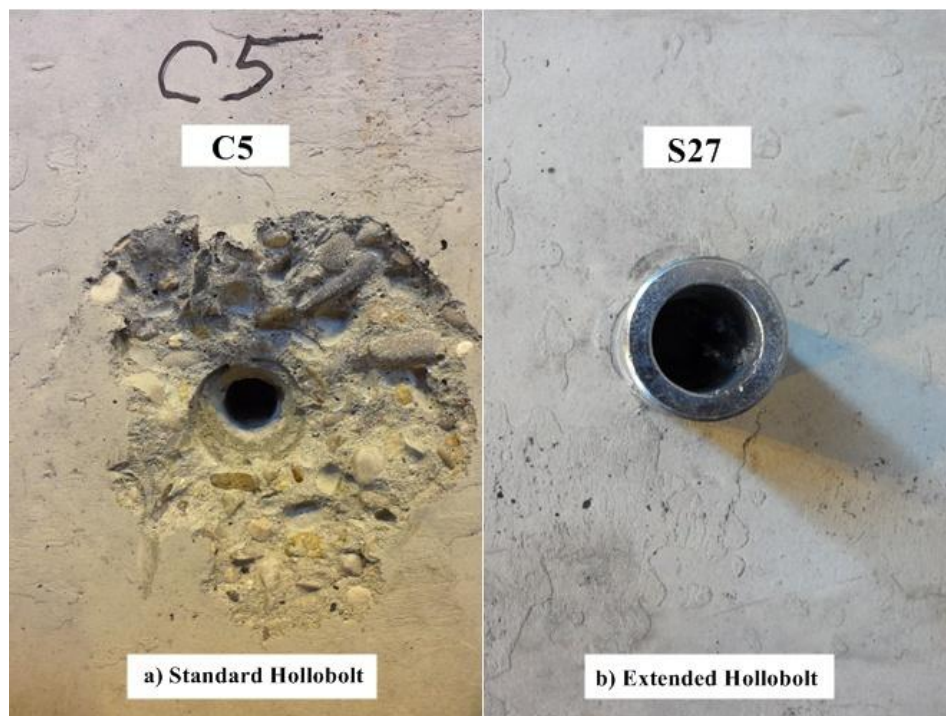


Figure 4.11 : Concrete surface of the standard HB and EHB test specimens

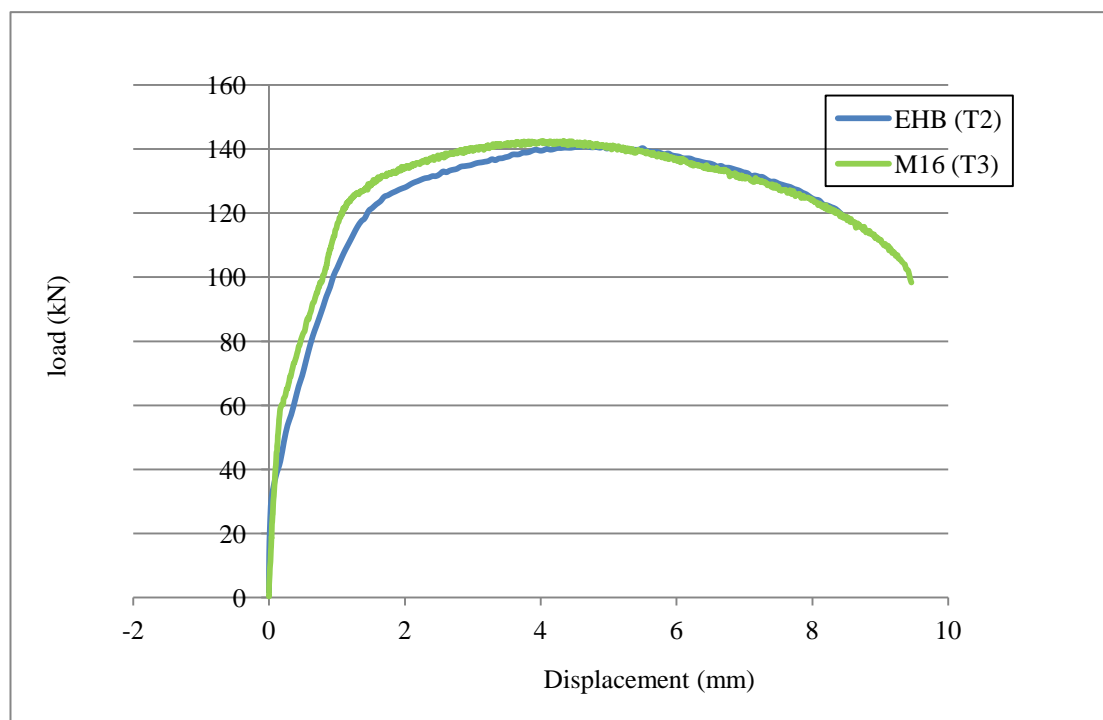


Figure 4.12 : Static test results of Extended Hollobolt and standard bolt concrete-filled hollow sections

---

#### 4.4.3 Fracture failure of bolt

A similar method to that applied to the EHB was conducted to present the fracture failure of the other types of bolt. A photograph of the bolt fracture was taken. A comparison of the shape trend is shown in Figure 4.13. Similarly shaped trends were found for the EHB and the standard HB at the stress range of  $584 \text{ N/mm}^2$ . However, the M16 bolt exhibited a different shape of fracture failure. Compared with the EHB and the standard HB, the M16 had a similar shape trend with other stress ranges. This shape trend can also be seen in the micrograph in Figure 4.14 where a similar fracture failure is shown. The possibility of increasing the plasticity at a higher stress range, as discussed in Section 4.3.2, seemed to occur in the standard HB but not in the M16. Therefore, the obvious shape trend occurred only in the Extended and the standard HB.

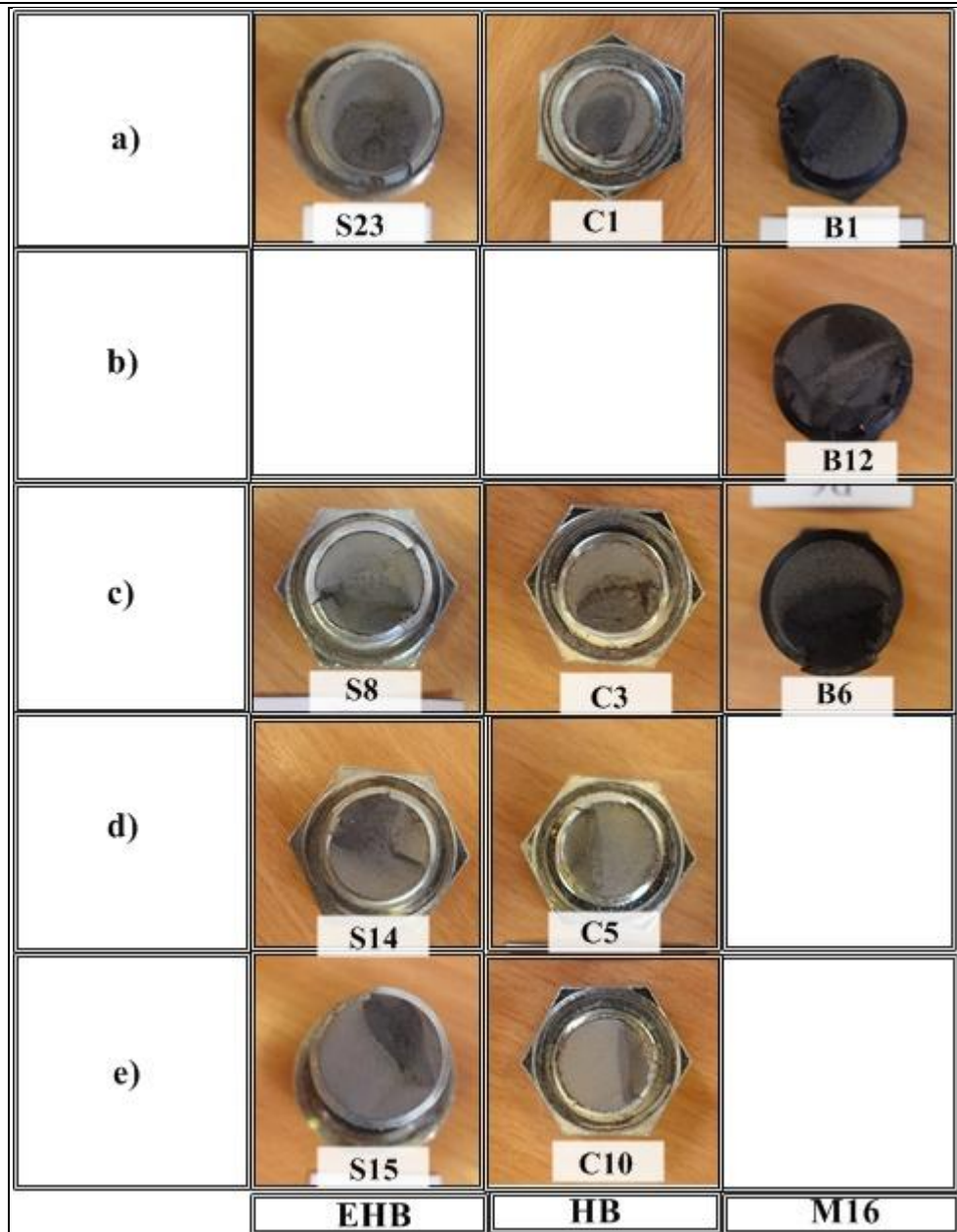


Figure 4.13 : Fracture failure of bolts: a) 584 N/mm<sup>2</sup>; b) 519 N/mm<sup>2</sup>; c) 454 N/mm<sup>2</sup>; d) 389 N/mm<sup>2</sup>; e) 325N/mm<sup>2</sup>

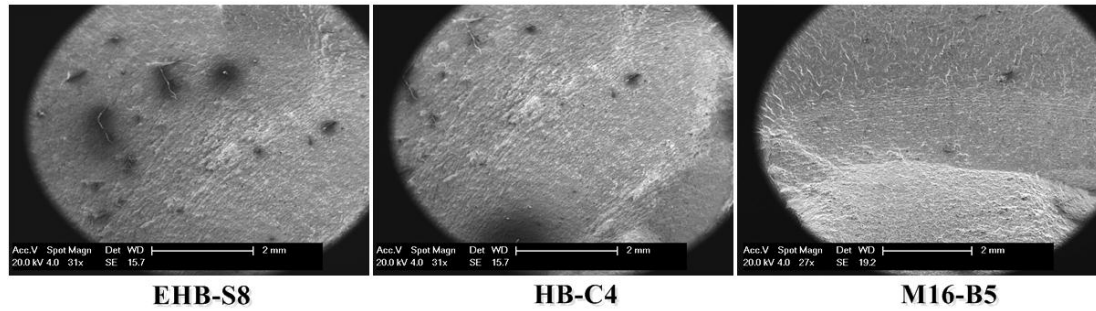


Figure 4.14 : Micrographic of fracture failure at  $\Delta\sigma=454 \text{ N/mm}^2$

The sleeve of the HB was observed to determine if any damage occurred during the fatigue test. Apparently, the sleeve did not incur any damage, except for the line mark at the sleeve opening, as shown in Figure 4.15. The line mark appeared in both the EHB and the standard HB.

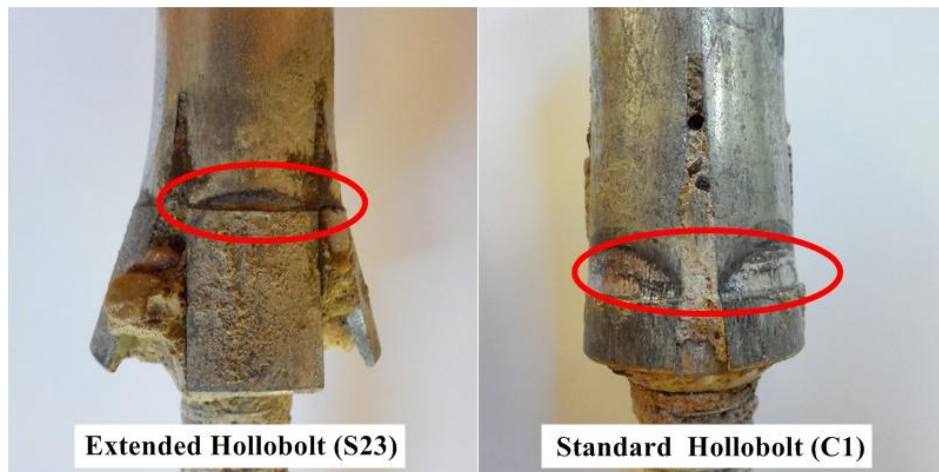


Figure 4.15 : Sleeve observation after test

#### 4.4.4 EC3 S–N curve classification

To validate the fatigue test of the bolt, the S–N curve characteristic was used. The proposed fatigue assessment according to the EC3 is equal to the category of 50. Category of 50 consists of the bolts and rod with roller or cut threads in tension. According to EN1993-1-9 (2005), to determine the appropriate detail category for a particular constructional detail (for example category 50 in EC3), the value of the

---

stress range  $\Delta\sigma_c$  corresponding to a value of  $N_c= 2$  million cycles were calculated with 75% confidence level of 95% probability of survival for log N. The standard deviation, the sample size and residual stress effect were taking into account in calculation. The member of data point (not lower than 10) is considered in statistical analysis.

In this study the guideline proposed by the EC3 is followed to perform the S-N curve characteristic. From the test result, fatigue life of the EHB was stronger compared with the EC3 requirement. As shown in Figure 4.16, several test results demonstrated that the EHB was equal to the category of 100 and above. Because of the scatter of fatigue life, accurately categorizing it in accordance with EC3 is difficult. To categorize the EHB, further validation using statistical analysis is required, and will be the focus of the next chapter of this thesis.

The HB can be categorized between Classes 71 and 112. As illustrated by the equation in Figure 4.9, the slope of the HB fatigue test is equal to the slope of the S–N curve in EC3, which is equal to 3. Based on the overall test data, we can conclude that the EHB and the standard HB are safe in terms of fatigue assessment. As expected, the standard bolt M16 has a longer fatigue life because the additional concrete gives it a greater stress range.

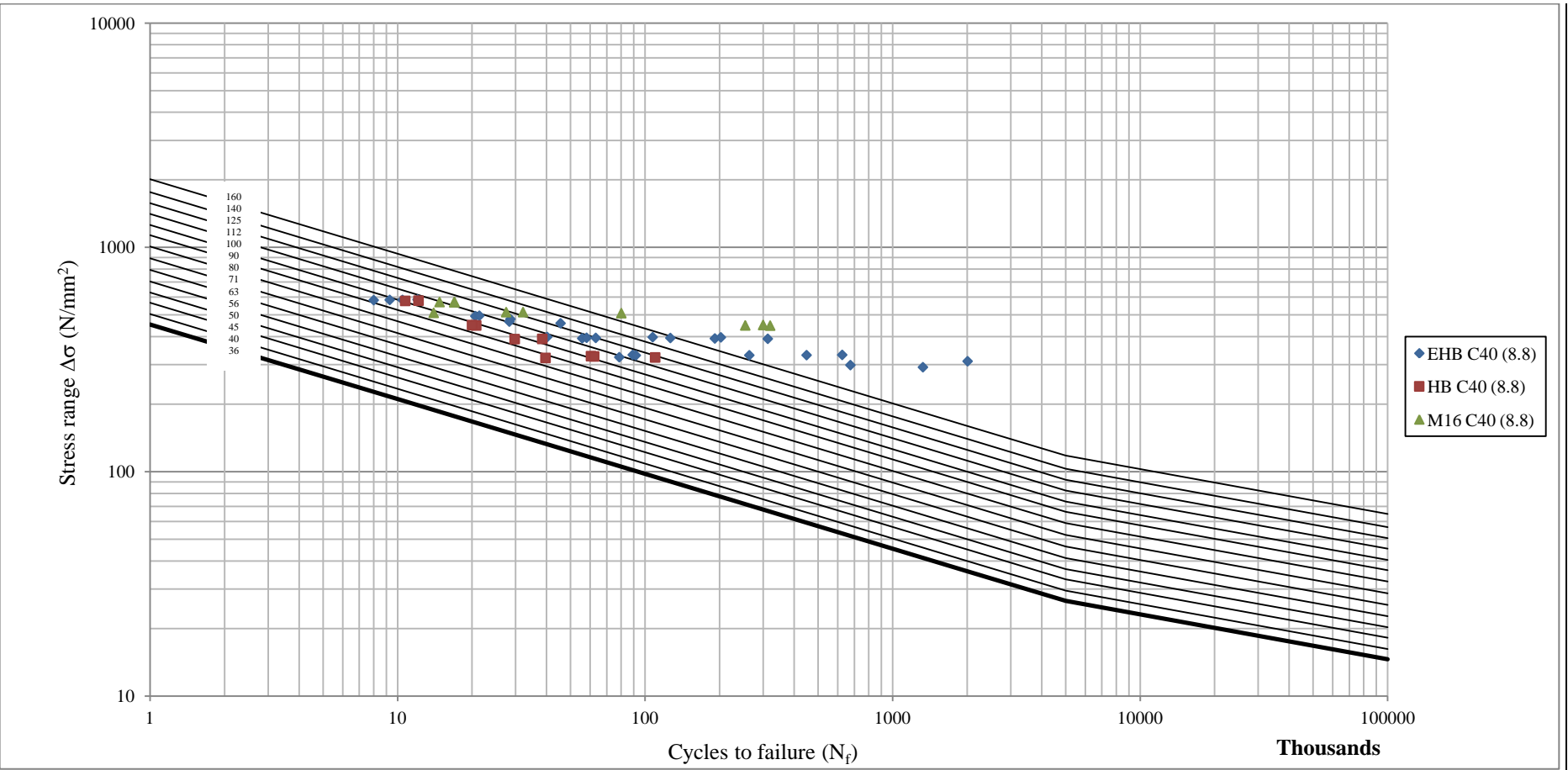


Figure 4.16 : S-N curve according to EC3 characteristics (BS EN1993, 2006)

---

#### 4.5 Effect of concrete strength

Concrete is one of the main components in connections that use EHB as fasteners. Static tests show that concrete improves the performance of the connection by significantly increasing the stiffness of the connection compared with unfilled connections (France et al., 1999).

In this study, concrete was used as a filled material confined in the tube section. In each test, the confined concrete behaved as a rigid mass. Based on the EHB fatigue test, no obvious bending of the tube section was observed. Failure of concrete was seen in the failure sample cored 100 mm diameter from the center of the bolt. Figure 4.17 shows the crack propagation on the concrete at different stress ranges. The crack line is located beside the red line. The crack pattern is nearly similar for each fatigue test of the EHB.



Figure 4.17 : Crack propagation on the concrete at stress ranges 584, 455, and 325  $\text{N/mm}^2$

A series of tests using higher concrete strengths was conducted. Here, C60 was used to investigate the effect of the concrete strength under fatigue load. A fatigue life-displacement graph and an S–N curve were employed to compare the two concrete

strengths. Figure 4.18 presents the results of the fatigue life test at a stress range of  $584 \text{ N/mm}^2$ .

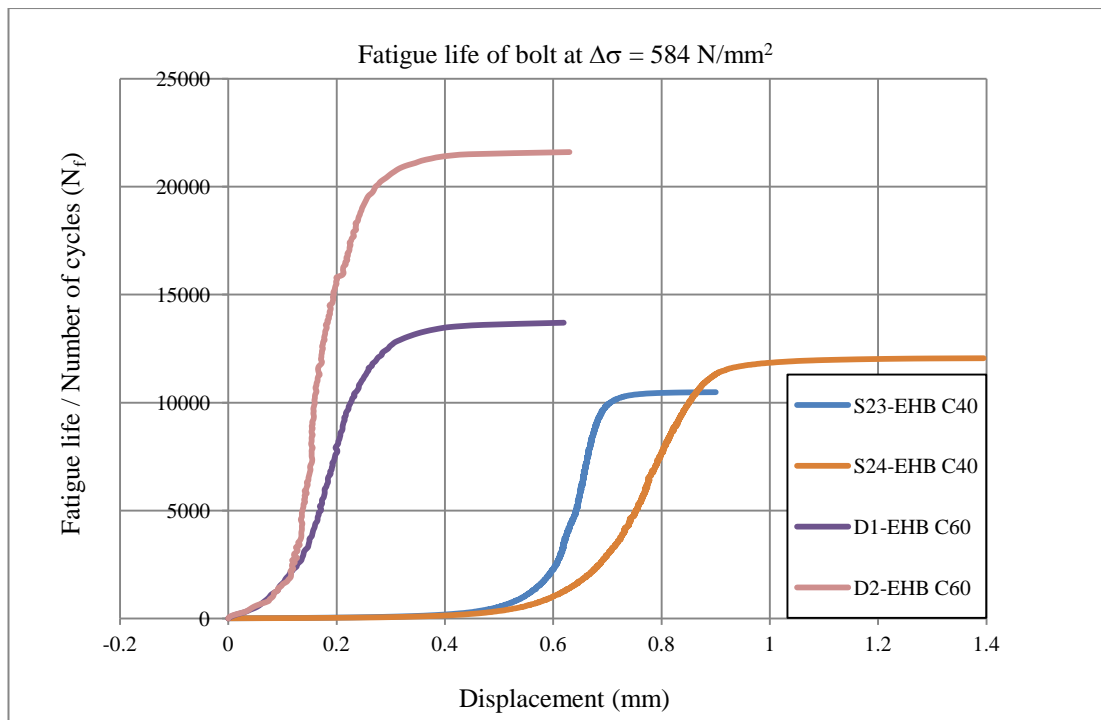


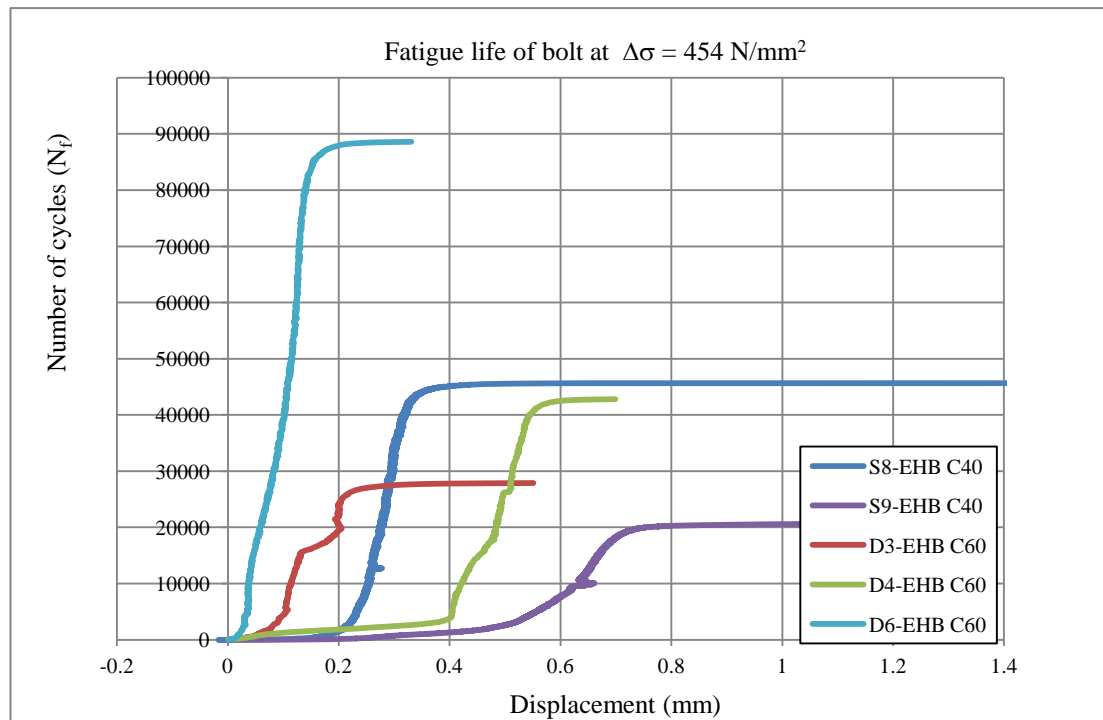
Figure 4.18 : Fatigue life-displacement graph at  $584 \text{ N/mm}^2$  stress range for C40 and C60

The two tests behaved similarly with an improvement in stiffness seen in the C60 samples. The sample's fatigue life was also improved, as shown in Table 4.7. An average of 40% improvement in fatigue life at a stress range of  $584 \text{ N/mm}^2$  was observed. This improvement could be explained by the increased bond strength between the EHB, the nut, and the concrete. At stress range  $454 \text{ N/mm}^2$ , the fatigue life using C60 was not consistent, even though the test was conducted on the same days (D3 and D4). This situation can be explained by the fatigue life–actuator movement graph in Figure 4.19. At this level, C40 and C60 did not exhibit similar behaviours, which might have led to the inconsistency in the fatigue life of the bolt. However, two out of three tests demonstrated that fatigue life increased with an

increase in concrete strength. Therefore, at this point, concrete strength does influence the fatigue life of the EHB, especially at a higher stress range.

Table 4.7 : Fatigue life of EHB using C40 and C60

Stress range (N/mm <sup>2</sup> )	C40		C60	
	Sample No.	Fatigue life (N <sub>f</sub> )	Sample No.	Fatigue life (N <sub>f</sub> )
584	S23	10,489	D1	13,840
	S24	12,063	D2	21,624
			D5	17,707
454	S8	45,631	D3	27,919
	S11	28,331	D4	42,862
	S12	28,632	D6	88,765

Figure 4.19 : Fatigue life displacement at  $454 \text{ N/mm}^2$  stress range for C40 and C60

---

**4.6 Chapter summary**

This chapter has presented the results of the fatigue tests conducted in this study. The results demonstrated that frequency does not influence the fatigue life of the EHB at high stress levels, but slightly influences the fatigue life at low stress ranges. The EHB was found to have a longer fatigue life than the standard HB, but has lower fatigue life than standard bolts when used in concrete-filled sections. For the three types of bolts investigated, a common failure mode was observed due to bolt fracture. The longer fatigue life of the EHB can be attributed to the bolt anchorage and the nut. The nut at the end of the EHB prevents the bolt from pulling out and gives the EHB more strength. In addition, concrete strength has a significant effect on the fatigue life of the EHB, especially at high stress levels. At lower levels, increasing the fatigue life does not indicate clear results in two out of three tests.

---

## Chapter 5 : Statistical and Reliability Analysis

---

### 5.1 Introduction

This chapter discusses the validation of fatigue test data, to perform the statistical analysis and to assess the reliability of the Extended Hollobolt. The statistical analysis is performed to assess the behaviour of EHB using S-N curve and using the limit state design technique. To assess the reliability index of EHB, the reliability is calculated and compare with target reliability index according to BS EN 1990 (2002). To perform the statistical and reliability analysis, only fatigue test data of the Extended Hollobolt (EHB, grade 8.8) with concrete strength C40 was analysed.

Currently, the most popular technique used for both research and applications in structural design is the limit state design technique. Limit state design focuses on the prediction of the actual load capacity at which failure will occur in the structure. The two types of limit states are listed below.

1. *Ultimate limit state* refers to the load at which the structure will collapse and at which it can no longer serve its intended function. This type of limit state is concern about the safety of structure. It can be threat as ultimate limit state when the structure loss of equilibrium, failure by excessive deformation, rupture, loss of stability of the structure including supports and foundation and failure cause by fatigue or other time-dependent effects.

- 
2. *Serviceability limit state* refers to the load at which the structure is damaged but can still accept additional load. Repair is usually required to restore the structure to an acceptable state. This type of limit state is concern about the functioning of the structure or structural members under normal use. The verification of serviceability limit states should be based on criteria concerning deformation that affect the appearance or the functioning the structure, vibrations and etc.

Eventhough fatigue is design under ultimate limit state design condition, in order to determine the fatigue behaviour under normal working load, it is appropriate to conduct this study under serviceability limit state design.

The limit state is usually combined with a type of probabilistic analysis to determine whether the calculated strength is sufficient enough to guarantee safety of use. In this study, probability analysis is conducted to validate the data from the fatigue test. Thus, suitable probability distribution is define to choose the appropriate method for statistical and reliability analysis.

## **5.2 Probability Distribution Function**

Fatigue testing determines the relationship between the fatigue resistance of a given material, component, or structural detail, and cyclic loading. The results of the fatigue endurance test are plotted on a graph that compares the applied loading (force, stress, strain, and etc) with the number of cycles prior to failure. Test specimens do not always meet testing conditions. Thus, the resulting data are invariably hampered by uncertainties that exist in the fatigue process (Schneider and

---

Maddox, 2003, Wirsching, 1998) although testing conditions are maintained as identical as possible. Consequently, critical judgement is essential in analysing the test data. Statistical methods assist in analysing fatigue test data and in providing recommendations on the use of such data for analysis, such as in the case of BS 2846 (BS 2846, 2002).

Given that individual fatigue failures are impossible to predict, failure from a given set of test conditions is assumed to be distributed randomly within a fairly predictable distribution function. The basic practice for the statistical analysis of fatigue test data, as outlined in Eurocode 3 Parts 1- 9 (BS EN1993, 2006) and in ECCS (1985), is available to guide the design. The fatigue life of a component is typically determined by tests that apply constant amplitude stress. Cycles to failure are measured, and a curve is fitted to the data. Mean and standard deviation are determined in accordance with the distribution function.

Probability distribution function is a general term used to express the variability in fatigue test results/data. In statistical quality studies, the underlying assumption is that the data are obtained from normal distribution (Chandrupatla, 2009, Schneider and Maddox, 2003). The other functions commonly used to represent fatigue data are the lognormal and Weibull distribution. In this study, only three distributions are discussed, namely, normal, lognormal, and Weibull distributions. The properties of these types of distributions are summarized in Table 5.1, where  $\beta$  is shape parameter of distribution,  $\alpha$  is scale parameter,  $\zeta$  is the Weibull shape parameter, and  $\Gamma$  is the gamma function.

Table 5.1: Properties of the normal, lognormal, and Weibull distributions (Walpole et al., 1998)

Distribution	Normal	Lognormal	Weibull
Parameters	$\mu_x, \sigma_x$	$\lambda_x, \zeta_x$	$\alpha, \beta$
Range of x	$-\infty < x < \infty$	$0 \leq x < \infty$	$0 \leq x < \infty$
Probability density function, $f_x(x)$	$\frac{1}{\sigma_x \sqrt{2\pi}} \exp\left(-\frac{1}{2}\left(\frac{x - \mu_x}{\sigma_x}\right)^2\right)$	$\frac{1}{\zeta_x x \sqrt{2\pi}} \exp\left(-\frac{1}{2}\left(\frac{\ln(x) - \lambda_x}{\zeta_x}\right)^2\right)$	$\left(\frac{x}{\epsilon}\right)^\beta \frac{\beta}{x} \exp\left(-\left(\frac{x}{\alpha}\right)^\beta\right)$
Cumulative distribution function, $F_x(x)$	$\int_{-\infty}^x f_x(x) dx$	$\int_{-\infty}^x f_x(x) dx$	$1 - \exp\left(-\left(\frac{x}{\alpha}\right)^\beta\right)$
Mean	$\mu_x$	$\exp\left(\lambda + \frac{1}{\zeta^2}\right)$	$\alpha \Gamma\left(1 + \frac{1}{\beta}\right)$
Variance	$\sigma_x^2$	$\left(\exp\left(\lambda + \frac{1}{\zeta^2}\right)\right)^2 (\exp(\zeta^2) - 1)$	$\alpha^2 \left(\Gamma\left(1 + \frac{2}{\beta}\right) - \left(\Gamma\left(1 + \frac{1}{\beta}\right)\right)^2\right)$

A distribution function is dependent on the data collection. For some data, a suitable distribution is difficult to define because not every distribution provides the best fit in defining the mean and standard deviation of fatigue life of selected data (Young and Ekvall, 1981). The form of distribution for the mean is typically defined using either lognormal or Weibull distribution. Normal and lognormal distributions are often used to represent material properties or strength estimates (Hess et al., 2002). The advantage of the lognormal distribution is that it excludes negative values. The choice of function is a matter of preference, given that most studies indicated that either function can be used to represent fatigue scatter on identical testing specimens with the probability  $P$  range of  $0.05 < P < 0.95$ , where the fatigue data should lie within the range.

---

### 5.2.1 Lognormal distribution

The lognormal distribution is commonly used for general reliability analysis, cycles to failure in fatigue, material strengths, and loading variables in the probabilistic design. The data follow the lognormal distribution when the natural logarithms of times or cycles to failure are normally distributed. The probability plot of  $i^{th}$  data in lognormal distribution is calculated using Equation 5-1, which is called median rank (MR) or Bernard's approximation (Johnson, 1951). The MR evaluates the probability of failure with a confidence level of 0.5. Figure 5.1 presents the probability graph of lognormal distribution for the proposed EHB. The standard  $z$  value in the  $y$ -axis is the  $NORMSINV(MR)$ , and MR is defined using Equation 5-1. Appendix B presents detailed data for the plotted graph.

$$P_i / MR = \frac{i - 0.3}{n + 0.4}, \quad \text{Equation 5-1}$$

where  $P_i$  = Probability at  $i$

$i$  = 1, 2, 3...  $n$

$n$  = number of test sample

MRs estimate the unreliability for each failure. The  $j^{th}$  failure in a sample of  $n$  units at 50% confidence level obtains the true value of probability of failure, which means that it is the best estimate for unreliability or reliability. Sometimes, the true value will be greater than the 50% confidence estimate (Johnson and G, 1951).

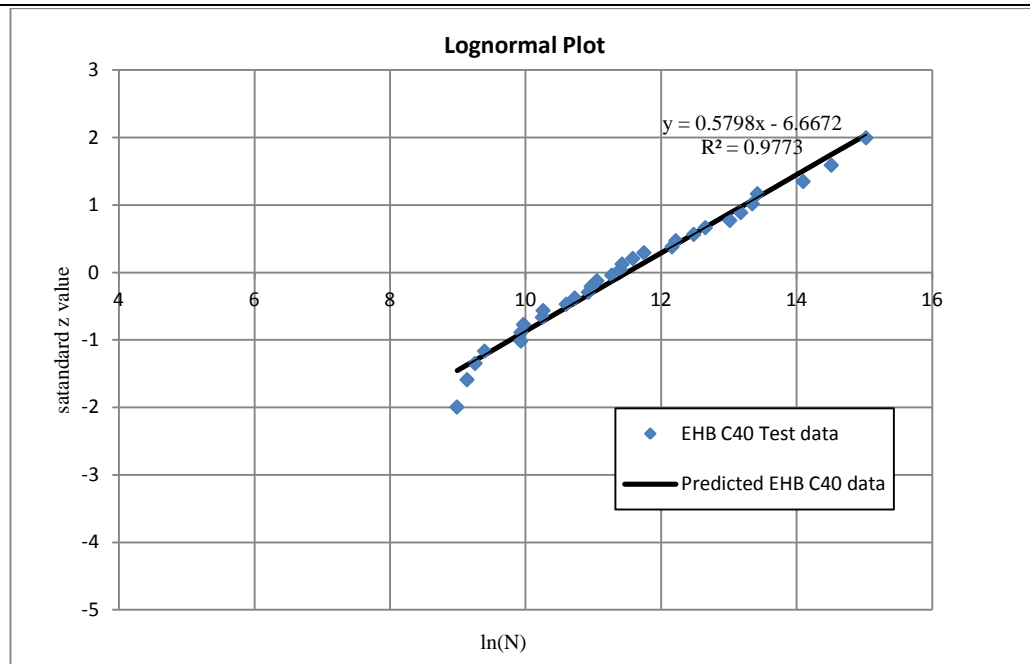


Figure 5.1 : Probability plot using lognormal distribution

The type of lognormal parameter should be determined to estimate the reliability of cycles to failure of a test using distribution function and to help define the shape of distribution. The effects of the shape parameter of a distribution are reflected in the shapes of the probability density function (PDF), the reliability function, and the failure rate function of the test data. The lognormal distribution assumes several shapes depending on the value of the shape parameter. The lognormal distribution is skewed to the right, where skewness increases as the value of  $\sigma$  increases (Figure 5.2).

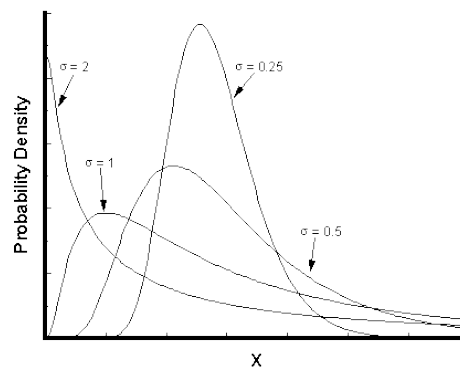


Figure 5.2 : Lognormal PDF

The shape parameter is used to predict the reliability of the cycles to failure in the fatigue test. Using the approximation of MR or Bernard's approximation, the reliability at the  $j^{\text{th}}$  failure is evaluated (Chandrupatla, 2009).

$$R(t_j) = 1 - MR_j \quad \text{Equation 5-2}$$

The shape parameter is defined by the lognormal parameters  $\mu$  and  $\sigma$ . Using the best-fit line, values of  $\mu$  and  $\sigma$  are calculated, where  $\mu = 16.6672/0.5798 = 1.500$ , and  $\sigma = 1/6.6672 = 1.7248$ . The graph of probability density, also known as the survival probability graph, is presented in Figure 5.3. Analysis of data is detailed in Appendix B.

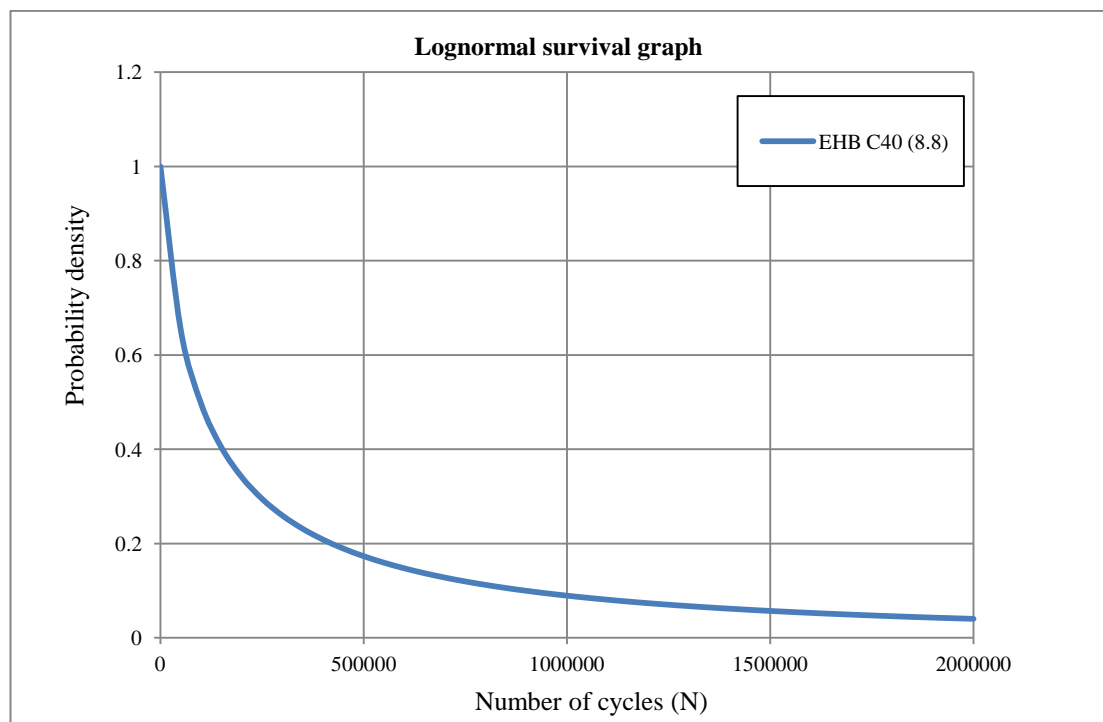


Figure 5.3 : Lognormal survival graph

### 5.2.2 Weibull distribution

The Weibull distribution is one of the most commonly used distributions in the assessment of reliability. This type of distribution is commonly used to model material strength; time to failure of electronic and mechanical components, equipment, or systems; and time to repair. The MR is used in a manner similar to lognormal distribution to evaluate the probability of failure of the  $i^{th}$  data point with a confidence level of 0.5 (50%) or with the mean value of the data. The probability of the data plot is shown in Figure 5.4.

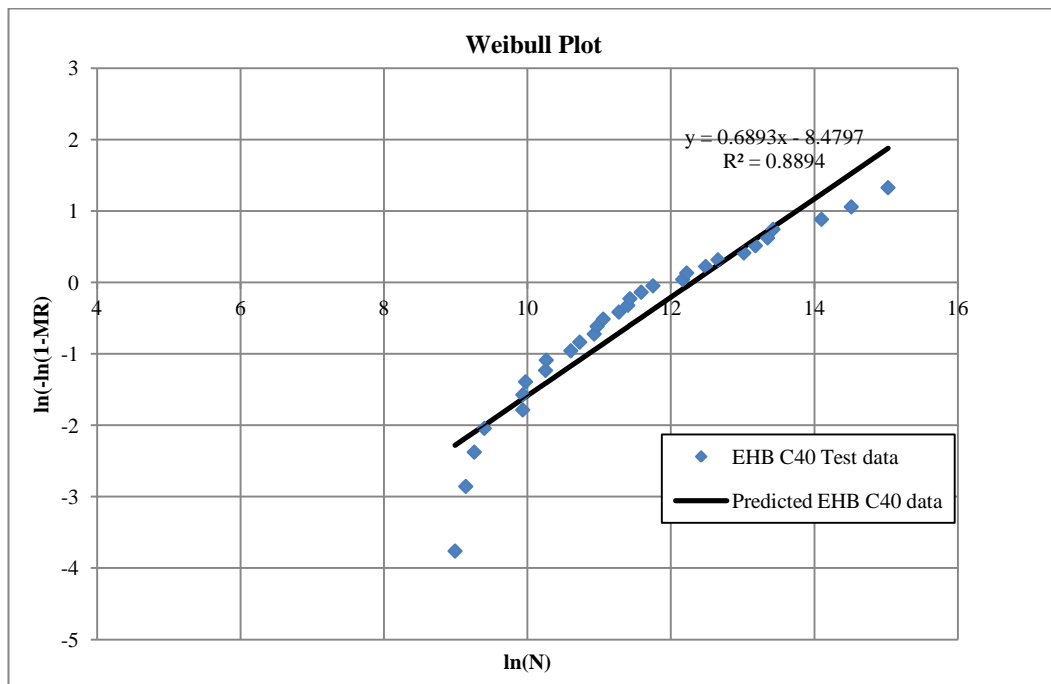


Figure 5.4 : Probability plot using Weibull distribution

After the Weibull distribution is plotted, the Weibull parameters can be defined. The shape of the PDF plot depends on the value of the Weibull parameter  $\beta$  (Figure 5.5).

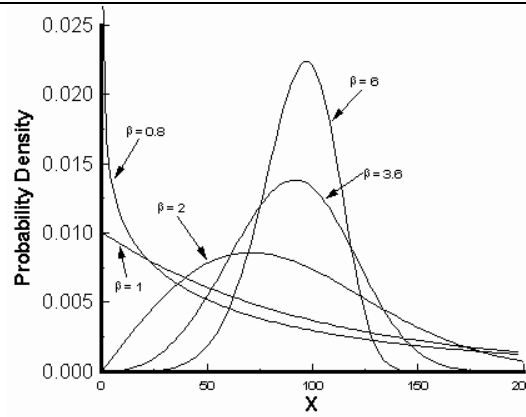


Figure 5.5 : Weibull PDF (Survival graph)

By changing the value of the shape parameter  $\beta$ , the Weibull distribution can model a wide variety of data. If  $\beta = 1$ , the Weibull distribution is identical to the exponential distribution; if  $\beta = 2$ , the Weibull distribution is identical to the Rayleigh distribution; and if  $\beta$  is between 3 and 4, the Weibull distribution approximates the normal distribution. The Weibull distribution approximates the lognormal distribution for several values of  $\beta$ .

In the EHB C40 data analysis, the shape parameter is  $\beta = 0.7$ , which is close to the exponential distribution function. This study does not discuss the exponential distribution. The shape parameter or survival graph predicts the reliability of the fatigue life at  $x$  for the EHB connection to the concrete-filled tube. For example, based on the graph, the reliability of EHB is predicted to be 0.059 at a 1 million cycle fatigue life.

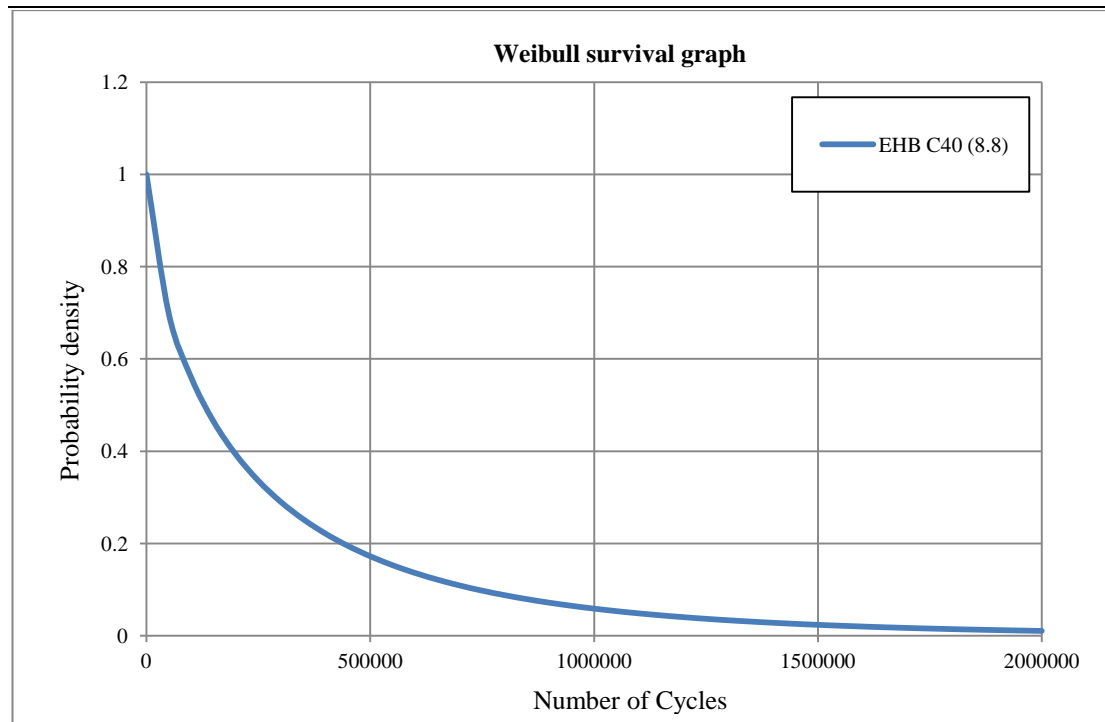


Figure 5.6 : Survival graph using the Weibull distribution of EHB C40 test data

### 5.2.3 Normal distribution

Normal distribution is the most commonly used distribution in statistical analyses of data. The normal distribution can describe the statistical behaviour of a large number of real events. The shape of the normal distribution is completely defined by the mean and standard deviation (Table 5.1). Given the mean and standard deviation, the probability of normal distribution can be computed. The first step is to plot the probability of the data. Basically,  $n$  data points are arranged in ascending order. Therefore, the probability value for the  $i^{\text{th}}$  data point is assumed to be the following:

$$P_i = \frac{i - 0.5}{n} \quad \text{Equation 5-3}$$

The  $z$ -value corresponding to  $P_i$  is defined using the standard normal inverse ( $z_i$ ) to plot normal probability, and  $x_i$  versus  $z_i$  is plotted (Figure 5.7).

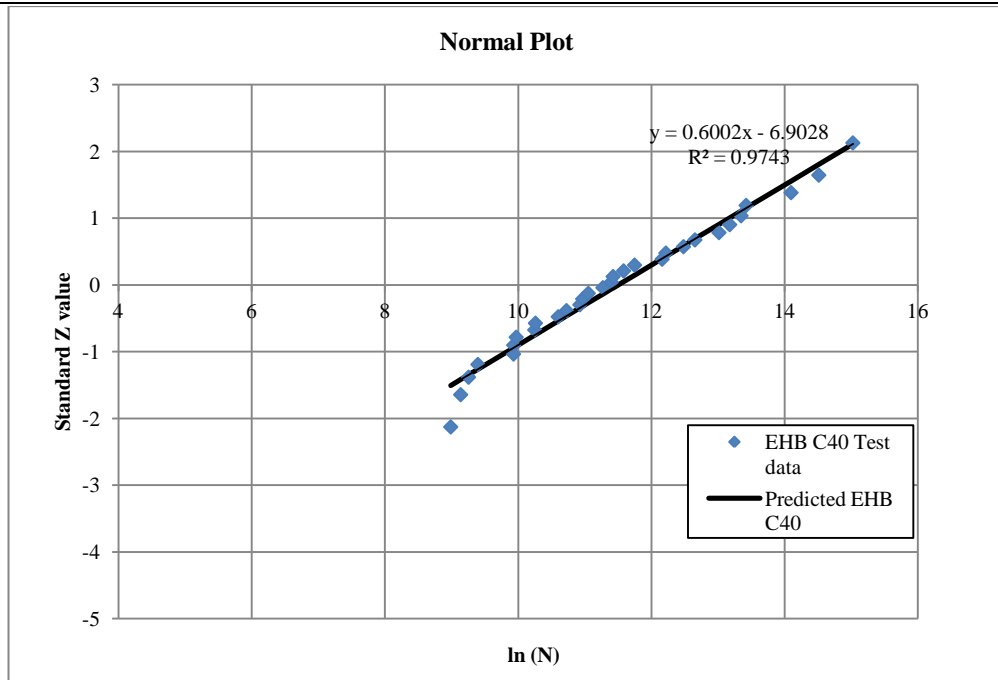


Figure 5.7 : Probability plot using Normal distribution

The shape of normal distribution is the familiar bell shape. Therefore, no shape parameter exists.

#### 5.2.4 Distribution Discussion

The best-fit equations and corresponding  $R^2$  values obtained from the three distributions are summarized in Table 5.2. The EHB test data are not widely scattered, according to the  $R^2$  value of the fitted probability distribution, which is almost equal to 1 for the normal distribution and lognormal distribution.

In all graphs (Figure 5.1, Figure 5.4, and Figure 5.7) above and in Table 5.2 below, the distribution of the fatigue life data best fit with normal or lognormal distribution based on their respective R-squared value (goodness-of-fit). The R-squared value was 0.9743 for normal distribution and 0.9773 for lognormal distribution. When the data are plotted in Weibull scales, the linear fits are less accurate, with R-squared values ranging down to 0.8894.

Table 5.2 : Comparison of the three distributions

	Normal distribution	Lognormal distribution	Weibull distribution
Line fit equation	$y = 0.6028x - 6.9028$	$y = 0.5798x - 6.6672$	$y = 0.6893x - 8.4797$
$R^2$	0.9743	0.9773	0.8894

Among the three graphical analyses, lognormal and normal distribution are considered the appropriate distribution types for the fatigue test of EHB connected to a concrete-filled hollow section. The fatigue tests are capable of investigating the reliability of the EHB. Therefore, the characteristic S-N curve can be defined using the statistical equation of lognormal format, as suggested in the British Standard (BS ISO, 2003), the details of which are discussed in the next section.

### 5.3 Extended Hollobolt S-N curve characteristic

For typical S-N curves, a linear fit is obtained using  $\log(N)$  and  $\log(S)$ . The fitting technique (least squares) should identify the best-fit straight line through the data. A standard practice in analysing fatigue data using the fitting technique is offered by the British Standard (BS ISO 12107, 2003). The best-fit straight line through the data is estimated by ordinary linear regression, as described by Gurney and Maddox (1973). A general method to estimate the slope and intercept coefficients is called “least square estimation.” Therefore, the basic equation that represents the S-N curve is given by:

$$\log N = \log A - m \log \Delta \sigma, \quad \text{Equation 5-4}$$

---

where  $\log$  corresponds to base 10,  $m$  is the slope, and  $A$  is the intercept. This equation can be rewritten in the following form, which is commonly used to describe S-N curves in design rules:

$$\Delta\sigma^m N = A \quad \text{Equation 5-5}$$

Using Equation 5-5, the strength model can be written as the following linear regression (Schneider and Maddox, 2003):

$$Y = a + bX \quad \text{Equation 5-6}$$

where

$$X = \log\Delta\sigma, Y = \log N, a = \log A, b = -m$$

Fatigue strength can be computed over a fatigue life range covered by the straight line if the slope of the line and one point on the line are known. However, only one type of stress cycle and one detail are represented on an individual S-N curve. In this case, the S-N curve is represented by the curve for bolt in tension (BS EN1993, 2006), where a similar assumption is applied in the classification of bolts in EC3. Using the equation above, the mean value of the scattered fatigue data can be defined by plotting the data using a log-log graph. The British Standard (BS ISO 12107, 2003) offers a standard practice for this class of analysis.

Figure 5.8 presents the fitting graph of mean values for three types of bolts. Thus, the EHB has a fatigue life performance in between that of the HB and the standard bolt (M16). Further details are provided in Chapter 4.

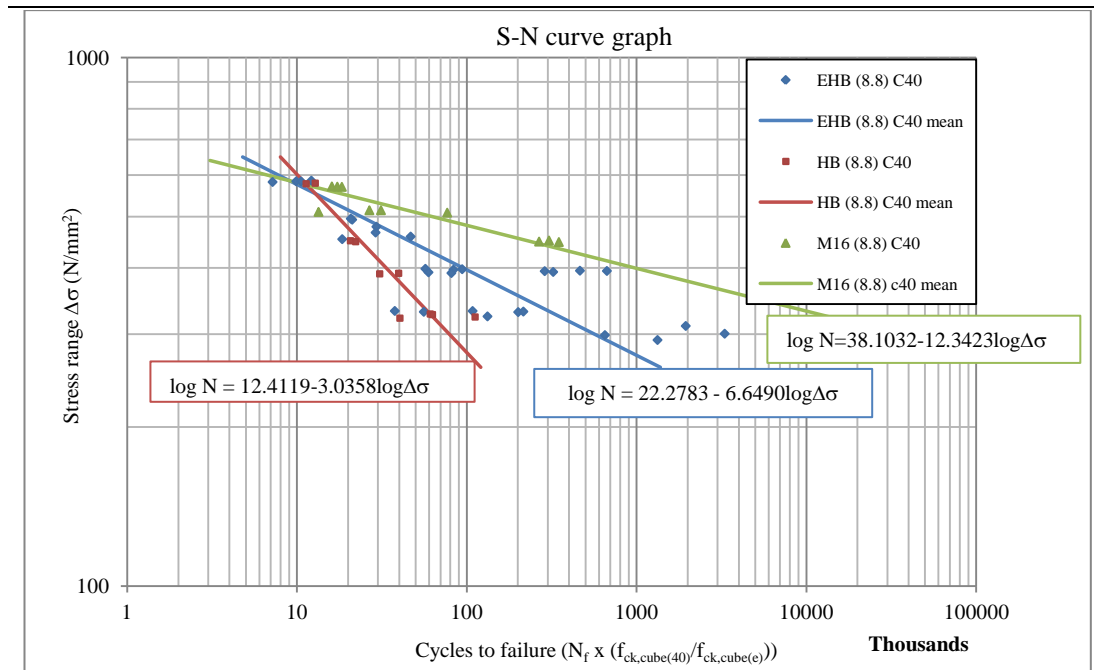


Figure 5.8 : Curve-fitting graph

At  $580 \text{ N/mm}^2$  nominal stress range, the fatigue lives of the three types of bolts were almost identical. When a lower stress range was applied, the fatigue life of the EHB spread more compared with those of the other types of bolts. This phenomenon has already been discussed in Chapter 4.

The confidence and tolerance limit for the test data need to be defined to establish the S-N curves. The difference between confidence limits and tolerance limits should be emphasized. The confidence limit/interval provides a method to measure the precision of an estimate. If the sampling distribution of the parameter in question is known, the confidence limit is easily set. In many cases, given sufficient accuracy, the distribution may be normal. Meanwhile, the tolerance limit/interval is significantly more accurate in determining whether the data fall within the range.

### 5.3.1 Tolerance Limits

Typical curve fitting determines the average fatigue behaviour of materials given an appropriate range of stress levels. Scattered data indicate that some materials have lower strength and some have higher strength than the average. A distribution of strengths typically underlies the scatter of fatigue data.

An alternative methodology for the establishment of a characteristic curve is called tolerance limit. Tolerance limits are based on the estimation of confidence limits. Tolerance limits are a valuable tool for the study of the sensitivity of design curves and can be used to justify design curves that are based on small samples, especially for sample sizes smaller than 40 (Schneider and Maddox, 2003).

In this study, tolerance limit ensures that test data are within the range of  $0.05 < P < 0.95$ , as discussed in Section 5.2, where  $P$  denotes the probability of the specimen.

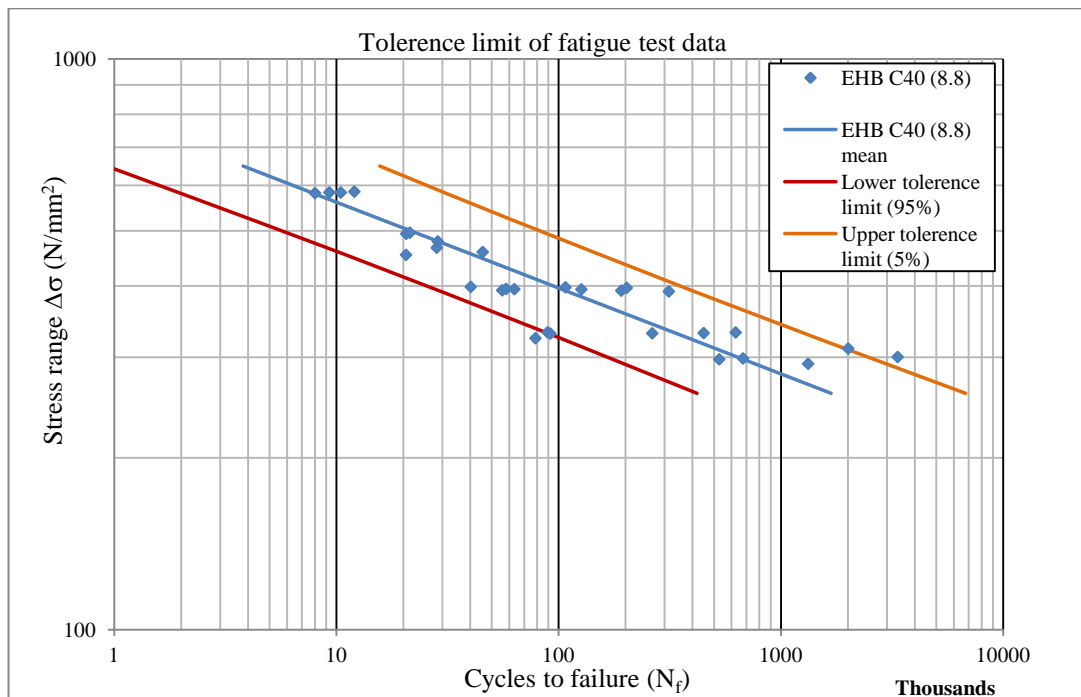


Figure 5.9 : Tolerance limit for fatigue test data

---

Statistical analysis based on Eurocodes (BS ISO 12107, 2003) was used to analyze experimental fatigue data. Figure 5.9 shows the tolerance limit of the test data. The fatigue test data based on the tolerance limit prediction value are considered acceptable because all data are between the range 5% to 95% of the tolerance limit, which is  $\pm 45\%$  from mean of test data. Two-sided tolerance limit has always been discussed or practically used in numerous statistical analyses. However, Little (1981) proposed the one-sided lower statistical tolerance limit and confirmed its suitability for analysing fatigue data. When the one-sided lower case is considered, the minimum limit for the study becomes 95% (-45% from mean test data), a value that is called the confidence limit. Therefore, the confidence limit is used to define the S-N curve of the EHB connection to the concrete hollow section. A 95% confidence level is adopted by EC3 for the design of the S-N curve, along with a 95% probability level, which is applicable for structures exposed to normal atmospheric conditions (ISSC Committee III.2, 2009)

### **5.3.2 Confidence limit/level**

For design purposes, establishing limits between the boundaries of data proportions (typically 95%) is necessary. These boundaries are often called “confidence limits.” The established confidence limit properties of fatigue strength provided by the designer are used with confidence in design (Herbet J. Sutherland and Veers, 2000). In case of actual data, the prediction limits at stress range  $\Delta\sigma$  can be expressed explicitly in the following form (Schneider and Maddox, 2003, BS ISO 12107, 2003):

$$\log N_{p\%} = (\log A + m \log \Delta \sigma) - t \hat{\sigma} \sqrt{1 + \frac{1}{n} + \frac{(\log \Delta \sigma - \overline{\log \Delta \sigma})^2}{\sum_{i=1}^n (\log \Delta \sigma_i - \overline{\log \Delta \sigma})^2}} \quad \text{Equation 5-7}$$

or

$$y_{p\%} = (a + bx) - t \hat{\sigma} \sqrt{1 + \frac{1}{n} + \frac{(x - \bar{x})^2}{\sum_{i=1}^n (x_i - \bar{x})^2}} \quad \text{Equation 5-8}$$

where  $\log A(a)$  and  $m(b)$  are the coefficients of the regression line through the  $n$  data points,

$\overline{\log \Delta \sigma}$  is the mean of the  $n$  values of  $\log \Delta \sigma_i$ ,

$t$  is the appropriate percentage points of  $t$  distribution, with  $n-2$  degrees of freedom ( $v$ ), and

$\hat{\sigma}$  is the best estimate of the standard deviation of the data about the regression line.

The value of  $t$  is defined from the student's  $t$  distribution. The  $t$  distribution of the student (Appendix C) is applied if sample  $n > 30$  is used to estimate the confidence limit/level of the mean when the standard deviation is unknown. All terms inside the root sign in Equation 5-8 is a correction to the estimated standard deviation for the population. This correction depends on the number of tests and on the range covered by the tests. When the number and the range of the tests are sufficient, the correction term is close to 1 and may be neglected. Equation 5-9 is used to calculate the estimated standard deviation of the fatigue life from the mean of the S-N curve as follows:

$$S_x = \sqrt{\frac{\sum_{i=1}^n [y_i - (a - bx_i)]^2}{n - 2}} \quad \text{Equation 5-9}$$

where

$a$  and  $b$  are the coefficients of the regression line through the  $n$  data points, and

$S_x$  is the standard deviation of  $x$  data.

The predicted lower limit of the fatigue data is also known as the design characteristic (Collate, 2005), where the lower limit provides low stresses. The definition of characteristic design is illustrated in Figure 5.10. In conventional usage (e.g., in design), the load or strength is described only by this value (Melchers, 2001). A linear extrapolation of the S-N curve at lower stresses will normally tend to be safe because of the approach to the fatigue limit (Gurney, 1979).

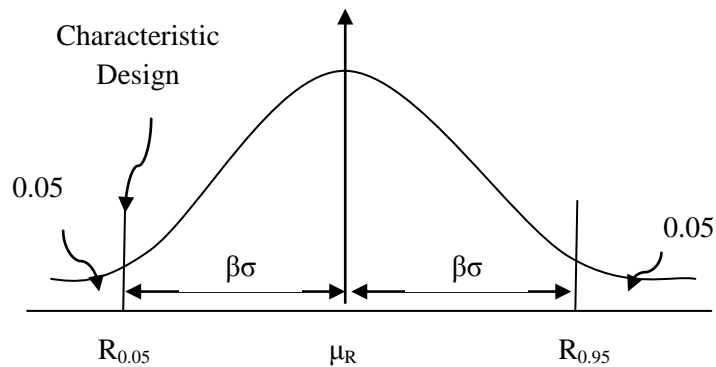


Figure 5.10 : Definition of characteristic resistance

Using the equations from the available design code (BS ISO 12107, 2003), that is, Equations 5-6 and 5-8, the S-N curve of characteristic design is plotted and is shown in Figure 5.11, and the S-N curve result is summarized in Table 5.3. Therefore, the characteristic design of the EHB can be written as

$$\log N = 21.4863 - 6.5747 \log \Delta \sigma \quad \text{Equation 5-10}$$

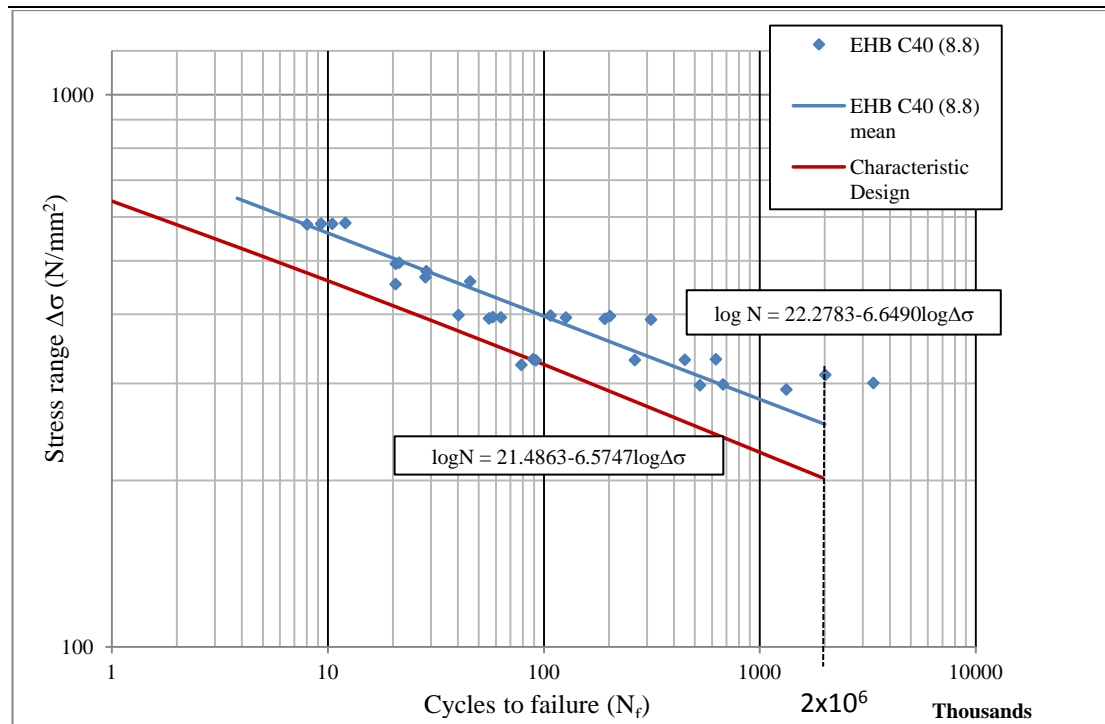


Figure 5.11 : S-N curve characteristic design

Table 5.3 : S-N Curve result of the EHB

Description	Slope m	Stress at 2 million cycles (N/mm <sup>2</sup> )
Mean value	6.6	253
Characteristic value	6.6	204

Using Equation 5-10, the stress range of the EHB can be classified as 204 N/mm<sup>2</sup> at 2 million cycles, which is above the recommendation of Eurocode 3, parts 1-9.

### 5.3.3 Standard deviation

Standard deviations vary from test to test and from the type of details studied. A higher stress concentration factor generally results in a lower standard deviation for fatigue testing. Table 5.4 shows the standard deviation of fatigue strength of the EHB

---

compared with other types of detail categories that appear in Appendix C of ECCS (1985). These values were obtained from the statistical analysis.

Table 5.4 : Standard deviation of various types of detail category

<b>Type of detail</b>	<b>Range of standard deviation</b>
Rolled beam	0.125– 0.315
Welded beam	0.150– 0.230
Vertical stiffener	0.115– 0.190
Longitudinal attachment	0.115– 0.140
Cover plate on flange	0.070– 0.140
Extended Hollobolt	0.05

The table of standard deviation shows that EHB has higher stress concentration compared with other types of materials. The calculation of the standard deviation of EHB in Table 5.4 is based on the statistical analysis method provided by Eurocode, as shown in Equation 5-9.

#### **5.4 Introduction to fatigue reliability**

Reliability analysis is used to ensure safe resistance factor evaluation of blind bolts (Tabsh and Mourad, 1997). Several related topics on fatigue reliability design have been discussed by such researchers as (Park et al., 2010), Xu and Wang (2011), and Carpenter (Carpenter, 2011). Wirsching (1998) discussed this topic and proposed a procedure for determining fatigue reliability. The first step in fatigue reliability analysis is defining the fatigue model. Two fatigue models are typically used in

---

determining the fatigue reliability: the S-N approach and the fracture mechanics approach. The S-N approach is a traditional model that describes fatigue life under constant amplitude. This method is based on the experimental measurement of fatigue life in terms of failure cycles at different loading levels. The fracture mechanics approach, on the other hand, is based on the existence of an initial crack in a stress-free structure. The fracture mechanics approach is more detailed and involves the examination of crack growth and determines the number of load cycles needed for small initial defects to grow into cracks that are sufficiently large to cause fracture.

Constant amplitude is applied in this study. Therefore, the S-N approach is more suitable for analysing the reliability of the EHB connected to concrete-filled hollow sections under fatigue loading.

## **5.5 Fatigue reliability analysis**

Several numerical methods can be used to evaluate the failure probability of safety index. These methods include the first-order reliability method (FORM), the second-order reliability method (SORM), and the Monte Carlo method. FORM is one of the methods used for utilizing the reliability index and is the most used method in providing the safety index with the application of lognormal distribution. SORM is recommended if lognormal is not applied. The FORM technique emerged from the efforts to find a simple method of estimating the failure probability of the linear state functions of several variables by initially assuming that the variables follow a normal distribution. The technique was proven quite powerful for handling complex cases involving non-normal variables, non-linear limit state functions, and correlated variables. Approximately 90% of all applications that use this first-order theory

---

fulfill all practical needs because the numerical accuracy is more than sufficient (Rackwitz, 2000).

The development of the reliability, safety index, and safety factor of the experimental data is discussed in Annex C of BS EN 1990 (2002) and in Appendix C of ECCS (ECCS, 1985). The FORM method, which is based on the first-order Taylor series approximation of limit state function defined below, is used in this study:

$$g(R, S) = R - S \quad \text{Equation 5-11}$$

where

R = Resistance normal variables

S = Load normal variable.

Assuming that R and S are statistically independent from the normally distributed random variables, variable g is also normally distributed. Failure occurs when  $R < S$ , that is,  $g < 0$ . In this case, the failure probability can be stated as:

$$P_f = \text{Prob}(g \leq 0) = \text{Prob}(g \leq \mu_g - \beta \sigma_g) \quad \text{Equation 5-12}$$

$$P_f = \Phi(-\beta)$$

where  $\mu_g$  and  $\sigma_g$  are the mean and standard deviation of the variable g, respectively;  $\Phi$  is the cumulative distribution function for the standard normal variables; and  $\beta$  is the safety index or the reliability index. The coefficient of variance is denoted as:

$$\beta = \frac{\mu_g}{\sigma_g} = \frac{\mu_R - \mu_S}{\sqrt{\sigma_R^2 + \sigma_S^2}} \quad \text{Equation 5-13}$$

$$C.O.V = \frac{\sigma_{xi}}{\mu_{xi}}$$

Equation 5-14

### 5.5.1 Safety index and probability of EHB

The first step in evaluating the reliability of the grade 8.8 EHB with concrete strength C40 is to calculate the safety index ( $\beta$ ). Hesofer–Lind (1974) defined safety index as the probability of failure as the distance from the origin to the failure surface becomes shorter, as shown in Figure 5.12.

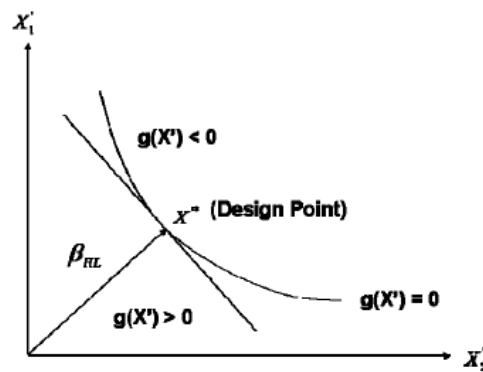


Figure 5.12 : Geometric representation of the safety index  $\beta$  based on the Hesofer–Lind approach

In this study, the fatigue life is expressed in terms of the number of cycles of stress, therefore the R values becomes the number of cycles required to cause failure  $f$  the material (experimental data) and S the required number of cycles to satisfy design requirement (Eurocode 3 part 1-9) for a given lifetime (Melchers, 2011).

Equation 5-13 defines the value of  $\beta$  as 4.2. The probability table (Appendix E) defines the value of  $\Phi(-\beta)$  as  $0.1332 \times 10^{-4}$ . The probability of the EHB using the safety index value is determined by Equation 5-12. Therefore, from the experiment result, the failure probability of the EHB can be concluded as equal to  $0.1332 \times 10^{-4}$ . (Appendix D).

### 5.5.2 Discussion on the reliability of the Extended Hollobolt

Based on the statistical and reliability analyses discussed above, the FORM method proposed by the British Standard is used. The reliability index or the probability of survival of the proposed blind bolt is 0.999, and the failure probability ( $P_f$ ) is  $0.1332 \times 10^{-4}$ . Reliability can be defined from  $1 - P_f$ .

To performed the reliability check on fatigue design for proposed bolt, the computed reliability safety index ( $\beta$ ) resulting from reliability assessment using FORM should not be less than the target safety index ( $\beta_o$ ) (Ayyub et al., 2002) as given by equation

$$\beta \geq \beta_o \quad \text{Equation 5-15}$$

From the computed safety index ( $\beta = 4.2$ ) is higher than target safety index (Table 5.5). It shows the Extended Hollobolt is adequate to use in connection design under serviceability limit state. Other safety index calculation is involved the characteristic design of Extended Hollobolt and the safety index is 1.76. It shows the EHB is reliable under fatigue assessment.

Table 5.5 : Target reliability index  $\beta_o$  for class RC2 structural members<sup>1</sup> (BS EN1990, 2002)

Limit State	Target Reliability Index	
	1 Year	50 Years
Ultimate	4.8	3.8
Fatigue		1.5 to 3.8 <sup>2)</sup>
Serviceability (Irreversible)	2.9	1.5
<sup>1)</sup> See Annex B		
<sup>2)</sup> Depends on the degree of inspectability and damage tolerance		

---

## 5.6 Chapter summary

Three probability distributions were investigated, namely, lognormal, normal, and Weibull distributions. Lognormal and normal distributions have the best fit for the probability function. These distributions are used for statistical and reliability analyses to define such parameters as mean and standard deviation values.

Tolerance limits were defined to establish the S-N curve using BS ISO 12107(BS ISO, 2003) as a guideline for establishing the S-N curve of the EHB. Fatigue life prediction for the EHB was proposed with a 95% confidence interval. The equation  $\log N = 21.4863 - 6.5747 \log \Delta \sigma$  was used to predict the fatigue life of the EHB.

Two methods are typically used to determine the reliability of a material, a connection, and so on. These methods are the S-N Curve and the fracture mechanic methods. The S-N curve method is adopted in this study because the samples were tested using constant amplitude. Applying the so-called FORM method, the safety index of the EHB was found to be 4.2, and probability of failure was  $0.13 \times 10^{-4}$ . These results show that the reliability of EHB is 99.99, which indicates that the EHB is reliable for connection design.

---

# Chapter 6 : Conclusions and Recommendations for Future Work

---

## 6.1 Introduction

This thesis has presented the results of an experimental program aimed at examining the behaviour of an Extended Hollobolt under repeated load. A statistical analysis of the experimental data has also been discussed. In this chapter, the research conclusions are presented. Recommendations for future work aimed at defining the fatigue behaviour of the investigated blind bolt connection are also proposed.

The results of previous studies have shown that the use of blind bolt fasteners to connect to a concrete-filled tube provides stiffer behaviour compared with an unfilled hollow section. An Extended Hollobolt is a type of blind bolt that is a modification of the Standard Hollobolt with added anchorage. The Extended Hollobolt presents an improvement in the behaviour of the connection because the load can be shared between the tube wall and the anchorage.

One of the tests conducted by Elghazouli (2009) showed that fatigue behaviour considered as low-cycle fatigue occurs during the cyclic test performed on the Hollobolt. Therefore, a series of fatigue test was conducted to investigate the behaviour of an Extended Hollobolt connected to a concrete-filled hollow section.

---

## 6.2 Conclusion

This work aimed to investigate the fatigue behaviour and reliability of the Extended Hollobolt when connected to a concrete-filled hollow section. In this section, a summary of the key findings and observations are listed as follows:

- Frequencies less than 3 Hz, shows no difference in fatigue life because the actual load during the test is equal to the applied load before the test started. However at a frequency of 5 Hz, the actual load produced during the test was higher than the applied load. Therefore, frequencies ranging from 0.25 Hz to 3 Hz are more suitable for an Extended Hollobolt connected to a concrete-filled hollow section.
- The fatigue life and strength of an Extended Hollobolt were lower than those of a Standard bolt but higher than those of a Standard Hollobolt. This finding was proven by an S-N curve, where the fatigue strength at two million cycles of the Extended Hollobolt was 253 N/mm<sup>2</sup>, M16 was 377 N/mm<sup>2</sup>, and Hollobolt was 103 N/mm<sup>2</sup>.
- The fatigue fracture of an Extended Hollobolt is located at the shank and is near the head of the bolt. A close-up of the pattern of the fracture was compared using photography. The comparison shows no obvious trend in shape at the lower stress range but a different trend at the highest stress range. The difference can be attributed to the increased plasticity at the higher stress range, which is near the yield stress of the bolt in this study.
- Using different concrete strengths, the fatigue life of an Extended Hollobolt was shown to increase using the concrete strength 60 N/mm<sup>2</sup>.

---

However, further studies should be conducted to obtain a more accurate understanding of the fatigue characteristic effect of concrete strength.

- A statistical analysis was conducted to analyze fatigue data, as well as the performance of an Extended Hollobolt connected to a concrete-filled hollow section using S-N curve characteristics. An equation of the characteristic design with 95% confidence is proposed. This equation is limited to an Extended Hollobolt grade of 8.8 with a concrete strength  $35 < f_{ck,cube} < 42$ .

$$\log N = 21.4863 - 6.5747 \log \Delta \sigma$$

- The S-N curve method was used to determine the reliability of the Extended Hollobolt connected to a concrete-filled hollow section. From the reliability analysis using the First Order Reliability Method, calculated safety index ( $\beta$ ) is larger than target safety index ( $\beta_0$ ), therefore the Extended Hollobolt was found to be adequate and reliable for design of connection.

### 6.3 Recommendations for further study

The results of this study indicate that the Extended Hollobolt connected to a concrete-filled hollow section is reliable for use. However, further studies under fatigue load should be conducted to improve the behaviour and reliability of the proposed bolt. Further studies will facilitate the establishment of a design procedure for Extended Hollobolts in practical connections. The recommendations for further study can be concluded as follows:

- 
- Further tests for grade 10.9 bolt connections should be conducted following the same design parameters used for grade 8.8 to determine the differences and the effects of fatigue using different bolt grades.
  - Bolts with different diameters and connected with different concrete strengths should be tested to complete the assessment of Extended Hollobolts connected to concrete-filled hollow section under fatigue load.
  - The effects of axial loading resulting from torque on the fatigue life of bolts should be tested to assess the fatigue life of actual bolts.
  - Variable amplitudes should be used in conducting the fatigue test to determine the cumulative damage and fracture mechanics of the Extended Hollobolt.
  - Tests on displacement control should also be conducted to study its influence on the Extended Hollobolt.
  - Further investigations on reliability and probability using more experimental data to compare with other types of bolt should also be conducted.
  - Finite element modeling should be used to investigate the behaviour of Extended Hollobolts under fatigue load for comparison with the experimental results and for parametric studies.

---

**References**

1. AL-MUGHAIRI, A. S. (2009) The Behaviour of Moment Resisting Connection to Concrete Filled Hollow Sections Using Extended Hollowbolts University of Nottingham.
2. ASTM (1991) Standard practice for statistical analysis of linear or linearized stress-life and strain-life fatigue data. PA, ASTM.
3. ASTM, Committee E-9 on Fatigue American Society for Testing and Materials: American Society For Testing And material. (1963) A Guide for Fatigue testing and the statistical Analysis of Fatigue Data. American Society For Testing And material.
4. AYYUB, B. M., ASSAKKAF, I. A., KIHLE, D. P. & SIEV, M. W. (2002) Reliability-Based Design Guidelines for Fatigue of Ship Structures. *Naval Engineers Journal*, 114, 113-138.
5. AZIZINAMINI, A. & SCHNEIDER, P.S. (2004) Moment connection to circular concrete filled steel tube columns. *Journal of structural Engineering*, 213-222.
6. BALLIO, G. & CASTIGLIONI, C. A. (1995) A Unified Approach for the Design of Steel Structures under Low and/or High Cycle Fatigue. *Journal Construction Steel Research*, 34, 75-101.
7. BARNETT, T., TIZANI, W. & NETHERCOT, D. A. (2000) Blind bolted moment resisting connection to structural hollow section. *Connections in Steel Structures IV: Steel Connections in the New Millennium*. Roanoke, Virginia, USA.
8. BARNETT, T.C. (2001) The Behaviour of a Blind Bolt for Moment Resisting Connections in Hollow Steel Section. PhD thesis. *Department of Civil engineering* University of Nottingham.
9. BARNETT, T.C., TIZANI, W. & NETHERCOT, D.A. (2001) The Practice of Blind Bolting Connection to Structural Hollow Sections: A Review. *Steel and Composite Structures*, 1, 1-16.
10. BARSOM, J. M. & ROLFE, S. T. (1999) *Fracture and Fatigue Control in Structures - Applications of Fracture Mechanics: (MNL 41)*, ASTM International.
11. BEER, F. P. & JOHNSTON, E.R. (1981) *Mechanics of Materials* McGraw Hill.Inc.

- 
12. BENJAMIN V. FELL & KANVINDE, A. M. (2009) Recent Fracture and Fatigue Research in Steel Structures. *STRUCTURE*.
  13. BERETTA, S., CLERICI, P.& MATTEAZZI, S. (1995) The effect of sample size on the confidence of endurance fatigue tests. *Fatigue Fracture Engineering Material Structure*, 18, 129-139.
  14. BIRKEMOE, P. C. & SRINIVASAN, R. (1971) Fatigue of Bolted High Strength Structural Steel. *Journal of Structural Division Proceedings of the American Society of Civil Engineering*, 97, 935-950.
  15. BIRKEMOE, P. C., MEINHEIT, D. F.& MUNSE, H.W. (1969) Fatigue of A514 Steel In Bolted Connections. *Journal of the Structural Division Proceedings of the American Society of Civil Engineers*, 95, 2011-2030.
  16. BOUWMAN, I. L. P. (1979) Fatigue of bolted connections and bolts loaded in tension. The Netherlands, Delft University of Technology.
  17. BS EN, B. S. (2001) Metallic material-Tensile testing. *Annex D*. BSi British Standard.
  18. BS 2846, B. S. (2002) UK National Annex for Eurocode Basis of structural design. *BS 2846-1-2:2002*. BSi British Standard.
  19. BS EN1990, B. S. (2002) UK National Annex for Eurocode Basis of structural design. *BS EN 1990:2002, Annex C*. BSi British Standard.
  20. BS EN1993, B. S. (2005) Eurocode 3: Design of steel structures —Part 1-8: Design of joints. *BS EN 1993 - 1 - 8*. BSi British Standard.
  21. BS EN1993, B. S. (2006) Eurocode 3: Design of steel structures —Part 1-9: Fatigue. *BS EN 1993-1-9:2005*. BSi British Standard.
  22. BS EN ISO 898, B. S. (2009) Mechanical properties of fasteners made of carbon steel and alloy steel : Part 1. *BS EN ISO 898-1:2009*. BSi British Standard.
  23. BS ISO 12107, B. S. (2003) Metallic materials- Fatigue testing-Statistical planning and analysis data. *BS ISO 12107:2003*. BSi British standard.
  24. CARPENTER, J. (2011) Reliability: the practical application of Eurocode. *The Structural engineer*. London, United Kingdom, The Institute of Structural Engineers.
  25. CHANDRUPATLA, T. R. (2009) *Quality and reliability in engineering*, New York, Cambridge University press.

- 
26. COLLATE, M. (2005) Strength and Reliability of Aluminium Stiffened Panels. *School of Marine Science Technology*. Newcastle upon Tyne, University of Newcastle.
  27. COUNTS, W. A. & JOHNSON, W. S. (2002) Bolt bearing fatigue of polymer matrix composites at elevated temperature. *International Journal of fatigue*, 24, 197-204.
  28. ECCS (1985) Recommendation for the Fatigue Design of Steel Structure. Brussels, European Convention for Constructional Steelwork.
  29. ECCS (1986) Recommended testing procedure for assessing behaviour of structural steel elements under cyclic loads. Belgium, European Convention for Constructional Steelwork.
  30. ELGHAZOULI, A.Y., MALAGA-CHUQUITAYPE, C., CASTRO, J.M. & ORTON, A.H. (2009) Experimental Monotonic and Cyclic Behaviour of Blind -Bolted Angle Connections *Engineering Structures*.
  31. ESDEP (2011) ESDEP Course  
[http://www.fgg.uni-lj.si/kmk/esdep/master/wg12/10600.htm#SEC\\_2\\_1](http://www.fgg.uni-lj.si/kmk/esdep/master/wg12/10600.htm#SEC_2_1). Last accessed on June 2011
  32. FLOWDRILL (2012). <http://www.flowdrill.com/flowdrillprocess>. Last accessed on october 2012.
  33. FRANCE, J. E. (1997) Bolted connection between open section beams and box columns. PhD Thesis. *Department of civil Engineering*. England, University of Sheffield.
  34. FRANCE, J. E., DAVISION, J. B. & KIRBY, P. A. (1999) Moment-capacity and rotational stiffness of endplate connections to concrete filled tubular columns with flowdrilled connectors. *Journal of Construction Steel Research*, 50, 35-48.
  35. FRANCE, J. E., DAVISION, J. B. & KIRBY, P. A. (1998) Strength and rotational stiffness of simple connections to tubular columns using flowdrill connectors. *Journal of Construction Steel Research*, 50, 15-34.
  36. GHAZALI, T.H.& DIN, K. (2004) Fatigue Life of Bolt Subjected to Fatigue Loading Condition. *International Journal of Engineering and Technology*, 1, 20-27.
  37. GURNEY T R & MADDOX S J (1973) A re-analysis of fatigue data for welded joints in steel. *Welding Research International*, 3.
  38. GURNEY, T.R. (1979) *Fatigue of welded structures*, Cambridge, Cambridge University Press.

- 
39. HASOFER, A. M. & LIND, N. C. (1974) An Exact and Invariant First Order Reliability Format. *Journal of the Engineering Mechanics Division, ASCE*, 100, 111-121.
  40. HERBET J. SUTHERLAND & VEERS, P. S. (2000) The development of confidence limits for fatigue strength data. *2000 ASME Wind Energy Symposium*. AIAA/ASME.
  41. HESS, P. E., BRUCHMAN, D., ASSAKKAF, I. A. & AYYUB, B. M. (2002) Uncertainties in Material and Geometric Strength and Load Variables. *Naval Engineers Journal*, 114, 139-166.
  42. HOBBS, J. W., BURGUETE, R. L., HEYES, P. F. & PATTERSON, E. A. (2000) The effect of eccentric loading on the fatigue performance of high-tensile bolts. *International Journal of Fatigue*, 22, 531-538.
  43. HSU, H. L. & LIN, H. W. (2003) Performance of concrete filled tube base under repeated load. *International workshop on steel and composite construction, NCREE*.
  44. HUCK INTERNATIONAL LTD. (2012)  
[http://www.alcoa.com/fastening\\_systems/commercial/en/product.asp?cat\\_id=557&prod\\_id=884](http://www.alcoa.com/fastening_systems/commercial/en/product.asp?cat_id=557&prod_id=884). Last accessed on October 2012.
  45. HUGHES, O. F. (1998) *Ship Structural design , A rationally based, Computer-Added Optimization Approach*, Jersey City, New York, The Society of Naval Architects and Marines Engineers.
  46. IOANNIS VAYAS, SOPHOCLEOUS, A. & DINU, F. (2003) Fatigue Analysis of Moment Resisting Steel Frames. *Journal of Earthquake Engineering*, 7, 635-654.
  47. ISSC COMMITTEE III.2 (2009) Fatigue and Fracture. *17th International Ship and Offshore Structure Congress* Seoul. Korea.
  48. JIANI, H. (2012) An Investigation into the fatigue behaviour of the Extended Hollobolt connected to the concrete filled hollow section. Master Dissertations. *Department of Civil engineering*. University of Nottingham.
  49. JOHNSON & G, L. (1951) The Median Ranks of Sample Values in their Population With an Application to Certain Fatigue Studies. *Industrial Mathematics*, 2.
  50. JOHNSON, L. G. (1951) The Median Ranks of Sample Values in their Population With an Application to Certain Fatigue Studies. *Industrial Mathematics*, 2.

- 
51. KORIN, I. & PEREZ IPIÑA, J. (2010) Experimental evaluation of fatigue life and fatigue crack growth in a tension bolt-nut threaded connection. *International Journal of Fatigue*, 33, 166-175.
  52. KOROL, R. M., GHOBARAH, A. & MOURAD., S. (1993) Blind bolting W-shape beams to HSS columns. *Journal of Structural Engineering*, 119, 3463-3481.
  53. LINDAPTER (2012) Lindapter Hollo-Bolt. [http://www.lindapter.com/products/Cavity\\_Fixings/2/Type\\_HB\\_Hollo-Bolt](http://www.lindapter.com/products/Cavity_Fixings/2/Type_HB_Hollo-Bolt). Last accessed on october 2012.
  54. LITTLE, R. E. (1981) *Review of Statistical Analyses of Fatigue Life Data Using One-Sided Lower Statistical Tolerance Limits*, American Society for Testing and Materials.
  55. MARINEDIESELS.CO.UK. [http://www.marinediesels.info/2\\_stroke\\_engine\\_parts/Other\\_info/fatigue.htm](http://www.marinediesels.info/2_stroke_engine_parts/Other_info/fatigue.htm). Last accessed on 16 April 2011
  56. MELCHERS, R. E. (2001) *Structural Reliability analysis and prediction*, England, John wiley & Sons Ltd.
  57. NORWEGIAN PUBLIC COMMISSION (1981) The Alexander L.kielland accident, Report of Norwegian public commission appointed by Royal Decree of March 28,1980, presented to the Ministry of Justice and Police. ISBN B0000ED27N.
  58. O'BRIEN, M. & METCALFE, R. (2009) High Strength Engineering Fasteners: Design for Fatigue Resistance. *Journal of Failure Analysis and Prevention*, 9, 171-181.
  59. PARK, T.-G., CHOI, C.-H., WON, J.-H. & CHOI, J.-H. (2010) An efficient method for fatigue reliability analysis accounting for scatter of fatigue test data. *International Journal of Precision Engineering and Manufacturing*, 11, 429-437.
  60. PLUMIER, A., AGANTINO, M.R., CASTELLANI, A., CASTIGLIONI C.A. & CHESI, C. (1998) Resistance of steel connections to low cycle fatigue. *11th European on Earthquake Engineering* Balkema, Rotterdam.
  61. RACKWITZ, R. (2000) Reliability Analysis-Past, Present and Future. *8th ASCE Speciality Conference on Probabilistic Mechanics and Structural Reliability*. University of Notre Dome, Indiana.
  62. R-FUJCZAK, R. (1994) The effects of fatigue loading frequency on fatigue life of high strength pressure vessel steels. Watervliet, N.Y, US Army armament research, development and engineering center.

- 
63. SCHAUMANN, P. P. & MARTEN, D.-I. F. (2009) Fatigue resistance of high strength bolts with large diameters. *Proceeding of the International Symposium for Steel Structures ISSS 2009*. South Korea.
  64. SCHNEIDER, C. R. A. & MADDOX, S. J. (2003) Best Practice Guide on Statistical Analysis of Fatigue Data. Granta Park, Great Abington, Cambridge, UK, International Institute Welding, United Kingdom delegation
  65. SCI (1997) *Joints in steel Construction: Moment connection*, The Steel Construction Institute, London.
  66. SEAN ELLISON & TIZANI, W. (2004) Behaviour of blind bolted connections to concrete filled hollow sections. *The structural Engineer*. London, United Kingdom, The Institution of Structural Engineers
  67. SHOSUKE MORINO & TSUDA, K. (2002) Design and construction of concrete-filled steel tube column system in Japan. *Earthquake Engineering and Engineering Seismology*, 4.
  68. SOBCZYK, K. & B.F. SPENCER, J. (1992) *Random fatigue: From data to theory*, San Diego, CA 92101, Academic Press, INC.
  69. SWANSON, J. A. & LEO, R. T. (2000) Bolted steel connection: test on T-stub components. *Journal of structural Engineering, ASCE*, 126.
  70. TABSH, S. W. & MOURAD, S. (1997) Resistance factors for blind bolts in direct tension. *Engineering Structures*, 19, 995-1000.
  71. TABSH, S. W., MOURAD, S. & KOROL, R. M. (1997) Structural safety of ultra-twist blind fasteners in tension. *Canadian Journal of Civil Engineering*, 24, 211-217.
  72. TAMBOLI, A. R. (1999) *Handbook of Structural Steel Connection Design and Details*, New York, McGraw Hill.
  73. TAN, K., M. NICHOLAS, J. & PU, X. (2003) Mechanical properties of high strength concrete filled steel tubular column : Part 1-concentrically load. *ACI Journal*, 1-26.
  74. TANAKA, T. & TABUCHI, M. (2003) Flexural behaviour of H section beam webs connection with hollow section columns. IN M.A. ALONSO, A. CHICA & J.A. EDS (Eds.) *10th International symposium on tubular structure: Tubular structures X*. Madrid, Spain, Rotterdam: A.A. Balkema.

- 
75. TIZANI, W. & RIDLEY-ELLIS, D. J. (2003) The performance of a new blind bolt for moment resisting connections. IN: JAURRIETA, M. A. A., A. CHICA, J. A. EDS. (Ed.) *Proceeding of the 10<sup>th</sup> International Symposium on Tubular Structures: Tubular Structures X*. Madrid, Spain. , Rotterdam: A.A. Balkema.
  76. TRAHAIR, N.S., BRADFORD, M. A., NETHERCOT, D. A. & GARDNER, L. (2008) *The behaviour and design of steel structures to EC3*, Oxon OX14 4RN, Taylor & Francis.
  77. WALPOLE, E. R., MYERS, R. H. & MYERS, L.S. (1998) *Probability and Statistic for Engineers and Scientist*, New Jersey, Prentice Hall.
  78. WANG, J. F., HAN, L. H. & UY, B. (2009) Hysteretic behaviour of flush end plate joints to concrete filled steel tubular columns. *Journal Construction Steel Research*.
  79. WANG, J.-F., HAN, L.-H. & UY, B. (2009) Behaviour of flush end plate joints to concrete-filled steel tubular columns. *Journal of Constructional Steel Research*, 65, 925-939.
  80. WEIBULL, W. (1961) *Fatigue testing and analysis result*, Pergamon Press.
  81. WIRSCHING, P. H. (1983) Statistical summaries of Fatigue Data for Design Purpose. *NASA contractor report 3697*. Arizona, National Aeronautics and space administration (NASA).
  82. WIRSCHING, P. H. (1998) Fatigue reliability. *Structural Engineering and Material*, 1, 200-206.
  83. WOHLER A (1871) Test To Determine The Forces Acting on Railway carriage Axles and The Capacity of Resistance of The Axles. *Engineering*, 11.
  84. XU, J. & WANG, C. (2011) Reliability Design of Bolt Fatigue Strength of Hollow Axle in Cylinder of Ball Grinder. *International Conference on Information Science and Technology*. Nanjing, Jiangsu, China.
  85. YAO, H., GOLDSWORTHY, H. & GAD, E. (2008) Experimental and Numerical Investigation of the Tensile Behaviour of Blind-Bolted T-Stub Connections to Concrete-Filled Circular Columns. *Journal of Structural Engineering*, 134, 198-208.
  86. YOUNG, L. & EKVALL, J. C. (1981) Reliability of fatigue testing. IN LITTLE, R.E. & EKVALL, J. C. (Eds.) *Statistical analysis of fatigue data*. American Society for Testing Material.

- 
87. YOUNGWOON CHOI, BOKKYU LIM & BAE, S. (2007) Fatigue Life Prediction of High-Strength Bolt Subjecting to Torque. *Engineering Materials*, 345-346, 299-302.
88. YU, Z.-W., DING, F. X. & C.S.CAI (2006) Experimental behaviour of circular concrete filled steel tube stub columns. *Journal Construction Steel Research*, 165-174.

---

**Appendix A**

Prediction values of tensile resistance for Grade 8.8 bolts

A.1. Tensile resistance at ultimate

$$\begin{aligned}F_{t_{rd}} &= \frac{0.9 f_{ub} A}{\gamma_{m_2}} \\ &= \frac{0.9 \times 800 \times 157}{1.25} \times 10^{-3} \\ &= 90.43 \text{ kN}\end{aligned}$$

A.2. Tensile resistance at yield

$$\begin{aligned}F_{t_{rd}} &= \frac{0.9 f_{yb} A}{\gamma_{m_2}} \\ &= \frac{0.9 \times 650 \times 157}{1.25} \times 10^{-3} \\ &= 72.35 \text{ kN}\end{aligned}$$

---

**Appendix B**

Lognormal distribution fatigue test data

Rank	Sample Number	Number of cycles (N)	ln(N)	MR/P <sub>i</sub> = (j-0.3)/(n+0.4)	Standard z value
1	S1	8025	8.99032	0.02303	-1.99491
2	S4	9314	9.13927	0.05592	-1.58997
3	S23	10489	9.25808	0.08882	-1.34808
4	S24	12063	9.39790	0.12171	-1.16648
5	S2	20608	9.93343	0.15461	-1.01688
6	S9	20649	9.93542	0.18750	-0.88715
7	S10	21441	9.97306	0.22039	-0.77086
8	S11	28331	10.25171	0.25329	-0.66417
9	S12	28632	10.26228	0.28618	-0.56457
10	S14	40297	10.60403	0.31908	-0.47028
11	S8	45631	10.72834	0.35197	-0.38000
12	S5	55822	10.92992	0.38487	-0.29272
13	S25	58142	10.97064	0.41776	-0.20762
14	S27	63314	11.05586	0.45066	-0.12400
15	S17	78803	11.27471	0.48355	-0.04124
16	S15	89300	11.39976	0.51645	0.04124
17	S16	91878	11.42822	0.54934	0.12400
18	S21	107526	11.58549	0.58224	0.20762
19	S19	126731	11.74982	0.61513	0.29272
20	S18	191710	12.16374	0.64803	0.38000
21	S20	202742	12.21969	0.68092	0.47028
22	S6	264135	12.48422	0.71382	0.56457

---

<b>Rank</b>	<b>Sample Number</b>	<b>Number of cycles (N)</b>	<b>ln(N)</b>	<b>MR/P<sub>i</sub> = (j-0.3)/(n+0.4)</b>	<b>Standard z value</b>
23	S22	313697	12.65618	0.74671	0.66417
24	S33	450044	13.01710	0.77961	0.77086
25	S29	528703	13.17818	0.81250	0.88715
26	S34	626804	13.34839	0.84539	1.01688
27	S28	676386	13.42452	0.87829	1.16648
28	S3	1328102	14.09926	0.91118	1.34808
29	S13	2012778	14.51503	0.94408	1.58997
30	S7	3358810	15.02710	0.97697	1.99491

---

 Lognormal probability distribution function plotted data
 

---

<b>Cycles</b>	<b>Survival probability/ Reliability</b>	<b>Cycles</b>	<b>Survival probability/ Reliability</b>	<b>Cycles</b>	<b>Survival probability/ Reliability</b>
10	1.000	700000	0.128	1400000	0.062
50000	0.653	750000	0.120	1450000	0.060
100000	0.497	800000	0.113	1500000	0.057
150000	0.404	850000	0.106	1550000	0.055
200000	0.341	900000	0.100	1600000	0.053
250000	0.295	950000	0.095	1650000	0.051
300000	0.260	1000000	0.090	1700000	0.049
350000	0.232	1050000	0.085	1750000	0.048
400000	0.209	1100000	0.081	1800000	0.046
450000	0.190	1150000	0.077	1850000	0.045
500000	0.173	1200000	0.074	1900000	0.043
550000	0.160	1250000	0.071	1950000	0.042
600000	0.148	1300000	0.068	2000000	0.041
650000	0.137	1350000	0.065		

## Weibull distribution data

Rank	Sample Number	Number of cycles (N)	ln(N)	MR = $(j-0.3)/(n+0.4)$	1-MR	ln(-ln(1-MR))
1	S1	8025	8.9903	0.0230	0.9770	-3.7595
2	S4	9314	9.1393	0.0559	0.9441	-2.8552
3	S23	10489	9.2581	0.0888	0.9112	-2.3750
4	S24	12063	9.3979	0.1217	0.8783	-2.0419
5	S2	20608	9.9334	0.1546	0.8454	-1.7841
6	S9	20649	9.9354	0.1875	0.8125	-1.5720
7	S10	21441	9.9731	0.2204	0.7796	-1.3904
8	S11	28331	10.2517	0.2533	0.7467	-1.2307
9	S12	28632	10.2623	0.2862	0.7138	-1.0873
10	S14	40297	10.6040	0.3191	0.6809	-0.9563
11	S8	45631	10.7283	0.3520	0.6480	-0.8351
12	S5	55822	10.9299	0.3849	0.6151	-0.7217
13	S25	58142	10.9706	0.4178	0.5822	-0.6146
14	S27	63314	11.0559	0.4507	0.5493	-0.5124
15	S17	78803	11.2747	0.4836	0.5164	-0.4143
16	S15	89300	11.3998	0.5164	0.4836	-0.3194
17	S16	91878	11.4282	0.5493	0.4507	-0.2268
18	S21	107526	11.5855	0.5822	0.4178	-0.1360
19	S19	126731	11.7498	0.6151	0.3849	-0.0462
20	S18	191710	12.1637	0.6480	0.3520	0.0432
21	S20	202742	12.2197	0.6809	0.3191	0.1331
22	S6	264135	12.4842	0.7138	0.2862	0.2240
23	S22	313697	12.6562	0.7467	0.2533	0.3172

<b>Rank</b>	<b>Sample Number</b>	<b>Number of cycles (N)</b>	<b>ln(N)</b>	<b>MR = (j-0.3)/(n+0.4)</b>	<b>1-MR</b>	<b>ln(-ln(1-MR))</b>
24	S33	450044	13.0171	0.7796	0.2204	0.4137
25	S29	528703	13.1782	0.8125	0.1875	0.5152
26	S34	626804	13.3484	0.8454	0.1546	0.6243
27	S28	676386	13.4245	0.8783	0.1217	0.7448
28	S3	1328102	14.0993	0.9112	0.0888	0.8843
29	S13	2012778	14.5150	0.9441	0.0559	1.0591
30	S7	3358810	15.0271	0.9770	0.0230	1.3274

## Normal distribution data

Rank	Sample Number	Number of cycles (N)	ln(N)	$P_i=j-0.5/n$	Standard z value
1	S1	8025	8.9903	0.0167	-2.1280
2	S4	9314	9.1393	0.0500	-1.6449
3	S23	10489	9.2581	0.0833	-1.3830
4	S24	12063	9.3979	0.1167	-1.1918
5	S2	20608	9.9334	0.1500	-1.0364
6	S9	20649	9.9354	0.1833	-0.9027
7	S10	21441	9.9731	0.2167	-0.7835
8	S11	28331	10.2517	0.2500	-0.6745
9	S12	28632	10.2623	0.2833	-0.5730
10	S14	40297	10.6040	0.3167	-0.4770
11	S8	45631	10.7283	0.3500	-0.3853
12	S5	55822	10.9299	0.3833	-0.2967
13	S25	58142	10.9706	0.4167	-0.2104
14	S27	63314	11.0559	0.4500	-0.1257
15	S17	78803	11.2747	0.4833	-0.0418
16	S15	89300	11.3998	0.5167	0.0418
17	S16	91878	11.4282	0.5500	0.1257
18	S21	107526	11.5855	0.5833	0.2104
19	S19	126731	11.7498	0.6167	0.2967
20	S18	191710	12.1637	0.6500	0.3853
21	S20	202742	12.2197	0.6833	0.4770
22	S6	264135	12.4842	0.7167	0.5730
23	S22	313697	12.6562	0.7500	0.6745

<b>Rank</b>	<b>Sample Number</b>	<b>Number of cycles (N)</b>	<b>ln(N)</b>	<b><math>P_i=j-0.5/n</math></b>	<b>Standard z value</b>
24	S33	450044	13.0171	0.7833	0.7835
25	S29	528703	13.1782	0.8167	0.9027
26	S34	626804	13.3484	0.8500	1.0364
27	S28	676386	13.4245	0.8833	1.1918
28	S3	1328102	14.0993	0.9167	1.3830
29	S13	2012778	14.5150	0.9500	1.6449
30	S7	3358810	15.0271	0.9833	2.1280

## Appendix C

Student's  $t$  distribution ((E.Walpole et al., 1998)

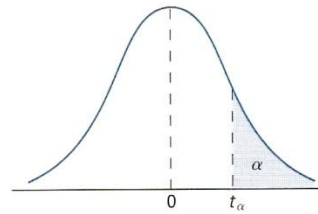


**TABLE A.4** Critical Values of the  $t$ -Distribution

$\nu$	$\alpha$						
	0.40	0.30	0.20	0.15	0.10	0.05	0.025
1	0.325	0.727	1.376	1.963	3.078	6.314	12.706
2	0.289	0.617	1.061	1.386	1.886	2.920	4.303
3	0.277	0.584	0.978	1.250	1.638	2.353	3.182
4	0.271	0.569	0.941	1.190	1.533	2.132	2.776
5	0.267	0.559	0.920	1.156	1.476	2.015	2.571
6	0.265	0.553	0.906	1.134	1.440	1.943	2.447
7	0.263	0.549	0.896	1.119	1.415	1.895	2.365
8	0.262	0.546	0.889	1.108	1.397	1.860	2.306
9	0.261	0.543	0.883	1.100	1.383	1.833	2.262
10	0.260	0.542	0.879	1.093	1.372	1.812	2.228
11	0.260	0.540	0.876	1.088	1.363	1.796	2.201
12	0.259	0.539	0.873	1.083	1.356	1.782	2.179
13	0.259	0.537	0.870	1.079	1.350	1.771	2.160
14	0.258	0.537	0.868	1.076	1.345	1.761	2.145
15	0.258	0.536	0.866	1.074	1.341	1.753	2.131
16	0.258	0.535	0.865	1.071	1.337	1.746	2.120
17	0.257	0.534	0.863	1.069	1.333	1.740	2.110
18	0.257	0.534	0.862	1.067	1.330	1.734	2.101
19	0.257	0.533	0.861	1.066	1.328	1.729	2.093
20	0.257	0.533	0.860	1.064	1.325	1.725	2.086
21	0.257	0.532	0.859	1.063	1.323	1.721	2.080
22	0.256	0.532	0.858	1.061	1.321	1.717	2.074
23	0.256	0.532	0.858	1.060	1.319	1.714	2.069
24	0.256	0.531	0.857	1.059	1.318	1.711	2.064
25	0.256	0.531	0.856	1.058	1.316	1.708	2.060
26	0.256	0.531	0.856	1.058	1.315	1.706	2.056
27	0.256	0.531	0.855	1.057	1.314	1.703	2.052
28	0.256	0.530	0.855	1.056	1.313	1.701	2.048
29	0.256	0.530	0.854	1.055	1.311	1.699	2.045
30	0.256	0.530	0.854	1.055	1.310	1.697	2.042
40	0.255	0.529	0.851	1.050	1.303	1.684	2.021
60	0.254	0.527	0.848	1.045	1.296	1.671	2.000
120	0.254	0.526	0.845	1.041	1.289	1.658	1.980
$\infty$	0.253	0.524	0.842	1.036	1.282	1.645	1.960

**TABLE A.4** (continued) Critical Values of the *t*-Distribution

<i>v</i>	$\alpha$						
	0.02	0.015	0.01	0.0075	0.005	0.0025	0.0005
1	15.895	21.205	31.821	42.434	63.657	127.322	636.590
2	4.849	5.643	6.965	8.073	9.925	14.089	31.598
3	3.482	3.896	4.541	5.047	5.841	7.453	12.924
4	2.999	3.298	3.747	4.088	4.604	5.598	8.610
5	2.757	3.003	3.365	3.634	4.032	4.773	6.869
6	2.612	2.829	3.143	3.372	3.707	4.317	5.959
7	2.517	2.715	2.998	3.203	3.499	4.029	5.408
8	2.449	2.634	2.896	3.085	3.355	3.833	5.041
9	2.398	2.574	2.821	2.998	3.250	3.690	4.781
10	2.359	2.527	2.764	2.932	3.169	3.581	4.587
11	2.328	2.491	2.718	2.879	3.106	3.497	4.437
12	2.303	2.461	2.681	2.836	3.055	3.428	4.318
13	2.282	2.436	2.650	2.801	3.012	3.372	4.221
14	2.264	2.415	2.624	2.771	2.977	3.326	4.140
15	2.249	2.397	2.602	2.746	2.947	3.286	4.073
16	2.235	2.382	2.583	2.724	2.921	3.252	4.015
17	2.224	2.368	2.567	2.706	2.898	3.222	3.965
18	2.214	2.356	2.552	2.689	2.878	3.197	3.922
19	2.205	2.346	2.539	2.674	2.861	3.174	3.883
20	2.197	2.336	2.528	2.661	2.845	3.153	3.849
21	2.189	2.328	2.518	2.649	2.831	3.135	3.819
22	2.183	2.320	2.508	2.639	2.819	3.119	3.792
23	2.177	2.313	2.500	2.629	2.807	3.104	3.768
24	2.172	2.307	2.492	2.620	2.797	3.091	3.745
25	2.167	2.301	2.485	2.612	2.787	3.078	3.725
26	2.162	2.296	2.479	2.605	2.779	3.067	3.707
27	2.158	2.291	2.473	2.598	2.771	3.057	3.690
28	2.154	2.286	2.467	2.592	2.763	3.047	3.674
29	2.150	2.282	2.462	2.586	2.756	3.038	3.659
30	2.147	2.278	2.457	2.581	2.750	3.030	3.646
40	2.125	2.250	2.423	2.542	2.704	2.971	3.551
60	2.099	2.223	2.390	2.504	2.660	2.915	3.460
120	2.076	2.196	2.358	2.468	2.617	2.860	3.373
$\infty$	2.054	2.170	2.326	2.432	2.576	2.807	3.291

---

**Appendix D**
Experimental data (R)

n	=	30	
$x_m(\log\Delta\sigma_R)$	=	2.5994	Mean value of stress
$y_m(\log N_R)$	=	4.9944	Mean value of fatigue life
$\hat{a}$	=	22.2783	
<b>b</b>	=	6.6490	
$s_y$	=	0.3301	Standard deviation of fatigue life
$s_x$	=	0.0496	Standard deviation of fatigue strength
$\log\Delta\sigma(2 \times 10^6)$	=	2.4029	Stress at 2 million cycles
$\Delta\sigma(2 \times 10^6)$	=	253N/mm <sup>2</sup>	

Equation =  $\log N = 22.2783 - 6.6490 \log \Delta\sigma$

Design requirement EC3 (S)

category			
n	=	5	
$x_m(\log\Delta\sigma_S)$	=	2.5984	Mean value of stress
$y_m(\log N_S)$	=	3.6027	Mean value of fatigue life
$\hat{a}$	=	11.3979	
<b>b</b>	=	3	
$s_y$	=	0	Standard deviation of fatigue life
$s_x$	=	0	Standard deviation of fatigue strength
$\log\Delta\sigma(2 \times 10^6)$	=	1.7	Stress at 2 million cycles
$\Delta\sigma(2 \times 10^6)$	=	50N/mm <sup>2</sup>	

Equation =  $\log N = 11.3979 - 3 \log \Delta\sigma$

---

Characteristic design (S)

category			
n	=	5	
$x_m(\log\Delta\sigma)$	=	2.5968	Mean value of stress
$y_m(\log N)$	=	4.4132	Mean value of fatigue life
$\hat{a}$	=	21.4863	
b	=	6.5747	
$s_y$	=	0	Standard deviation of Fatigue life
$s_x$	=	0	Standard deviation of Fatigue strength
$\log\Delta\sigma (2 \times 10^6)$	=	2.3	Stress at 2 million cycles
$\Delta\sigma (2 \times 10^6)$	=	204N/mm <sup>2</sup>	

$$\text{Equation} = \log N = 21.6181 - 6.6907 \log \Delta\sigma$$

Safety index calculations ( EC3 Design requirement)

$$\text{probability of failure } P = \Phi(-)\beta$$

Safety index ( $\beta$ )

$$\beta = \frac{\{\overline{\log N_R} - \overline{\log N_S}\}}{\sqrt{S_{\log N_R}^2 + S_{\log N_S}^2}}$$

$$= 4.22$$

From Standard Normal Table D.1 (Appendix E) (Melchers, 2001)

$$\beta = 4.22, \quad \text{Therefore } \Phi(-\beta) = 0.1332 \times 10^{-4}$$

$$\text{Probability of failure } P = \underline{\underline{0.1332 \times 10^{-4}}}$$

$$\text{Reliability} = 1 - P$$

$$= 0.999$$

---

**Safety index calculations( Characteristic design)**

probability of failure  $P = \Phi(-)\beta$

safety index

$$\beta = \frac{\{\overline{\log N_R} - \overline{\log N_s}\}}{\sqrt{S^2_{\log N_R} + S^2_{\log N_s}}}$$

$$= 1.76$$

From Table standard Normal Table

therefore  $\Phi(-\beta)$   
 $= 3.92 \times 10^{-02}$

$$\beta = 1.76$$

$$\text{Probability of failure } P = \underline{\underline{0.03921}}$$

$$\begin{aligned} \text{Reliability} &= 1 - P \\ &= 0.96079 \end{aligned}$$

## Appendix E

# Complementary Standard Normal Table

Table D.1  $N(0,1)$  distribution defined as  $\Phi(-\beta) = 1 - \Phi(\beta)$ .

$\beta$	$\Phi(-\beta)$	$\beta$	$\Phi(-\beta)$	$\beta$	$\Phi(-\beta)$
0.00	0.5000	0.40	0.3446	0.80	0.2119
0.01	0.4960	0.41	0.3409	0.81	0.2090
0.02	0.4920	0.42	0.3372	0.82	0.2061
0.03	0.4880	0.43	0.3336	0.83	0.2033
0.04	0.4841	0.44	0.3300	0.84	0.2005
0.05	0.4801	0.45	0.3264	0.85	0.1977
0.06	0.4761	0.46	0.3228	0.86	0.1949
0.07	0.4721	0.47	0.3192	0.87	0.1922
0.08	0.4681	0.48	0.3156	0.88	0.1894
0.09	0.4642	0.49	0.3121	0.89	0.1867
0.10	0.4602	0.50	0.3085	0.90	0.1841
0.11	0.4562	0.51	0.3050	0.91	0.1814
0.12	0.4522	0.52	0.3015	0.92	0.1788
0.13	0.4483	0.53	0.2981	0.93	0.1762
0.14	0.4443	0.54	0.2946	0.94	0.1736
0.15	0.4404	0.55	0.2912	0.95	0.1711
0.16	0.4364	0.56	0.2877	0.96	0.1685
0.17	0.4325	0.57	0.2843	0.97	0.1660
0.18	0.4286	0.58	0.2810	0.98	0.1635
0.19	0.4247	0.59	0.2776	0.99	0.1611
0.20	0.4207	0.60	0.2743	1.00	0.1587
0.21	0.4168	0.61	0.2709	1.01	0.1563
0.22	0.4129	0.62	0.2676	1.02	0.1539
0.23	0.4091	0.63	0.2644	1.03	0.1515
0.24	0.4052	0.64	0.2611	1.04	0.1492
0.25	0.4013	0.65	0.2579	1.05	0.1469
0.26	0.3974	0.66	0.2546	1.06	0.1446
0.27	0.3936	0.67	0.2514	1.07	0.1423
0.28	0.3897	0.68	0.2483	1.08	0.1401
0.29	0.3859	0.69	0.2451	1.09	0.1379
0.30	0.3821	0.70	0.2420	1.10	0.1357
0.31	0.3783	0.71	0.2389	1.11	0.1335
0.32	0.3745	0.72	0.2358	1.12	0.1314
0.33	0.3707	0.73	0.2327	1.13	0.1292
0.34	0.3669	0.74	0.2297	1.14	0.1271
0.35	0.3632	0.75	0.2266	1.15	0.1251
0.36	0.3594	0.76	0.2236	1.16	0.1230
0.37	0.3557	0.77	0.2207	1.17	0.1210
0.38	0.3520	0.78	0.2177	1.18	0.1190
0.39	0.3483	0.79	0.2148	1.19	0.1170

$\beta$	$\Phi(-\beta)$	$\beta$	$\Phi(-\beta)$	$\beta$	$\Phi(-\beta)$
1.20	0.1151	1.80	0.3593E-01	2.40	0.8198E-02
1.21	0.1131	1.81	0.3515E-01	2.41	0.7976E-02
1.22	0.1112	1.82	0.3438E-01	2.42	0.7760E-02
1.23	0.1094	1.83	0.3363E-01	2.43	0.7550E-02
1.24	0.1075	1.84	0.3289E-01	2.44	0.7344E-02
1.25	0.1057	1.85	0.3216E-01	2.45	0.7143E-02
1.26	0.1038	1.86	0.3144E-01	2.46	0.6947E-02
1.27	0.1020	1.87	0.3074E-01	2.47	0.6756E-02
1.28	0.1003	1.88	0.3005E-01	2.48	0.6569E-02
1.29	0.9853E-01	1.89	0.2938E-01	2.49	0.6387E-02
1.30	0.9680E-01	1.90	0.2872E-01	2.50	0.6210E-02
1.31	0.9510E-01	1.91	0.2807E-01	2.51	0.6037E-02
1.32	0.9342E-01	1.92	0.2743E-01	2.52	0.5868E-02
1.33	0.9176E-01	1.93	0.2680E-01	2.53	0.5703E-02
1.34	0.9013E-01	1.94	0.2619E-01	2.54	0.5543E-02
1.35	0.8851E-01	1.95	0.2559E-01	2.55	0.5386E-02
1.36	0.8692E-01	1.96	0.2500E-01	2.56	0.5234E-02
1.37	0.8535E-01	1.97	0.2442E-01	2.57	0.5085E-02
1.38	0.8380E-01	1.98	0.2385E-01	2.58	0.4940E-02
1.39	0.8227E-01	1.99	0.2330E-01	2.59	0.4799E-02
1.40	0.8076E-01	2.00	0.2275E-01	2.60	0.4661E-02
1.41	0.7927E-01	2.01	0.2222E-01	2.61	0.4527E-02
1.42	0.7781E-01	2.02	0.2169E-01	2.62	0.4397E-02
1.43	0.7636E-01	2.03	0.2118E-01	2.63	0.4269E-02
1.44	0.7494E-01	2.04	0.2068E-01	2.64	0.4145E-02
1.45	0.7353E-01	2.05	0.2018E-01	2.65	0.4025E-02
1.46	0.7215E-01	2.06	0.1970E-01	2.66	0.3907E-02
1.47	0.7078E-01	2.07	0.1923E-01	2.67	0.3793E-02
1.48	0.6944E-01	2.08	0.1876E-01	2.68	0.3681E-02
1.49	0.6811E-01	2.09	0.1831E-01	2.69	0.3573E-02
1.50	0.6681E-01	2.10	0.1786E-01	2.70	0.3467E-02
1.51	0.6552E-01	2.11	0.1743E-01	2.71	0.3364E-02
1.52	0.6426E-01	2.12	0.1700E-01	2.72	0.3264E-02
1.53	0.6301E-01	2.13	0.1659E-01	2.73	0.3167E-02
1.54	0.6178E-01	2.14	0.1618E-01	2.74	0.3072E-02
1.55	0.6057E-01	2.15	0.1578E-01	2.75	0.2980E-02
1.56	0.5938E-01	2.16	0.1539E-01	2.76	0.2890E-02
1.57	0.5821E-01	2.17	0.1500E-01	2.77	0.2803E-02
1.58	0.5706E-01	2.18	0.1463E-01	2.78	0.2718E-02
1.59	0.5592E-01	2.19	0.1426E-01	2.79	0.2635E-02
1.60	0.5480E-01	2.20	0.1390E-01	2.80	0.2555E-02
1.61	0.5370E-01	2.21	0.1355E-01	2.81	0.2477E-02
1.62	0.5262E-01	2.22	0.1321E-01	2.82	0.2401E-02
1.63	0.5155E-01	2.23	0.1287E-01	2.83	0.2327E-02
1.64	0.5050E-01	2.24	0.1255E-01	2.84	0.2256E-02
1.65	0.4947E-01	2.25	0.1222E-01	2.85	0.2186E-02
1.66	0.4846E-01	2.26	0.1191E-01	2.86	0.2118E-02
1.67	0.4746E-01	2.27	0.1160E-01	2.87	0.2052E-02
1.68	0.4648E-01	2.28	0.1130E-01	2.88	0.1988E-02
1.69	0.4552E-01	2.29	0.1101E-01	2.89	0.1926E-02
1.70	0.4457E-01	2.30	0.1072E-01	2.90	0.1866E-02
1.71	0.4363E-01	2.31	0.1044E-01	2.91	0.1807E-02
1.72	0.4272E-01	2.32	0.1017E-01	2.92	0.1750E-02
1.73	0.4182E-01	2.33	0.9903E-02	2.93	0.1695E-02
1.74	0.4093E-01	2.34	0.9642E-02	2.94	0.1641E-02
1.75	0.4006E-01	2.35	0.9387E-02	2.95	0.1589E-02
1.76	0.3921E-01	2.36	0.9138E-02	2.96	0.1538E-02
1.77	0.3836E-01	2.37	0.8894E-02	2.97	0.1489E-02
1.78	0.3754E-01	2.38	0.8657E-02	2.98	0.1441E-02
1.79	0.3673E-01	2.39	0.8424E-02	2.99	0.1395E-02

$\beta$	$\Phi(-\beta)$	$\beta$	$\Phi(-\beta)$	$\beta$	$\Phi(-\beta)$
3.00	0.1350E-02	3.60	0.1591E-03	5.00	0.2859E-06
3.01	0.1306E-02	3.61	0.1531E-03	5.05	0.2203E-06
3.02	0.1264E-02	3.62	0.1473E-03	5.10	0.1694E-06
3.03	0.1223E-02	3.63	0.1417E-03	5.15	0.1299E-06
3.04	0.1183E-02	3.64	0.1363E-03	5.20	0.9935E-07
3.05	0.1144E-02	3.65	0.1311E-03	5.25	0.7582E-07
3.06	0.1107E-02	3.66	0.1261E-03	5.30	0.5772E-07
3.07	0.1070E-02	3.67	0.1212E-03	5.35	0.4384E-07
3.08	0.1035E-02	3.68	0.1166E-03	5.40	0.3321E-07
3.09	0.1001E-02	3.69	0.1121E-03	5.45	0.2510E-07
3.10	0.9676E-03	3.70	0.1077E-03	5.50	0.1892E-07
3.11	0.9354E-03	3.71	0.1036E-03	5.55	0.1423E-07
3.12	0.9042E-03	3.72	0.9956E-04	5.60	0.1067E-07
3.13	0.8740E-03	3.73	0.9569E-04	5.65	0.7985E-08
3.14	0.8447E-03	3.74	0.9196E-04	5.70	0.5959E-08
3.15	0.8163E-03	3.75	0.8837E-04	5.75	0.4436E-08
3.16	0.7888E-03	3.76	0.8491E-04	5.80	0.3293E-08
3.17	0.7622E-03	3.77	0.8157E-04	5.85	0.2438E-08
3.18	0.7363E-03	3.78	0.7836E-04	5.90	0.1800E-08
3.19	0.7113E-03	3.79	0.7527E-04	5.95	0.1325E-08
3.20	0.6871E-03	3.80	0.7230E-04	6.00	0.9716E-09
3.21	0.6636E-03	3.81	0.6943E-04	6.10	0.5220E-09
3.22	0.6409E-03	3.82	0.6667E-04	6.20	0.2778E-09
3.23	0.6189E-03	3.83	0.6402E-04	6.30	0.1463E-09
3.24	0.5976E-03	3.84	0.6147E-04	6.40	0.7636E-10
3.25	0.5770E-03	3.85	0.5901E-04	6.50	0.3945E-10
3.26	0.5570E-03	3.86	0.5664E-04	6.60	0.2018E-10
3.27	0.5377E-03	3.87	0.5437E-04	6.70	0.1023E-10
3.28	0.5190E-03	3.88	0.5218E-04	6.80	0.5130E-11
3.29	0.5009E-03	3.89	0.5007E-04	6.90	0.2549E-11
3.30	0.4834E-03	3.90	0.4804E-04	7.00	0.1254E-11
3.31	0.4664E-03	3.91	0.4610E-04	7.10	0.6107E-12
3.32	0.4500E-03	3.92	0.4422E-04	7.20	0.2946E-12
3.33	0.4342E-03	3.93	0.4242E-04	7.30	0.1407E-12
3.34	0.4189E-03	3.94	0.4069E-04	7.40	0.6654E-13
3.35	0.4040E-03	3.95	0.3902E-04	7.50	0.3116E-13
3.36	0.3897E-03	3.96	0.3742E-04	7.60	0.1445E-13
3.37	0.3758E-03	3.97	0.3588E-04	7.70	0.6636E-14
3.38	0.3624E-03	3.98	0.3441E-04	7.80	0.3017E-14
3.39	0.3494E-03	3.99	0.3298E-04	7.90	0.1359E-14
3.40	0.3369E-03	4.00	0.3162E-04	8.00	0.6056E-15
3.41	0.3248E-03	4.05	0.2557E-04	8.10	0.2673E-15
3.42	0.3131E-03	4.10	0.2062E-04	8.20	0.1169E-15
3.43	0.3017E-03	4.15	0.1659E-04	8.30	0.5058E-16
3.44	0.2908E-03	4.20	0.1332E-04	8.40	0.2167E-16
3.45	0.2802E-03	4.25	0.1067E-04	8.50	0.9197E-17
3.46	0.2700E-03	4.30	0.8524E-05	8.60	0.3864E-17
3.47	0.2602E-03	4.35	0.6794E-05	8.70	0.1608E-17
3.48	0.2507E-03	4.40	0.5402E-05	8.80	0.6623E-18
3.49	0.2415E-03	4.45	0.4285E-05	8.90	0.2701E-18
3.50	0.2326E-03	4.50	0.3391E-05	9.00	0.1091E-18
3.51	0.2240E-03	4.55	0.2677E-05	9.10	0.4363E-19
3.52	0.2157E-03	4.60	0.2108E-05	9.20	0.1728E-19
3.53	0.2077E-03	4.65	0.1656E-05	9.30	0.6773E-20
3.54	0.2000E-03	4.70	0.1298E-05	9.40	0.2629E-20
3.55	0.1926E-03	4.75	0.1015E-05	9.50	0.1011E-20
3.56	0.1854E-03	4.80	0.7914E-06	9.60	0.3847E-21
3.57	0.1784E-03	4.85	0.6158E-06	9.70	0.1450E-21
3.58	0.1717E-03	4.90	0.4780E-06	9.80	0.5408E-22
3.59	0.1653E-03	4.95	0.3701E-06	9.90	0.1998E-22

**Standard Normal Probability Density Function  $\phi(x)$** 

The standard normal probability density function  $\phi(x)$  may be obtained, for low values of  $x$  from tables in standard statistics texts. For high values of  $x$  such tables generally are not helpful. A simple procedure may be used to estimate  $\phi(x)$  from Table D.1 using the approximation:

$$\phi(x) \approx \frac{\Phi(-x + \Delta x) - \Phi(-x - \Delta x)}{2\Delta x}$$

For example, to evaluate  $\phi(3.65)$ :

$$\Phi(-3.64) = 0.1363E - 3$$

$$\Phi(-3.66) = \underline{0.1261E - 3}$$

$$\text{difference} = 0.0102E - 3$$

$$\phi(3.65) = (0.0102E - 3) / (0.02) = \underline{0.51E - 3}$$

